DOT/FAA/AR-09/58

Air Traffic Organization
NextGen & Operations Planning
Office of Research and
Technology Development
Washington, DC 20591

Evaluating the Decomposition Products Generated Inside an Intact Fuselage During a Simulated Postcrash Fuel Fire

Timothy R. Marker
Louise C. Speitel

June 2011

Final Report

U.S. Department of Transportation
Federal Aviation Administration

NOTICE

Technical Report Documentation Page

1. Report No.	2. Government Accession No.	3. Recipient's Catalog No.
DOT/FAA/AR-09/58		

4. Title and Subtitle	5. Report Date
EVALUATING THE DECOMPOSITION PRODUCTS GENERATED INSIDE AN INTACT FUSELAGE DURING A SIMULATED POSTCRASH FUEL FIRE	June 2011
	6. Performing Organization Code

7. Author(s)	8. Performing Organization Report No.
Timothy R. Marker and Louise C. Speitel	

9. Performing Organization Name and Address	10. Work Unit No. (TRAIS)
Federal Aviation Administration William J. Hughes Technical Center Airport and Aircraft Research and Development Group Fire Safety Team Atlantic City International Airport, NJ 08405	11. Contract or Grant No.

12. Sponsoring Agency Name and Address	13. Type of Report and Period Covered
U.S. Department of Transportation Federal Aviation Administration Air Traffic Organization NextGen & Operations Planning Office of Research and Technology Development Washington, DC 20591	Final Report
	14. Sponsoring Agency Code ANM-114

15. Supplementary Notes

16. Abstract

This report summarizes the Federal Aviation Administration research effort to develop a laboratory-scale test method for evaluating the thermal decomposition products produced inside an intact transport category fuselage during exposure to a simulated external fuel fire. An oil-fired burner, configured in accordance with Title 14 Code of Federal Regulations Part 25.856(b) Appendix F Part VII, was used to simulate the fuel fire, and a 4- by 4- by 4-foot steel cube box was used to mount representative test samples. The cube box simulated an intact fuselage and served as an enclosure to collect emitted gases during fire exposure. Test samples representing a variety of fuselage constructions were evaluated, including a noncontemporary prototype structural composite material (without thermal acoustic insulation). A typical cross section consisted of a 40- by 40-inch aluminum panel representing the fuselage skin and the accompanying thermal acoustic insulation blanket behind the skin. Two thermal acoustic configurations were also tested. The first contained a heat-stabilized polyacrylonitrile fiber blanket. The second contained a ceramic paper barrier sandwiched under a fiberglass blanket. Each was encased by a thin metallized polyvinylfluoride moisture barrier. These burnthrough-resistant configurations were primarily run to provide a baseline for comparing the emitted gas concentrations with the prototype structural composite material.

A specialized Fourier Transform Infrared/total hydrocarbon gas analysis system was used to continually measure the products of combustion collected within the enclosure. Additional analyzers continuously measured the amount of carbon monoxide, carbon dioxide, and oxygen in the collected stream.

During the tests, it was determined that a prototype multi-ply structural composite material produced minimal quantities of toxic and flammable gases during a 5-minute fire exposure. Approximately 7 plies of the 16-ply carbon/epoxy structural composite material were delaminated by the fire exposure. By comparison, the aluminum skin/insulation configurations generated higher gas concentrations.

Subsequent full-scale tests were conducted using these material systems inside a Boeing 707 fuselage. These tests were run to determine realistic levels of combustion products that can be generated inside the fuselage during a fuel fire when using burnthrough-compliant materials identical to those previously tested in the laboratory-scale tests. The full-scale tests used a fire-hardened steel cylinder test section in which insulation materials could be installed and evaluated against a standard 8- by 10-foot fuel pan fire. A comparison of the laboratory- and full-scale gas analysis results was made to determine the scaling factor for gas concentrations. By determining the scaling factors, an appropriate gas concentration acceptance level could be established for the laboratory-scale apparatus. The goal was to use this laboratory-scale test and scaling factors to predict thermal decomposition product concentrations for burnthrough-resistant insulation. The predicted full-scale concentrations can be used to assess the survival and health hazards of various insulation systems exposed to external fuel fires.

17. Key Words	18. Distribution Statement
Prototype structural composite material, Postcrash, Burnthrough, Insulation batting, Heat-stabilized polyacrylonitrile fiber, Combustion gases, FTIR spectroscopy, Toxicity, Lower explosive limit	This document is available to the U.S. public through the National Technical Information Service (NTIS), Springfield, Virginia 22161. This document is also available from the Federal Aviation Administration William J. Hughes Technical Center at actlibrary.tc.faa.gov.

19. Security Classif. (of this report)	20. Security Classif. (of this page)	21. No. of Pages	22. Price
Unclassified	Unclassified	86	

TABLE OF CONTENTS

LIST OF FIGURES

LIST OF TABLES

LIST OF SYMBOLS AND ACRONYMS

CH_4	Methane
C_2H_2	Acetylene
C_2H_4	Ethylene
C_2H_6	Ethane
CH_2CHCHO	Acrolein
C_3H_8	Propane
C_6H_6	Benzene
$C_6H_5NH_2$	Aniline
$C_6H_5NHCH_3$	Methylaniline
$C_6H_5NHCH_2CH_3$	Ethylaniline
C_6H_5OH	Phenol
CO	Carbon monoxide
$COCl_2$	Carbonyl chloride
COF_2	Carbonyl fluoride
CO_2	Carbon dioxide
COS	Carbonyl sulfide
H_2O	Water
HBr	Hydrogen bromide
HC1	Hydrogen chloride
HCN	Hydrogen cyanide
HF	Hydrogen fluoride
NH_3	Ammonia
NO	Nitrogen oxide
N_2O	Nitrous oxide
NO_2	Nitrogen dioxide
O_2	Oxygen
SO_2	Sulfur dioxide
ZnSe	Zinc selenide
CLS	Classical least squares
ERPG	Emergency Response Planning Guidelines
FAA	Federal Aviation Administration
FED	Fractional effective dose
FID	Flame-ionization detector
FTIR	Fourier Transform Infrared
IDLH	Immediately Dangerous to Life and Health Concentrations
LC	Lethal concentration
LEL	Lower explosive limit
MCT	Mercury Cadmium Telluride
NDIR	Nondispersive infrared analyzer
NIOSH	National Institute for Occupational Safety and Health
PAN	Polyacrylonitrile
PVF	Polyvinylfluoride
THC	Total hydrocarbon

EXECUTIVE SUMMARY

This report summarizes the Federal Aviation Administration research effort to develop a laboratory-scale test method for evaluating the products of combustion inside an intact transport category fuselage during exposure to a simulated external fuel fire. A laboratory-scale test was developed to evaluate the thermal decomposition gases that could possibly be generated inside an intact fuselage during a postcrash fuel fire. The test consisted of an oil-fired burner, configured in accordance with Title 14 Code of Federal Regulations Part 25.856(b) Appendix F Part VII, to simulate the fuel fire, and a 4- by 4- by 4-foot steel cube box was used to mount representative test samples. The cube box simulated an intact fuselage and served as an enclosure to collect emitted gases during fire exposure. Test samples representing several fuselage constructions were evaluated. One sample was a prototype carbon/epoxy structural composite that was representative of the fuselage construction in a next-generation, all-composite transport aircraft. Two fuselage configurations were initially evaluated consisting of an aluminum skin panel and accompanying insulation materials that met the new burnthrough standard: a ceramic-based lightweight barrier in conjunction with standard fiberglass batting and a heat-stabilized polyacrylonitrile fiber. Each was encased by a thin, metallized polyvinylfluoride moisture barrier. These traditional configurations were primarily run to provide a baseline for comparing the emitted gas concentrations with those of the prototype structural composite material.

A process Fourier Transform Infrared analyzer was used to continuously measure the toxic and flammable gases collected within the enclosure. Additional analyzers measured the concentration of total hydrocarbons as propane, carbon monoxide, carbon dioxide, and oxygen. During the test, it was determined that the prototype structural composite material produced minimal quantities of toxic and flammable gases during a 5-minute fire exposure. Approximately 7 plies of the 16-ply composite panel were damaged by the fire. In contrast, the aluminum skin/insulation configurations generated higher gas concentrations than the composite materials during a 5-minute fire exposure.

Subsequent full-scale tests were conducted using these insulation systems inside a Boeing 707 fuselage. These tests were run to determine realistic levels of combustion products that could be generated during a fuel fire when using burnthrough-compliant materials identical to those previously tested in the laboratory-scale tests. The full-scale tests used a fire-hardened steel cylinder test section in which insulation materials could be installed and evaluated against a standard 8- by 10-foot fuel pan fire. A comparison of the laboratory- and full-scale gas analysis results was made to determine the ratio between the two. The resultant scaling factor was corrected for infiltration of external combustion gases into the fuselage and wall and reaction losses. By determining the corrected scaling factor, an appropriate gas concentration acceptance level could be established for the laboratory-scale apparatus. This information could be used in an assessment of the survival and health hazards of various burnthrough-resistant insulation by predicting full-scale gas concentrations of the systems when exposed to an external fuel fire.

1. INTRODUCTION.

1.1 PURPOSE.

This report describes the Federal Aviation Administration (FAA) research effort to develop a laboratory-scale test method for measuring toxic and flammable gaseous decomposition products inside an intact, burnthrough-resistant transport category fuselage during exposure to an adjacent external fuel fire. The results from this laboratory-scale test and subsequent full-scale burnthrough tests of identical materials were used to establish appropriate gas acceptance levels in the newly designed laboratory apparatus.

1.2 BACKGROUND.

In a majority of survivable accidents accompanied by fire, ignition of the interior of the aircraft is caused by burning jet fuel external to the aircraft as a result of fuel tank damage during impact. One important factor to occupant survivability is the integrity of the fuselage during an accident. Usually, there are two possibilities that exist in a survivable aircraft accident: (1) an intact fuselage and (2) a compromised fuselage from either a crash rupture or an opened emergency exit, which allows direct impingement of external fuel fire flames on the cabin materials. Based on a consideration of past accidents, experimental studies, and fuselage design, it is apparent that the fuselage rupture or opening represents the worst-case condition and provides the most significant opportunity for fire to enter the cabin [1]. Past FAA regulatory actions governing interior material flammability were based on full-scale tests employing a fuel fire adjacent to a fuselage opening in an otherwise intact fuselage. This scenario, in which the cabin materials were directly exposed to the intense thermal radiation emitted by the fuel fire, represented a severe but survivable fire condition and was used to develop improved material flammability test standards. However, in some accidents involving fire, the fuselage remained completely intact (no rupture or openings near the fire) and fire penetration into the passenger cabin was the result of a burnthrough of the fuselage shell [2].

There are typically three barriers that a fuel fire must penetrate to burnthrough to the cabin interior: aluminum skin, thermal acoustic insulation, and the interior sidewall and floor panel combinations. The burnthrough resistance of aluminum skin is well known, lasting between 30 to 60 seconds, depending on the thickness. Thermal acoustic insulation, typically comprised of several layers of fiberglass batting encased in a thin moisture barrier film, can offer an additional 1 to 2 minutes' protection if the material is not physically dislodged from the fuselage structure [3 and 4].

To evaluate potential improvements in burnthrough protection under realistic conditions, the FAA William J. Hughes Technical Center developed a full-scale fuselage burnthrough test apparatus in 1996. The construction of this apparatus was the most practical approach for repetitive testing and systematic evaluations of singular components. A 20-foot-long steel cylindrical test apparatus was fabricated, and the test apparatus was then inserted between two halves of a Boeing 707 fuselage (figure 1). This test apparatus has a 12- by 8-foot section of the outer skin removed and can be mocked up with representative airplane skin, thermal acoustic insulation, floor and sidewall panels, carpet, and cargo liner. The mocked up test apparatus extends beyond the 8- by 10-foot fire pan, eliminating problems that might occur if the edges of

the installed fuselage materials were in direct exposure to the fuel fire. Measurements of temperature, smoke, carbon monoxide (CO), carbon dioxide (CO_2), and oxygen (O_2) were taken inside the test apparatus along with video coverage at several locations to determine exact burnthrough locations and times.

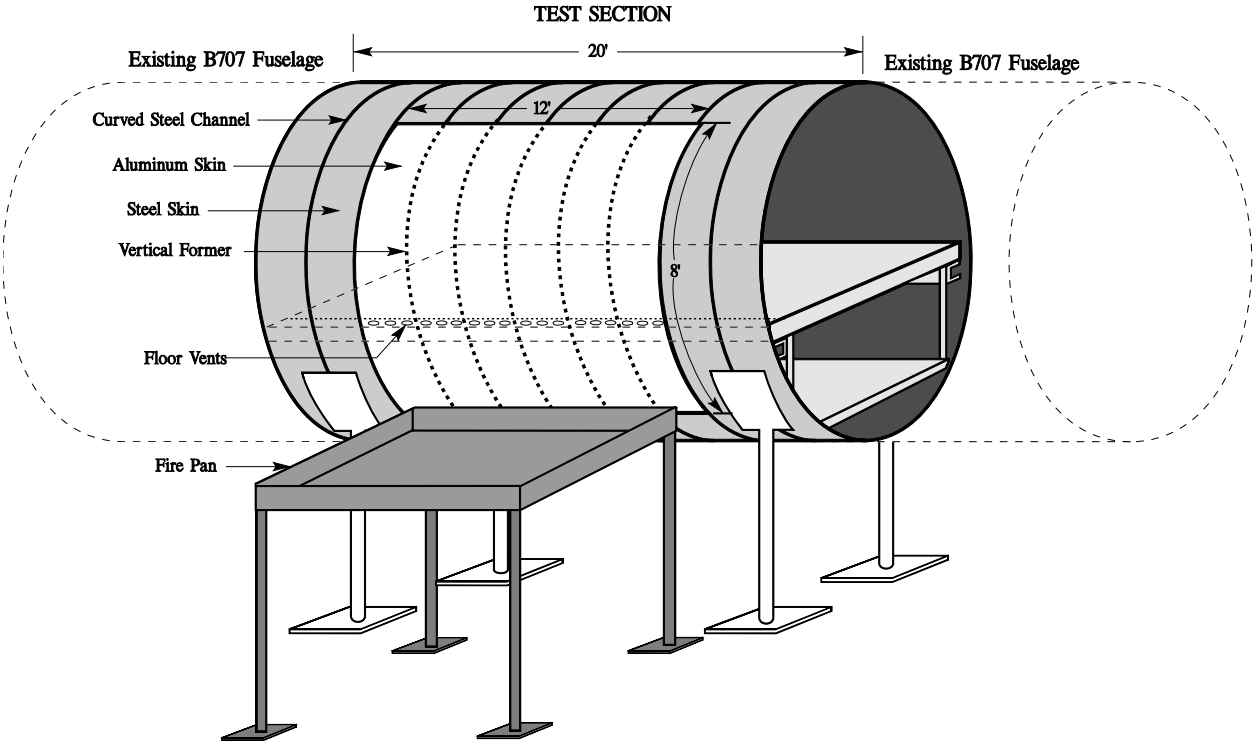

Figure 1. Full-Scale Fuselage Burnthrough Test Apparatus

Tests performed in this full-scale apparatus confirmed the enhanced burnthrough protection from a variety of materials including a thin, dot-printed, ceramic-based barrier that could be inserted into the existing fiberglass insulation bags. A heat-stabilized, oxidized polyacrylonitrile (PAN) fiber was equally capable at preventing a fully developed fuel fire from entering the cabin for as much as 8 minutes. When compared to current insulation materials, which were shown to fail in as little as 2 minutes, effective fire barriers offer increased life-saving potential during a postcrash fire accident in which the fuselage remains intact [5].

Based on the encouraging findings of the full-scale tests, which showed the potential benefit of increased burnthrough protection, the FAA began work on a laboratory-scale test that could replicate the full-scale conditions. The new laboratory test would evaluate the burnthrough protection capabilities of materials without the expense of running a full-scale test. The initial test apparatus used an oil-fired burner, similar to that used in other FAA flammability tests, along with a steel box used to mount a mock-up, 24- by 24-inch test sample, consisting of the outer aluminum skin and thermal acoustic insulation beneath it. The steel box also allowed combustion product monitoring of its contents and the viewing of the unexposed side of the sample using a video camera (figure 2).

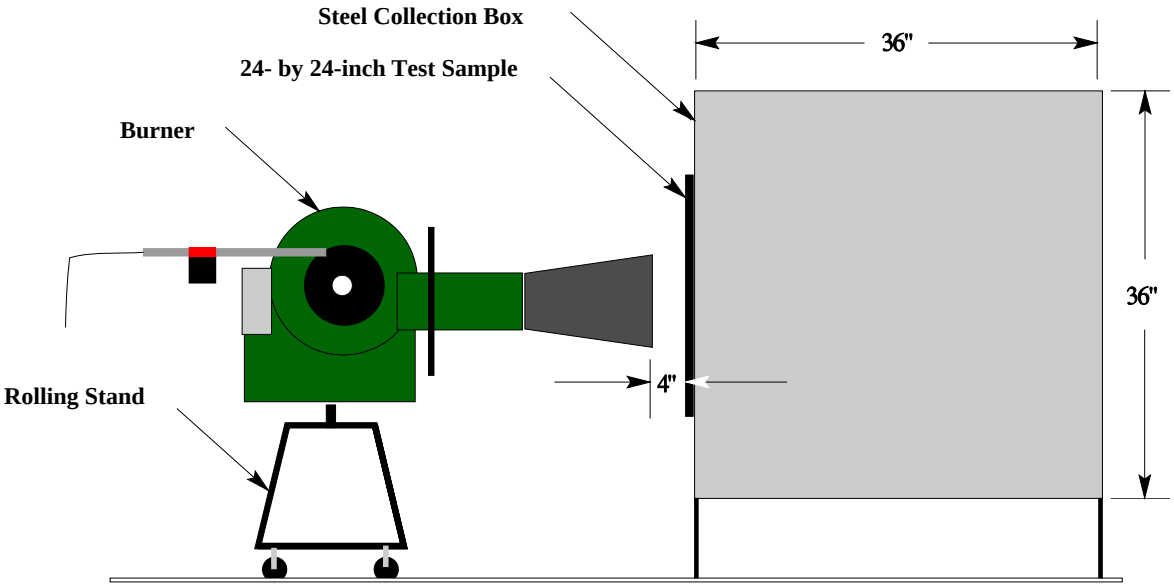

Figure 2. Initial Laboratory-Scale Burnthrough Test Apparatus

The box portion of the apparatus was eventually abandoned and replaced with a grid-style frame to mount insulation samples. Eventually, the aluminum skin sample on the exterior of the apparatus was also abandoned, as this became a cumbersome, time-consuming task. Since aluminum skin offers little practical opportunity for fire hardening, the focus of extending the burnthrough resistance has been on the thermal acoustic insulation and, to a much lesser extent, the floor/sidewall panel combination and related components. Full-scale fire tests have shown that appreciable gains in burnthrough resistance can be achieved by either protecting or replacing the current fiberglass thermal acoustic insulation.

In the finalized burnthrough test for insulation materials, samples of thermal acoustic insulation were mounted to the sample holder frame (figure 3), which resembled the former and stringer structure in transport aircraft, and exposed to the oil-fired burner flame for a period of 4 minutes (figure 4). The finalized test exposure condition consisted of a flame temperature of 1900°F and a heat flux of 16.0 Btu/ft^{2}sec. The burner output cone was situated 4 inches from the outer plane of the sample holder frame at an angle of 30° with respect to horizontal. This configuration yielded results that correlated with previous full-scale tests that used identical materials. During the tests, it was also determined that attaching the insulation blankets to the test sample structure had a critical impact on the effectiveness of the insulation material.

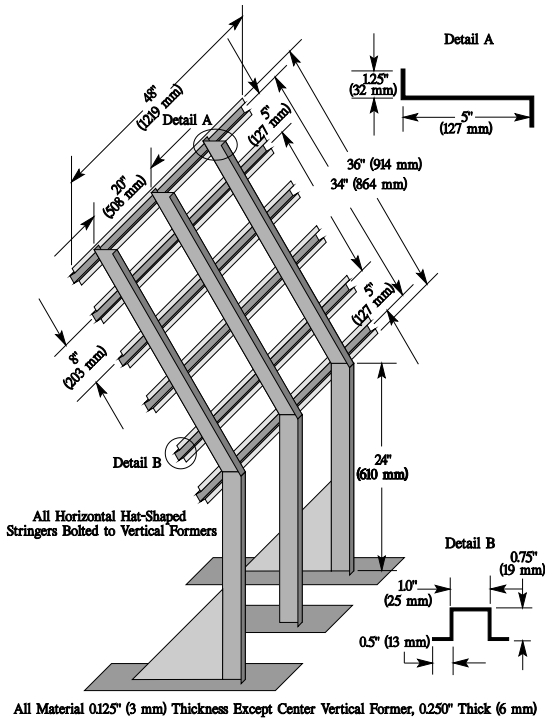

Figure 3. Insulation Burnthrough Test Sample Holder

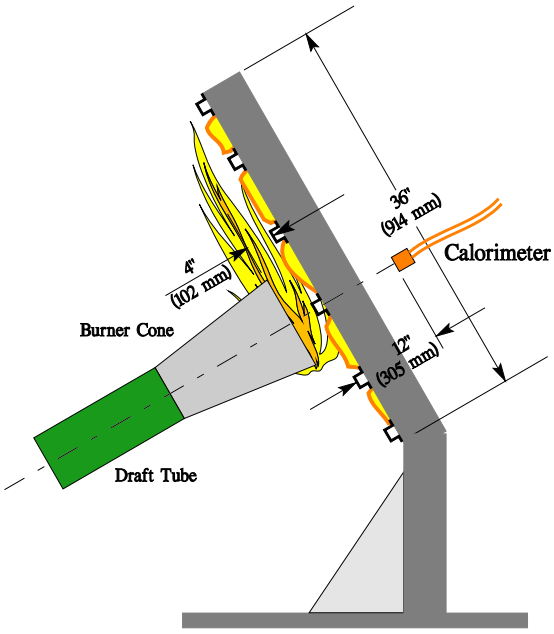

Figure 4. Finalized Insulation Burnthrough Test Apparatus

To evaluate and improve the reproducibility of the finalized test apparatus worldwide, a number of round-robin test series were conducted. During a typical round robin, several different types of insulation blanket test samples were identically prepared, shipped to participating laboratories, and tested. Test results were tabulated, compared, and analyzed to determine the degree of fluctuation or scatter of data from the laboratories. The standard deviation of test results from the four round-robin series showed that the data scatter had been reduced during each test series, indicating that the test was reproducible.

In September 2003, the FAA implemented a new regulation for the flammability of thermal acoustic insulation. The new regulation consisted of two new flammability test standards: one to measure the ability to prevent an in-flight fire and the other to resist postcrash fire flame penetration or burnthrough [6]. The new burnthrough requirement affected all primary thermal acoustic insulation in the lower half of the fuselage and specified resistance to flame penetration for 4 minutes. The burnthrough test standard is required in Title 14 Code of Federal Regulations Part 25.856(b) Appendix F Part VII (herein referred to as Appendix F Part VII).

1.3 EARLY TOXICITY TESTS OF PAN MATERIAL DURING FULL-SCALE TESTS.

Although full-scale tests in the late 1990s confirmed the enhanced burnthrough protection from a variety of materials, there were concerns over the potential toxicity of the PAN material during thermal decomposition because acrylonitriles generate hydrogen cyanide (HCN) when exposed to fire. Therefore, when the PAN material was tested in the full-scale test apparatus, HCN, CO, hydrogen fluoride (HF), and CO_2 were measured at two locations within the cabin, one close to the burnthrough area and another near the forward exit of the test fuselage, both at a height of 5′6″. Although the concentrations of HCN, HF, and CO were not trivial, it was determined that their levels would not cause incapacitation based on the 5-minute test exposures. From an analysis of past accidents (figure 5) [7 and 8], 5 minutes is a practical maximum time required to evacuate. Similar concerns were also raised over the potential toxicity of decomposition products generated inside an all-composite fuselage during exposure to a large external fuel fire. At least one commercial airplane manufacturer is developing an all-composite commercial transport fuselage.

Despite these concerns, it was apparent that a robust, burnthrough-resistant insulation system would prolong survivability much longer than a traditional, non-burnthrough-resistant system. However, the buildup of any toxic gases resulting from the decomposition of the barrier material was still of interest. For this reason, an additional laboratory test was developed to evaluate the decomposition products that could be generated inside an intact fuselage during a postcrash fuel fire.

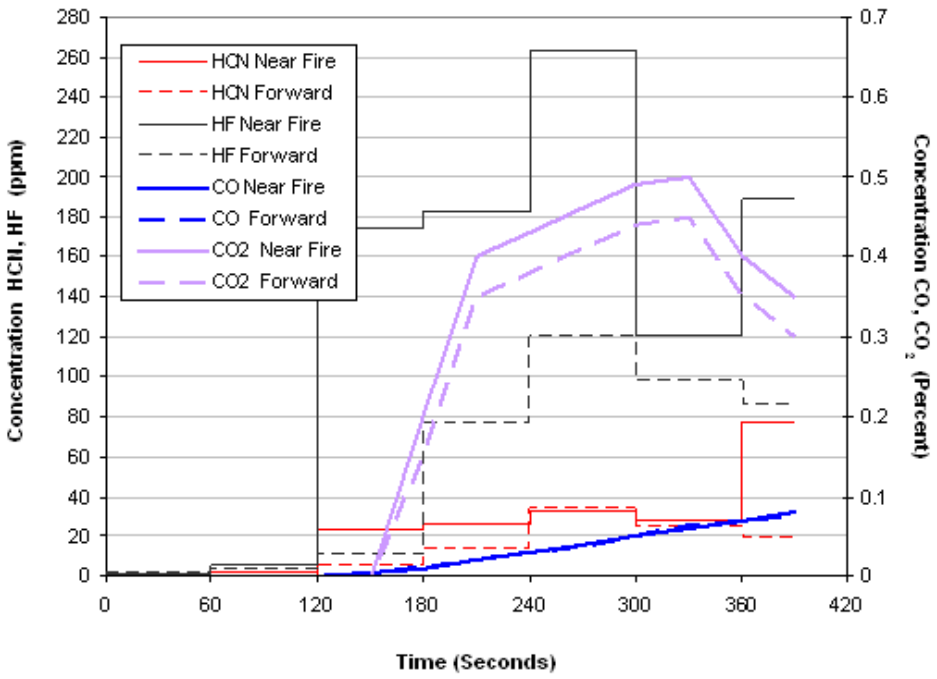

Figure 5. Gases Measured During Initial Full-Scale Test With PAN Insulation and Polyvinylfluoride Bagging Film With Polyester Reinforcement

2. EXPERIMENTAL TESTS.

2.1 DEVELOPMENT OF A LABORATORY-SCALE TEST APPARATUS FOR EVALUATING DECOMPOSITION PRODUCTS OF BURNTHROUGH-RESISTANT INSULATION.

To evaluate the decomposition products that could be generated inside an intact fuselage during a postcrash fuel fire, a test was devised that incorporated the burner apparatus used in the insulation burnthrough test. The burner equipment was configured in accordance with Appendix F Part VII, which requires a 1900°F flame and a heat flux of 16 Btu/ft^{2}sec. To capture all combustion products given off during exposure of a representative test sample to the fire, an enclosure was needed. The use of a large, 4- by 4- by 4-foot steel collection box was the most practical method. Due to its relatively large size, the top corner of the box was flattened to allow for clearance under the test area fume hood. A large 40- by 40-inch opening was used on the exposed face of the box to accommodate a test sample, and the face was positioned 4 inches from the burner cone, as would be the case in a test for certification. The steel collection box simulated an intact fuselage and served as an enclosure to collect gas emissions during fire exposure (figure 6). The exposed area/volume ratio was greater than what might be expected in an actual airplane to concentrate the gas levels and to better facilitate gas analysis.

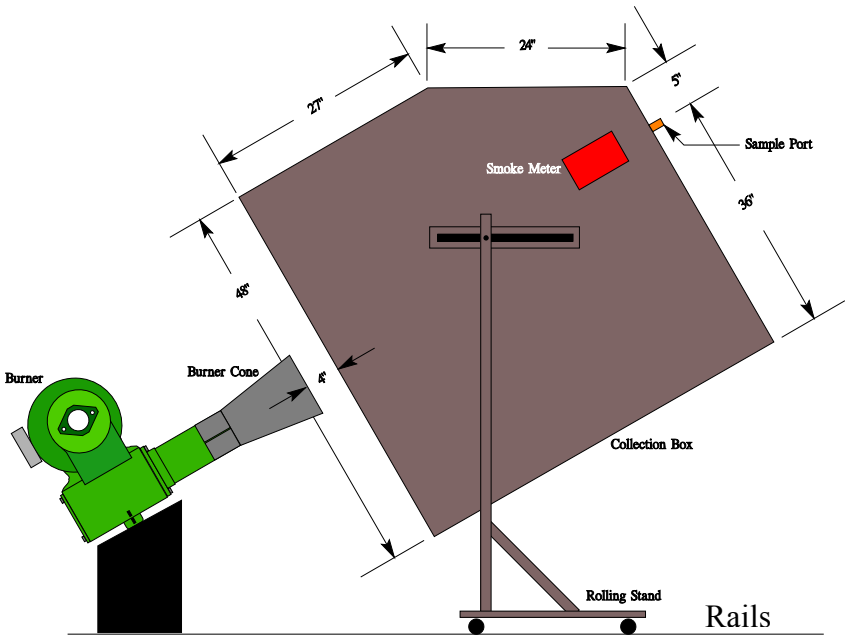

Figure 6. Test Apparatus for Evaluating the Toxicity of Insulation Materials

The insulation sample was mounted to the enclosure in a manner that prevented the intrusion of combustion products from the test burner flame. To accomplish this, the face of the steel box enclosure was recessed around the periphery of the opening, which allowed for a 40- by 40-inch test sample to be flush-mounted. A steel flange/gasket was mounted on top of the insulation sample and bolted into place around the perimeter using stud-mounted, 1/4-inch bolts (figure 7) to seal the sample edges.

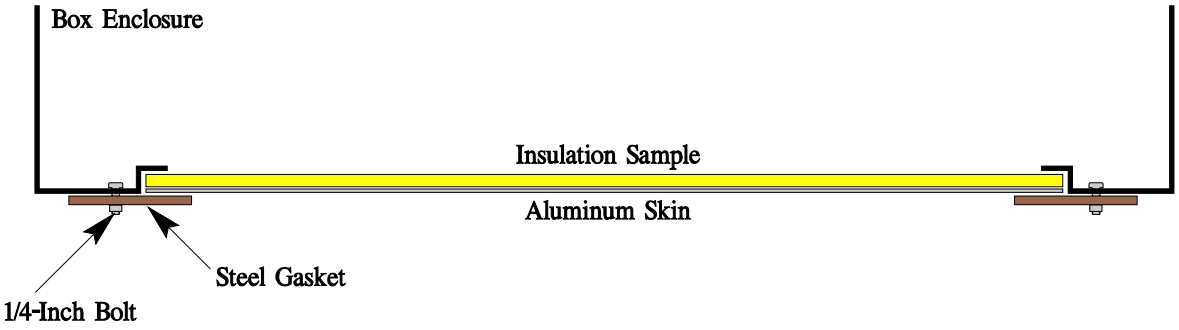

Figure 7. Box Enclosure Mounting System

During a typical test, the insulation sample and aluminum skin is mounted onto the box enclosure, and all bolts are securely tightened. The entire box enclosure is removed from the immediate burner area. The burner is then lit and warmed up for 2 minutes to ensure steady-state conditions. Following the warm-up period, the entire box is quickly rolled into position in front of the burner and subjected to the flame for 5 minutes. A rail-and-stop system ensures the correct position of the box. An in-box thermocouple can detect early burnthrough, and the test can be terminated to prevent damage to the gas-sampling equipment. All gas-sampling lines are

flexible and are supported from above so they do not interfere with the quick movement of the rolling box both into and away from the fire.

Under this test configuration, the thermal decomposition products in the enclosure were continuously monitored 5 inches below the top of the enclosure. A specialized extractive Fourier Transform Infrared (FTIR)/total hydrocarbon (THC) process analysis system was used for the analysis of the toxic gases CO, CO_2, carbonyl chloride ($COCl_2$), carbonyl fluoride (COF_2), acrolein (CH_2CHCHO), HCN, nitrogen oxide (NO), nitrous oxide (N_2O), nitrogen dioxide (NO_2), ammonia (NH_3), sulfur dioxide (SO_2), carbonyl sulfide (COS), benzene (C_6H_6), aniline ($C_6H_5NH_2$), phenol (C_6H_5OH), HF, hydrogen chloride (HCl), and hydrogen bromide (HBr), as well as water (H_2O) and the hydrocarbons methane (CH_4), acetylene (C_2H_2), ethylene (C_2H_4), ethane (C_2H_6), propane (C_3H_8), and THC as propane. This analysis system was designed to minimize errors found in conventional FTIR systems used for combustion gas analysis [9]. The selected gases include the primary decomposition products of epoxy-reinforced carbon and PAN materials identified in previous studies [10 and 11].

Additional continuous analyzers measured the concentration of CO, CO_2, and O_2 in the sample stream. The sampling line leading to the THC and FTIR analyzers was heated to minimize condensation of the sample gases. All gas histories were corrected for transit delays from the sampling point to the analyzers.

Measurement of the THC profiles enables the assessment of the flammability of the gases generated from the insulation systems. THC measurements were included to determine what levels of explosive thermal decomposition products of the insulation systems would build up in the fuselage. The lower explosive limit (LEL) is the smallest amount of a gas that supports a self-propagating flame.

2.2 METHODS OF ANALYSIS.

2.2.1 Gas Analyzers.

THCs were monitored for the laboratory-scale tests using a Rosemont Model NGA2000 total hydrocarbon analyzer, type MLT-2R. This is a nondispersive infrared analyzer (NDIR). A Beckman Model 402 total hydrocarbon flame-ionization detector (FID)-based analyzer was used for the full-scale tests. A Rosemount OM-11ea polarographic analyzer was used to monitor oxygen. CO and CO_2 were monitored using Rosemount 880a CO and CO_2 NDIR analyzers. These analyzers use Luft-type detectors filled with CO and CO_2, respectively. Additional optical filters enhanced selectivity. The Luft detector operates on the principle of common absorbance with the detector gas. The gas cells have a path length of approximately 3 mm for the CO and CO_2 analyzers. This short path length allows quantification at the strongest CO and CO_2 absorbance bands, resulting in greater accuracy for complex combustion gas mixtures. The CO and CO_2 analyzers were used to provide confidence in the FTIR method development for high concentrations of these gases.

2.2.2 The FTIR Analyzer.

2.2.2.1 The FTIR Spectometer and Data Acquisition.

A Midac Model I2001F FTIR Spectrometer[1] with a 4-meter cell was used for all tests. The optical path of this cell is over 1000 times longer than the 3-mm CO and CO_2 NDIR analyzer cells, contributing to a much greater sensitivity and lower limit of detection. The sample cell is nickel, the mirrors are coated with gold, and the windows are zinc selenide (ZnSe). The cell volume is approximately 160 ml. The interferometer, beam splitter, and windows are constructed of ZnSe with a germanium coating for moisture protection. The detector is a liquid nitrogen-cooled Mercury Cadmium Telluride (MCT) detector, providing more than an order of magnitude additional sensitivity. All interface optics are gold-coated for high light throughput and corrosion resistance. The sample cell has a horizontal orientation to minimize buildup of soot on the cell mirrors.

All tests were conducted in an extractive mode at 0.5 cm^{-1} resolution, with an average of 16 scans every 9 seconds for the laboratory-scale tests, and 8 scans every 5 seconds for the full-scale tests. All calibration spectra were obtained at 0.5 cm^{-1} and were prepared for the FAA by the FTIR manufacturer at 170°C for all gases except H_2O, CH_2CHCHO, $C_6H_5NH_2$, C_6H_5OH, C_6H_6, NH_3, N_2O, C_3H_8, and COS. The 170°C H_2O calibration spectra were prepared in-house at the FAA William J. Hughes Technical Center using a syringe calibration system, (which was built into the sampling system). The flow rate through the cell was 1-2 liters/min [9]. The NH_3, C_6H_6, and N_2O spectra were obtained at 25°C, and the COS and C_3H_8 spectra were obtained at 121°C from the Midac 0.5- cm^{-1} Spectral Library. Aniline, acrolein, and phenol spectra were obtained at 100°C and a 0.5-cm^{-1} resolution from the Environmental Protection Agency Standards Library.

Cell pressure and temperature are monitored and recorded with each spectrum. The FTIR software performs Beer's Law calculations for each analyte in each test spectra to correct the analyte concentration for any pressure and temperature variations from the calibration spectra.

Data were collected, analyzed, and plotted using the following commercial software: Midac Autoquant Pro™ software, Operant LLC: Essential FTIR®, and Microsoft® Excel®. Spectral bands for 24 gases were selected to have minimal common absorbance. Another requirement for spectral band selection is that it must have a low absorbance, so that the calibration is linear over a wide concentration range. Broad nonoverlapping bands were selected when possible.

2.2.2.2 The FTIR Method.

The FTIR method identifies the 24 gases to be analyzed and the spectral regions for performing a piecewise linear classical least squares (CLS) analysis within the 650- to 4500-cm^{-1} spectral range. Figure 8 illustrates the calibration spectra and spectral regions used in this FTIR method. Only the selected regions highlighted in figures 8 through 18 were used in the method. For each

[1] Certain commercial equipment, instruments, or materials are identified in this report to specify the experimental procedure. Such identification does not imply that the material or equipment is the best available for the purpose or endorsement by the FAA.

test spectrum and analyte gas, the method subtracts spectral regions that are common with the selected spectral regions of other gases in the method. A few very wide regions were selected for the water spectra, ensuring that water interferences would be subtracted from sample spectra. Spectral regions were selected for each gas to minimize interferences with other gases.

Many regions were used for CO and CO_2 for the various calibration concentrations to enable quantification in low-absorbing regions that exhibited the best linearity. Absorbencies less than 0.1 generally provide acceptable linearity. Calibration spectra were selected for each gas to define each piecewise-linear calibration curve. The minimum number of spectra needed to obtain accurate calibration curves was selected.

Figure 10 shows that the slope of the selected CO_2 region (the shoulder of the highly absorbing, clipped, CO_2 peak for the highest concentration CO_2 spectrum) is large, resulting in a decreased accuracy at the higher CO_2 concentrations.

All calibration spectra and test spectra were obtained at a unit gain. A triangular apodization, a Mertz phase correction, and a resolution of 0.5 cm^{-1} were used for all calibration and test spectra. The method creates a spreadsheet with the time profiles of the concentration and error (residuals) data for the 24 gases. Gas concentrations were reported as zero for each gas and spectra if the residuals for the spectral region were 50% or greater than the calculated concentration.

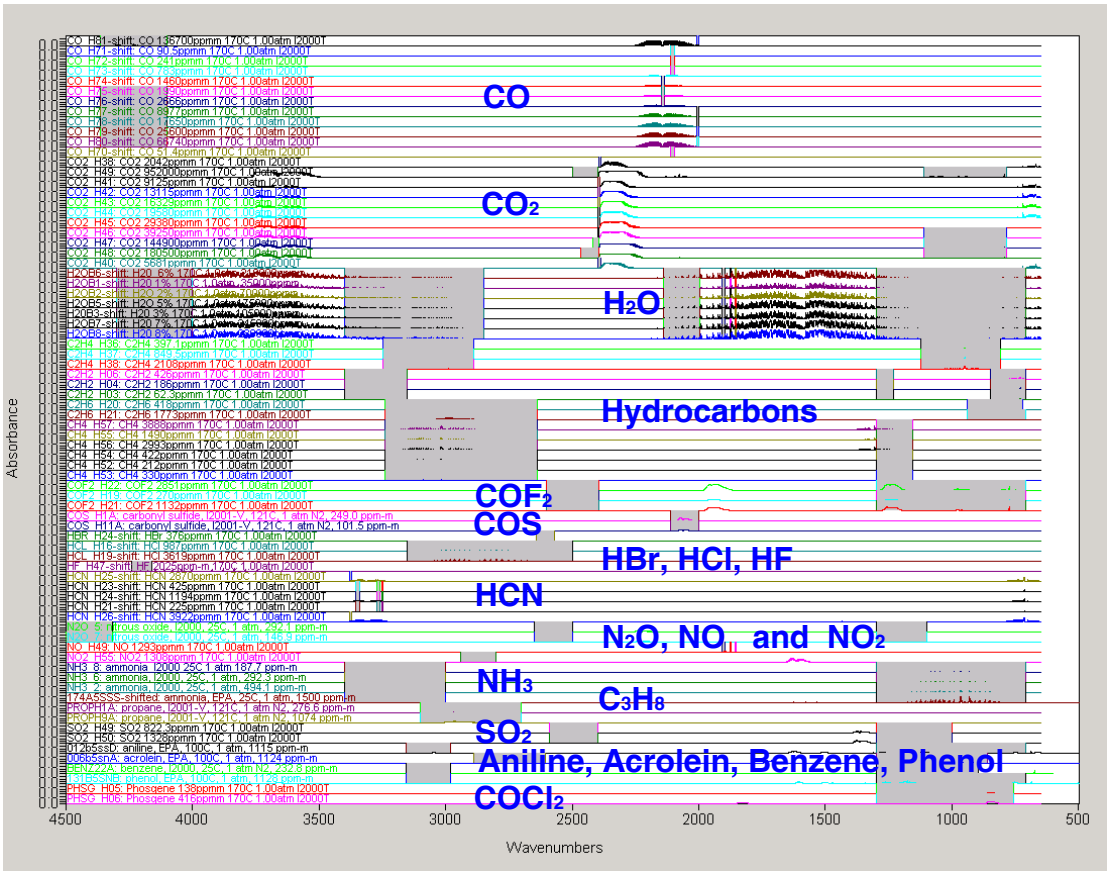

Figure 8. Calibration Spectra and Selected Regions for FTIR Analysis

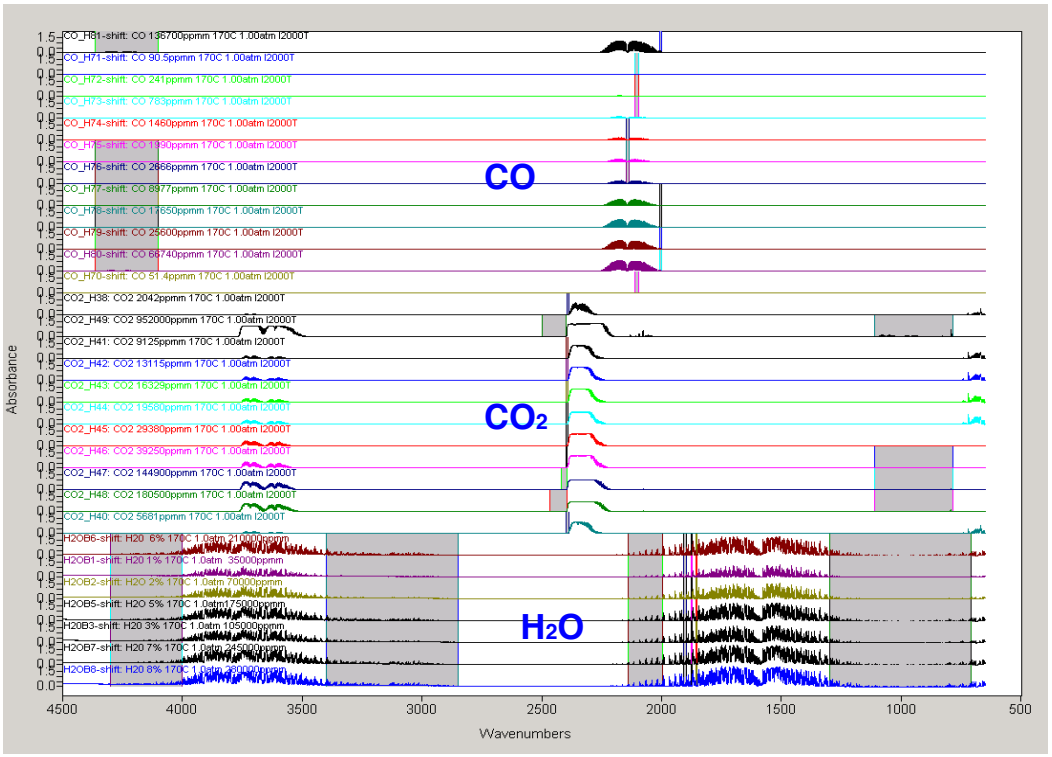

Figure 9. Calibration Spectra and Regions for CO, CO_2, and H_2O

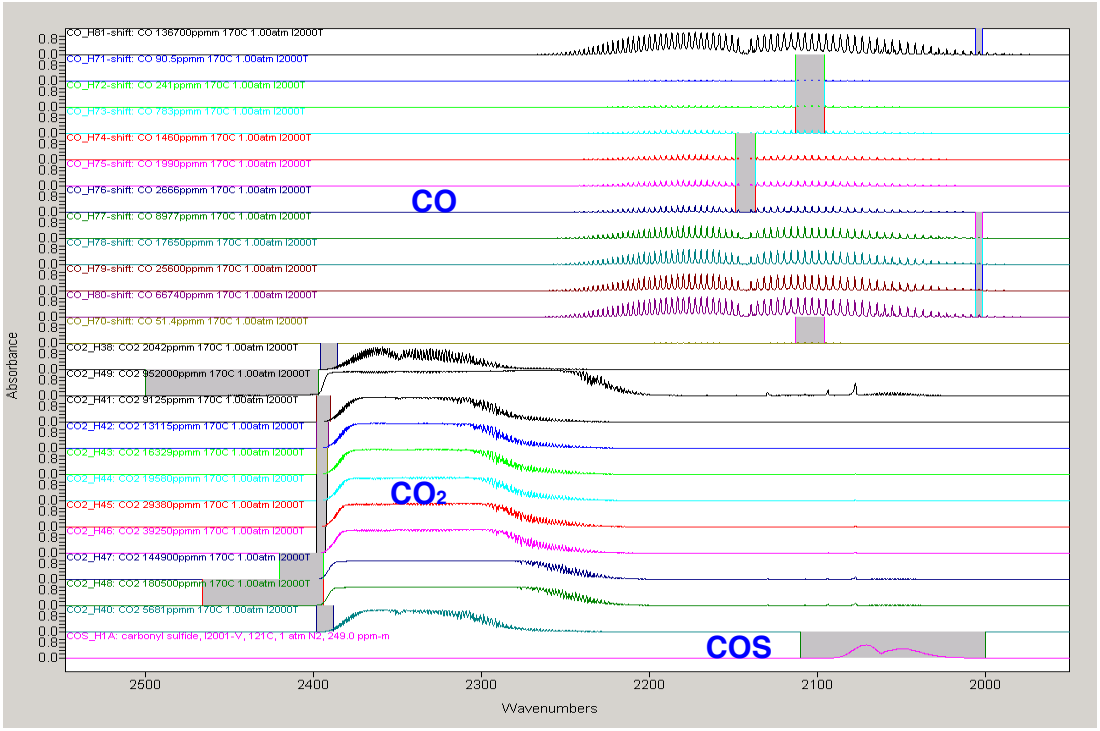

Figure 10. Expanded View of CO, CO_2, and COS Calibration Spectra and Regions

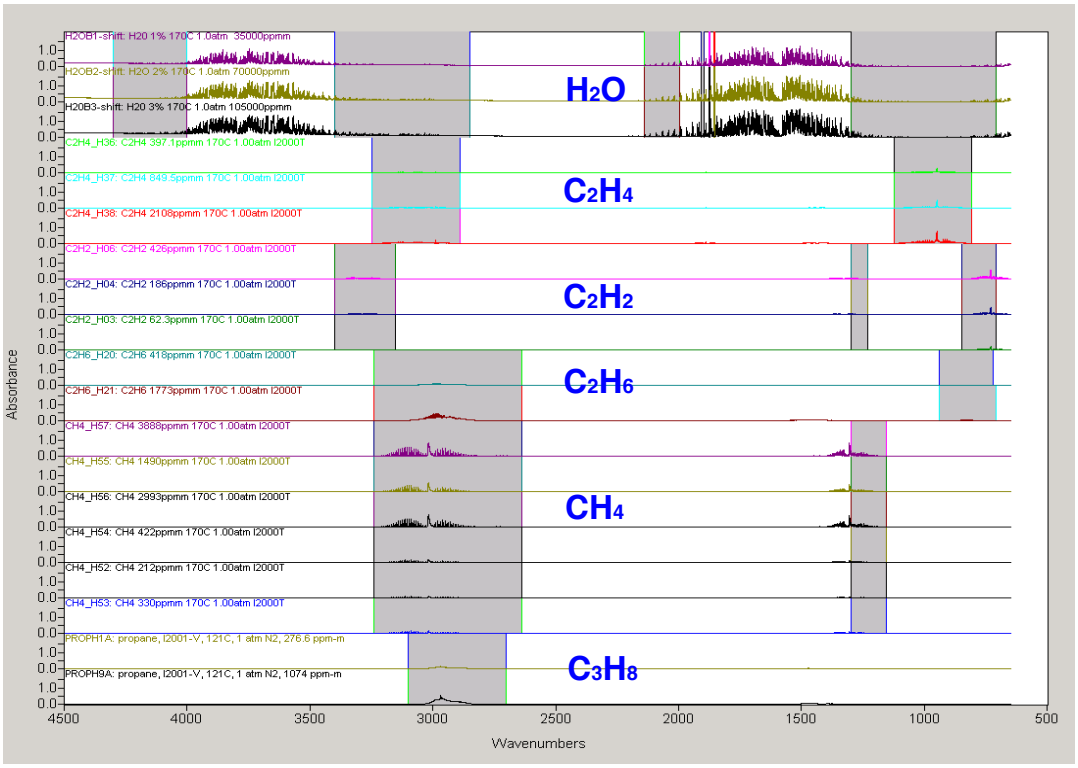

Figure 11. Calibration Spectra and Regions for H_2O, C_2H_4, C_2H_2, C_2H_6, CH_4, and C_3H_8

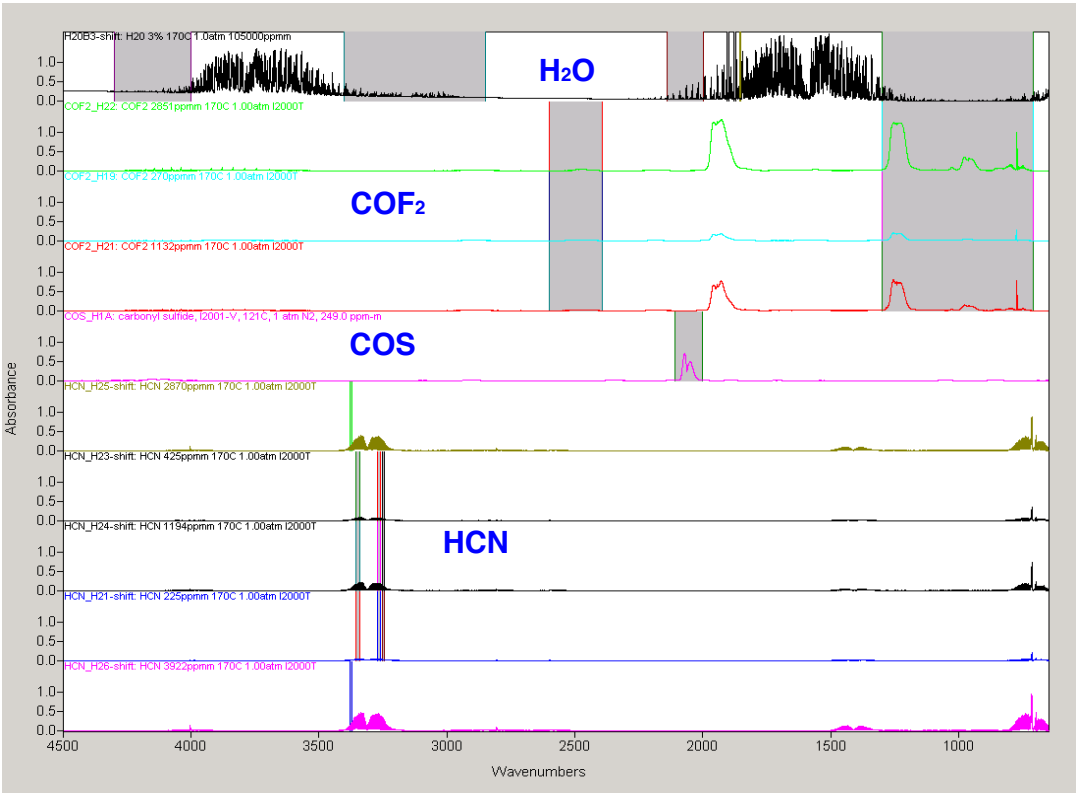

Figure 12. Calibration Spectra and Regions for H_2O, COF_2, COS, and HCN

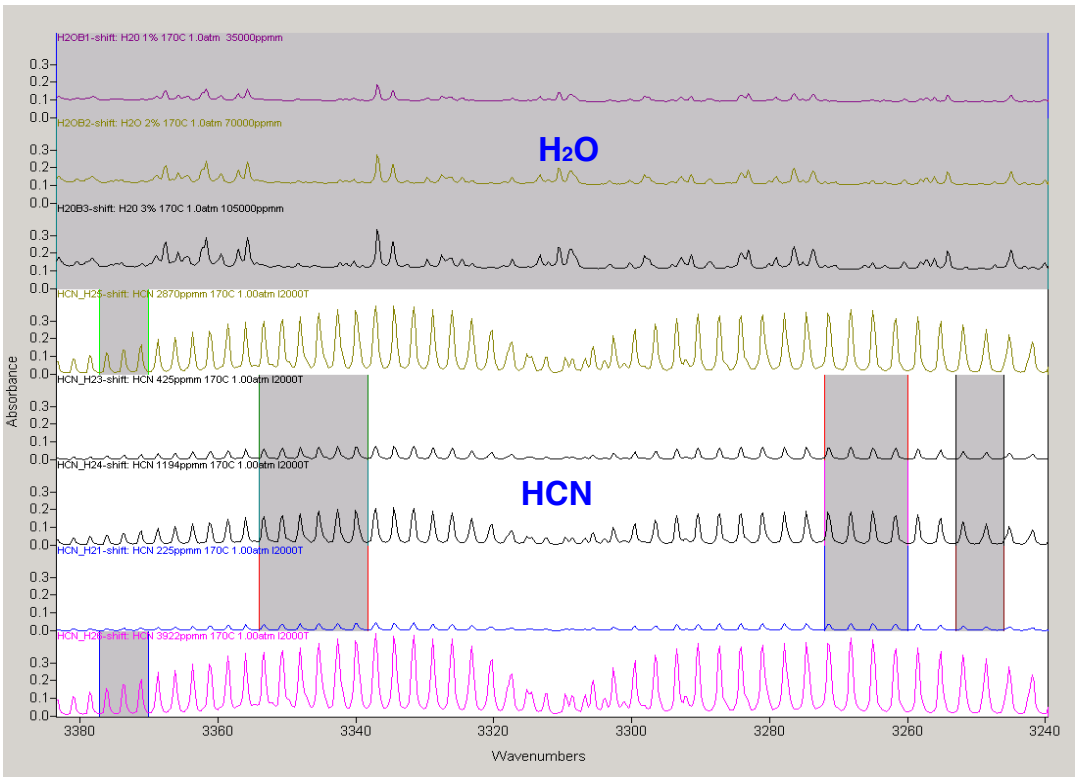

Figure 13. Expanded View of H_2O and HCN Calibration Spectra and Regions

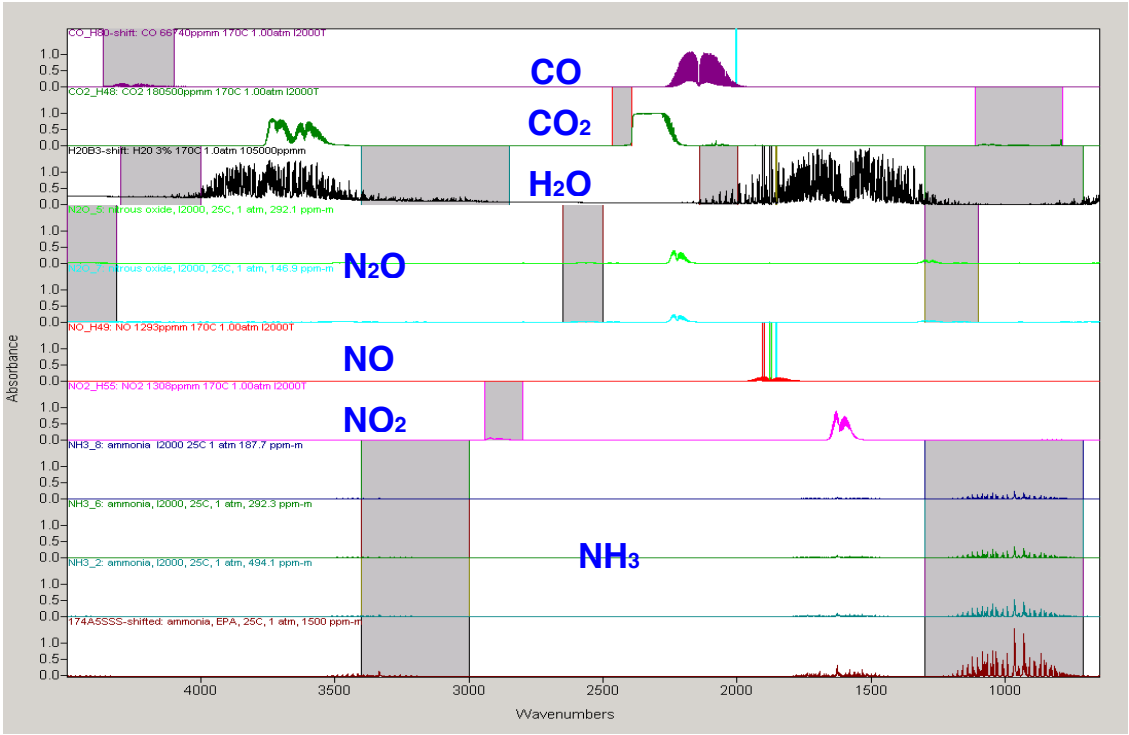

Figure 14. Calibration Spectra and Regions for N_2O, NO, NO_2, and NH_3

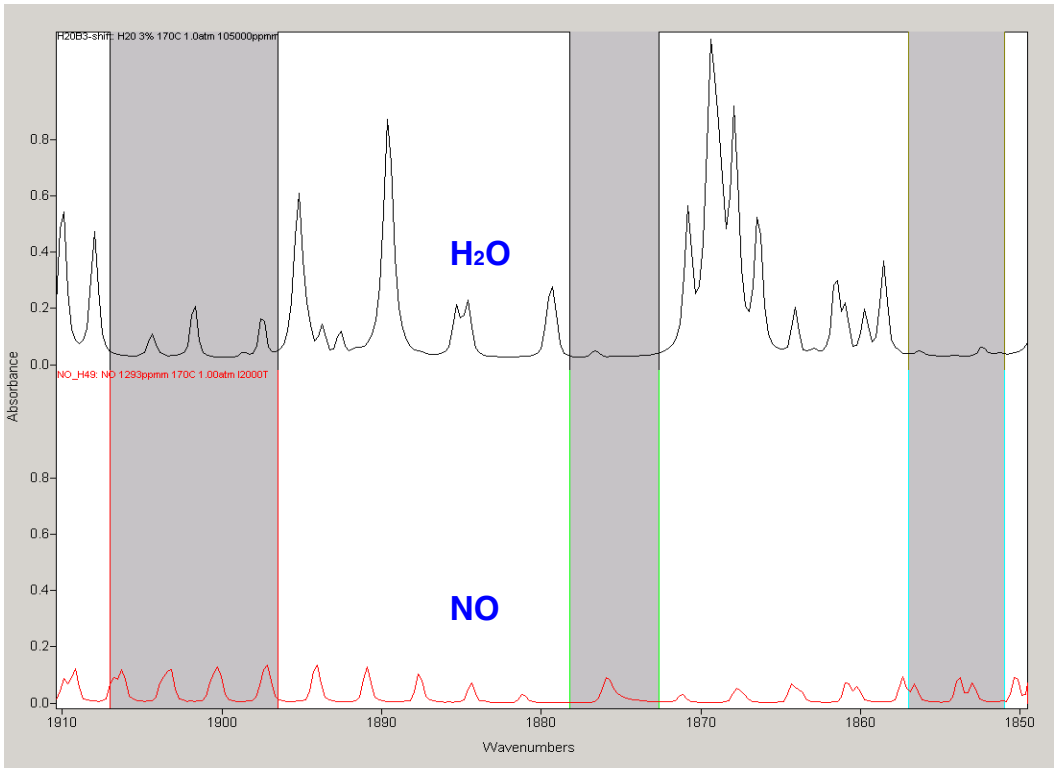

Figure 15. Expanded View of H_2O and NO Calibration Spectra and Regions

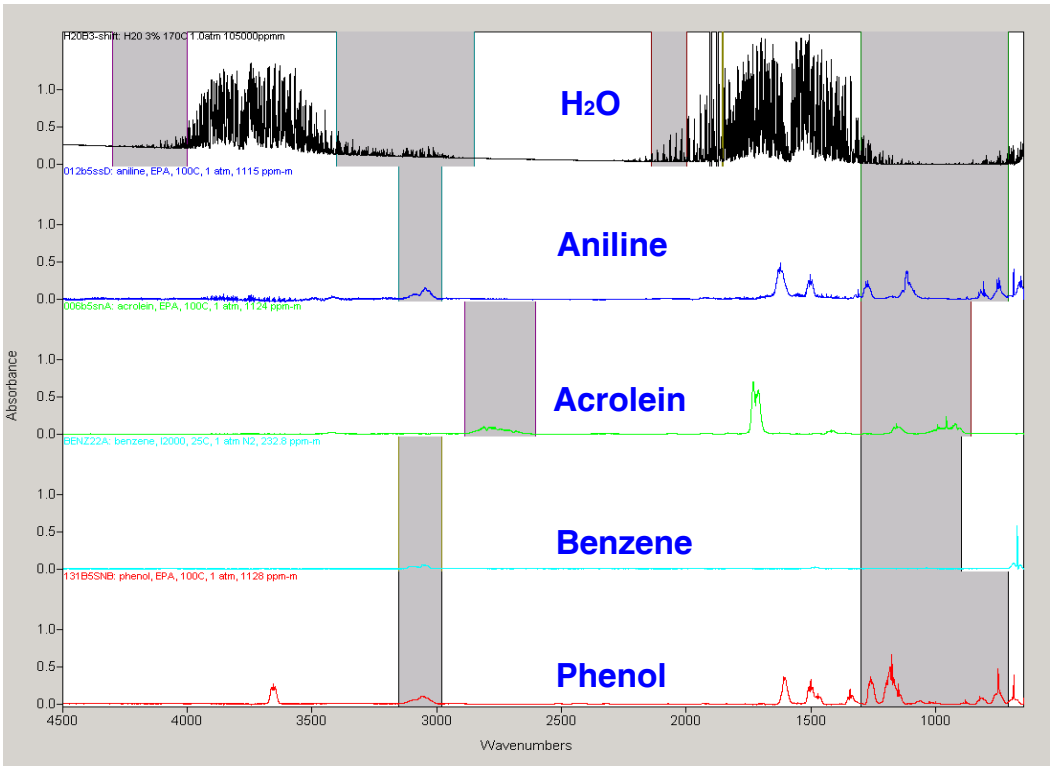

Figure 16. Calibration Spectra and Regions for H_2O, Aniline, Acrolein, Benzene, and Phenol

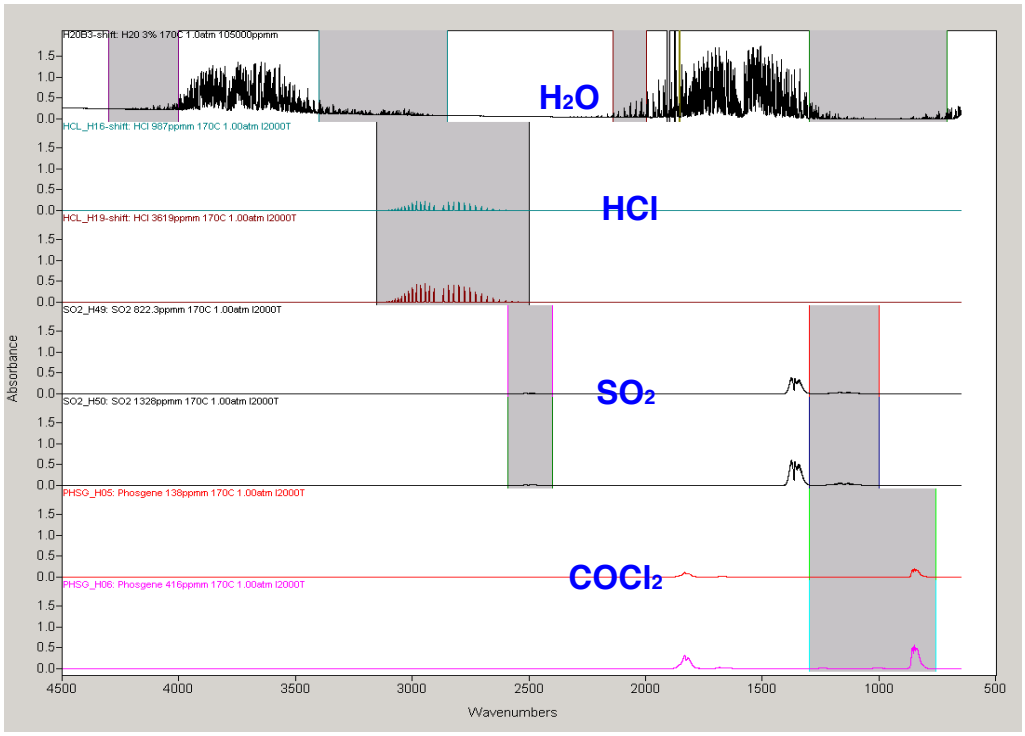

Figure 17. Calibration Spectra and Regions for H_2O, HCl, SO_2, and $COCl_2$

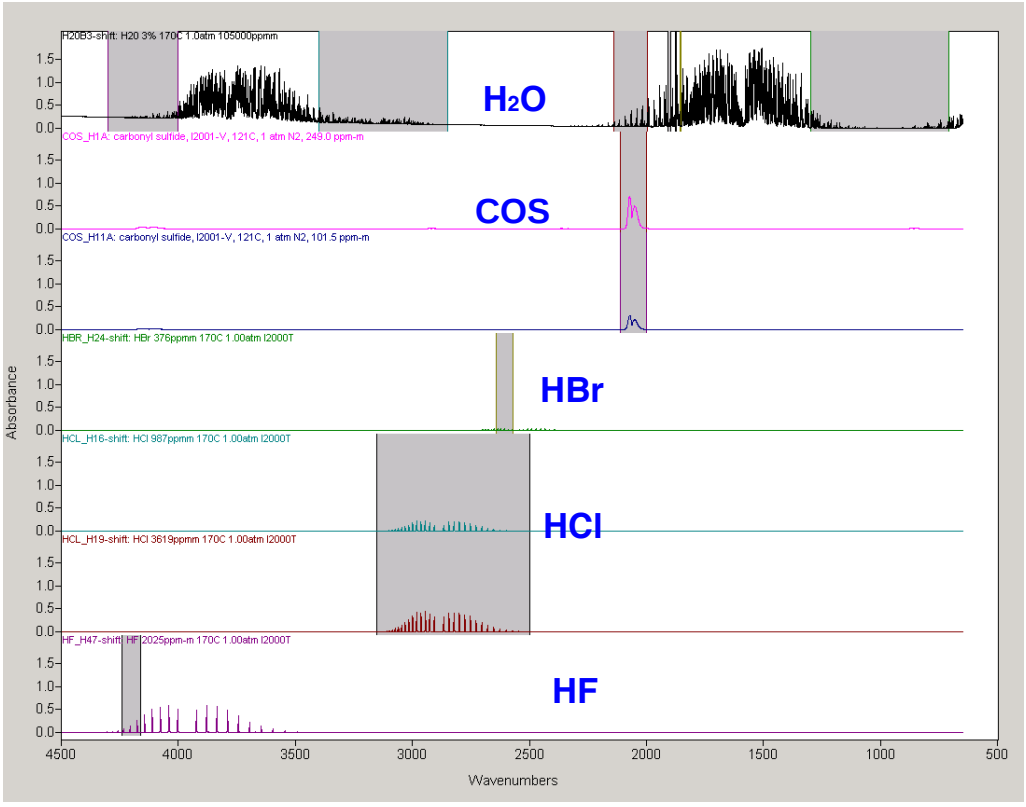

Figure 18. Calibration Spectra and Regions for H_2O, COS, HBr, HCl, and HF

2.2.3 Gas-Sampling Methodology for the FTIR and THC Analyzers During Laboratory-Scale Tests.

Figure 19 is a schematic of the FTIR and THC sampling system used for laboratory-scale tests. The entire path leading to the analyzers is heated to minimize condensation of analytes and absorption of water-soluble gases onto moist surfaces of the sampling system. The flexible, heated, Teflon®-lined, 20-ft (6.1-m) by 1/4-in.-diameter (0.64-cm) sample line runs from the test chamber to the sample conditioning filters that are housed in an oven. The heated sample line from the test chamber to the oven is composed of two 10-ft sections, each separately thermostated to 120°C. The entire sample path to the NDIR THC analyzer is thermostated to 120°C, the maximum design temperature of that analyzer. The line leading from the oven to the FTIR sample cell and the FTIR cell are thermostated to 170°C, the temperature at which the FTIR calibration standard library was developed. The separate thermostated circuits are also indicated in figure 19.

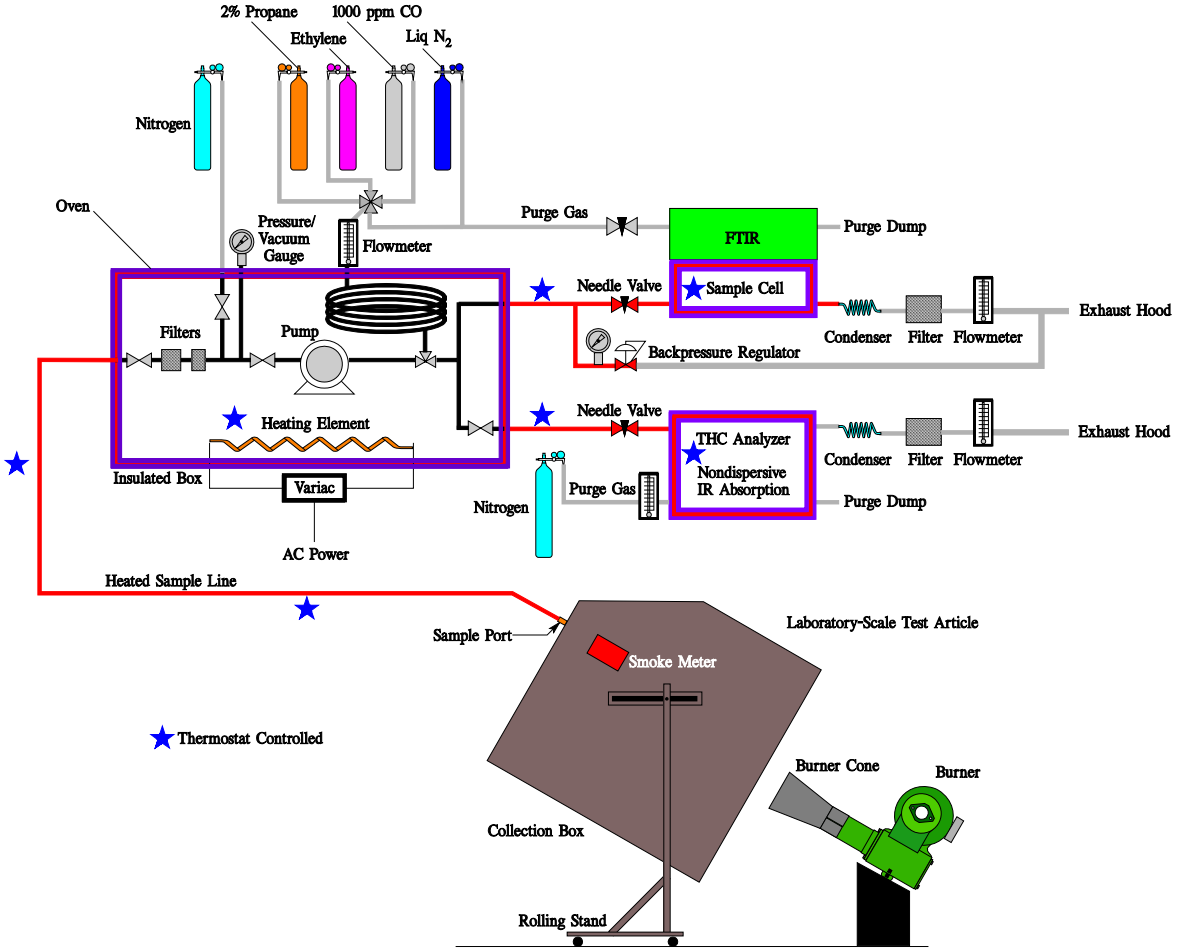

Figure 19. The FTIR and THC Sampling System

A three-way valve, downstream of the sample pump, can select either a calibration gas or a combustion gas input to the analyzers. The calibration gas flows from the gas cylinder through a heated, 13.1-ft (4-m) by 1/4-in.-diameter (0.64-cm) stainless steel coil. This coil enabled

preheating the calibration gas for analysis. The sample stream splits before it exits the oven to service the two analyzers. The tubing leading to the FTIR sample cell (and a point a few inches downstream of that cell) is maintained at 170°C, along with the sample cell. This preheated the sample stream to the FTIR calibration temperature of 170°C.

The gas sample is continuously drawn through the heated sample line, at a flow rate of approximately 11 liters per minute, and passes through a series of filters into the bellows pump. A backpressure regulator provides a constant flow rate through the 160-ml, 4-m optical path length sample FTIR cell and NDIR THC cell. This ensures a constant system response time throughout a fire test and from test to test, as particulates build up in the filters and the filter backpressure increases. It also ensures a constant cell pressure, enabling accurate quantification. The backpressure regulator output bypasses the analyzer, and a needle valve at the inlet to each analyzer is set to provide a flow rate of 2.0 liters/min. A cooling coil of 1/4-in.-diameter (0.064-cm) copper tubing and a high-capacity filter protect the flow meter, which is downstream of the sample cells.

A pressure/vacuum gauge located between the pump and the filter monitors the filter for excessive vacuum, indicating a restriction in flow and the need to replace the filter. The gauge can also be used to check for air leaks after filter replacement by pressurizing the filters with nitrogen, shutting adjacent valves, and checking if the pressure drops with time. This sampling system is not appropriate for quantitative sampling of HF, as the large particulate filter contains glass wool, which reacts with HF. Further details of the FTIR system can be found in reference 9.

3. LABORATORY-SCALE TEST RESULTS AND DISCUSSION.

3.1 INITIAL LABORATORY-SCALE BASELINE TEST RESULTS (NO INSULATION SYSTEM—OPEN BOX).

To determine the type and amount of combustion products yielded by the burner flame, an initial test was conducted without an insulation sample on the face of the steel cube box. A 1-ft-long, 1/4-inch-diameter stainless steel tube extension was attached to the sample probe, and a thermocouple was teed to the connection with the heated sampling line. The sampling was terminated after less than 1 minute when the temperature exceeded 150°C to prevent the thermal decomposition of the Teflon sample line.

Figures 20 and 21 illustrate the gas concentration histories obtained for the baseline (no sample) open-box test. The high CO_2/CO ratio of about 300/1 and low hydrocarbon concentrations observed in this test (at 30 seconds) is characteristic of well-ventilated flaming combustion. Concentrations of H_2O and CO_2 exceeded 7%, and CO reached 248 ppm at 45 seconds into the test. HF, NO, SO_2, HCN, NH_3, $C_6H_5NH_2$, C_2H_6, CH_4, and C_3H_8 were observed. The HF may have condensed on the surface of the box during a previous fire test. Consideration must be given to the possible contribution of the fuel decomposition products to the gas yields when interpreting the subsequent box test gas concentration profiles.

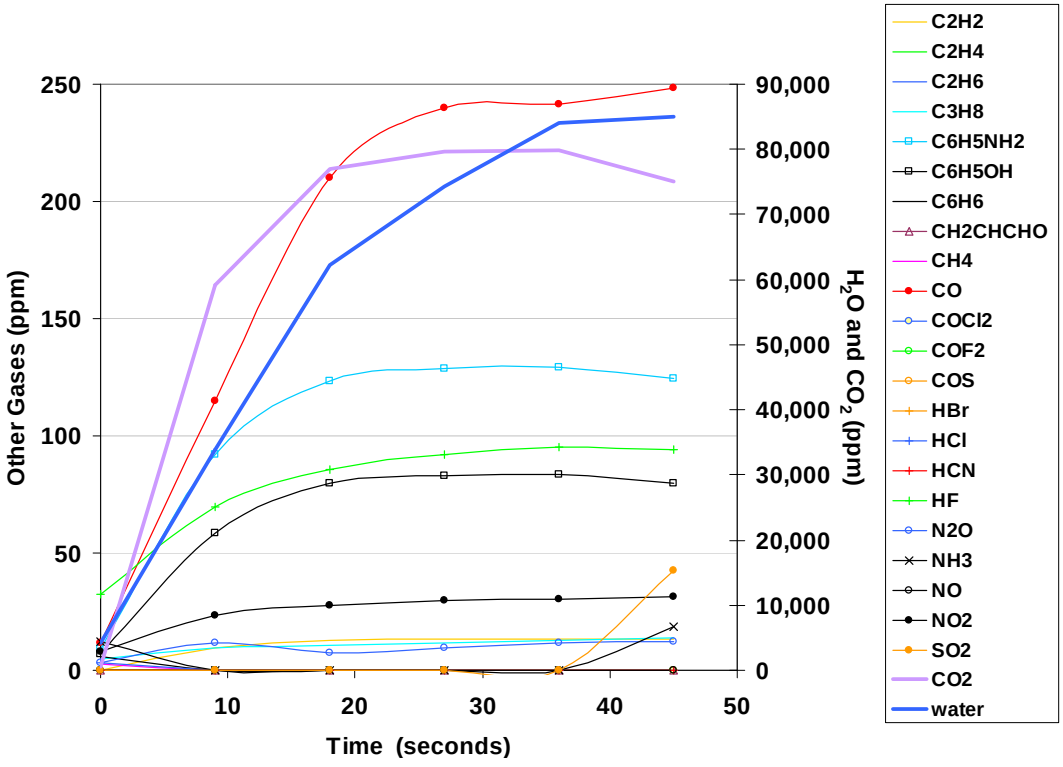

Figure 20. Concentration Histories for Baseline (no sample) Open-Box Test Obtained by FTIR Analysis

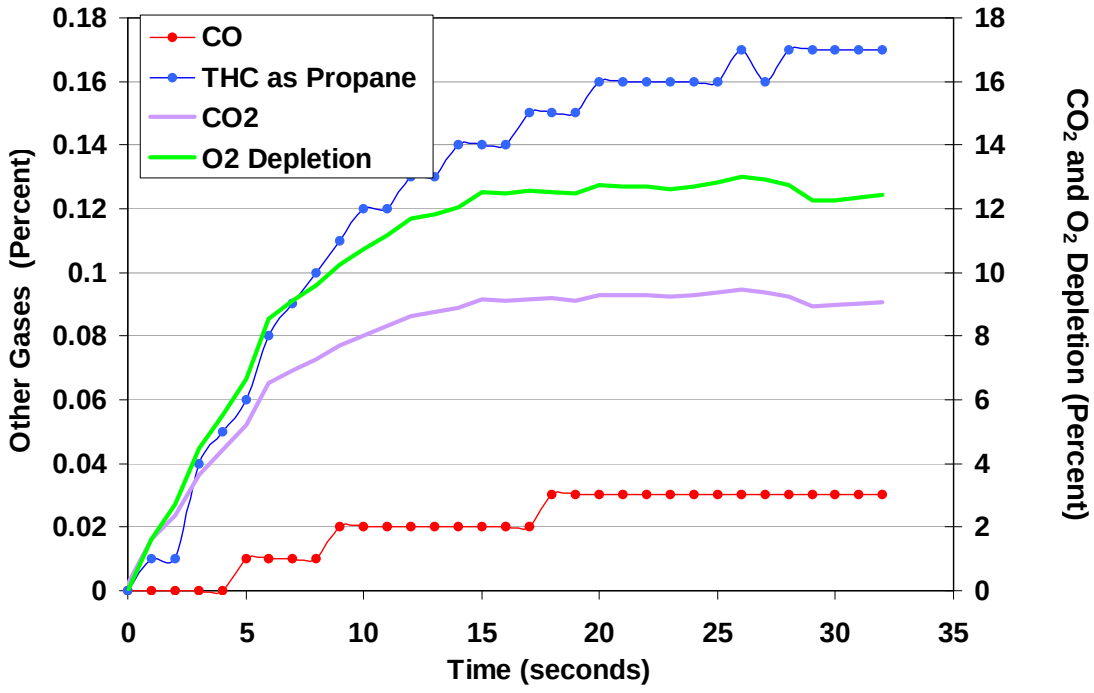

Figure 21. Yield Histories for Baseline (no sample) Open-Box Test Obtained by Gas Analyzers

3.2 FUSELAGE CONSTRUCTIONS EVALUATED.

The following material systems were tested and are illustrated in figure 22.

- Aluminum skin panel with a ceramic paper-like barrier sandwiched under a fiberglass insulation blanket. The barrier and insulation blanket were encased by a thin, metallized polyvinylfluoride (PVF) film.
- Aluminum skin panel with a heat-stabilized PAN fiber insulation blanket encased by a thin metallized PVF film.
- A prototype carbon/epoxy structural composite material with no insulation blanket.

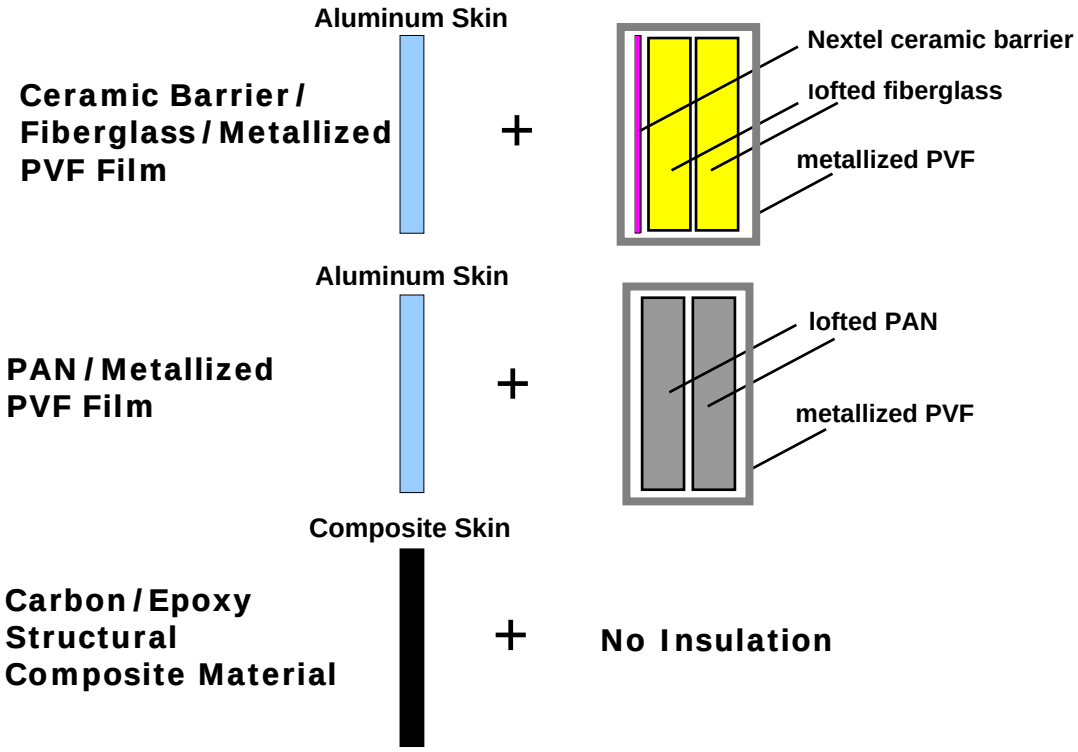

Figure 22. Material Systems Tested in the Laboratory-Scale Apparatus

The FTIR spectra obtained 5 minutes into the test for the three material systems are shown in figure 23.

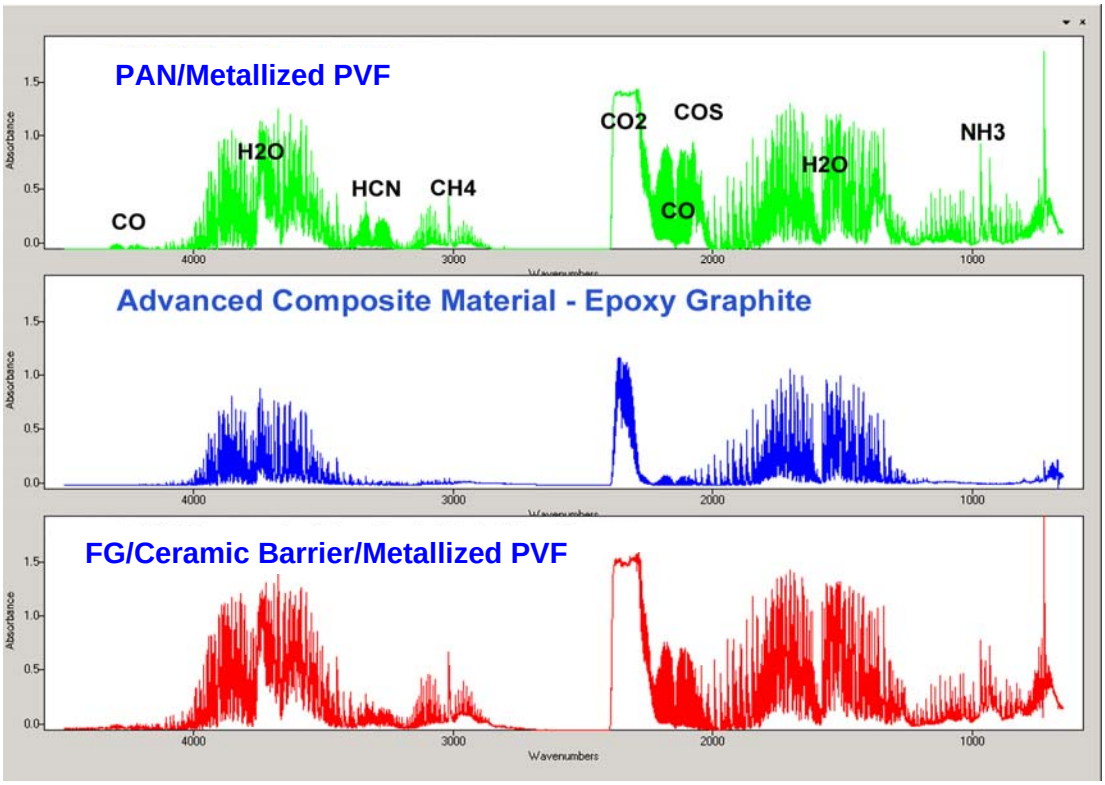

FG = Fiberglass

Figure 23. The FTIR Spectra of the Three Material Systems Obtained 5 Minutes Into the Test

3.3 LABORATORY-SCALE EVALUATION OF INSULATION MATERIALS MEETING THE NEW BURNTHROUGH STANDARD.

3.3.1 Fiberglass and Dot-Printed Ceramic Insulation System.

A thin, fire-resistant layer of ceramic fiber material known as Nextel™ was evaluated. Developed by the 3M Company, Nextel ceramic oxide fibers are continuous, polycrystalline metal oxide fibers suitable for producing textiles without the aid of other fiber or metal inserts. The polycrystalline fibers are typically transparent, nonporous, and have a diameter of 10-12 μm. The continuous nature and flexibility of the ceramic oxide fibers allows them to be processed into a variety of textile shapes and forms using conventional weaving and braiding techniques and equipment. In this particular arrangement, a nonwoven mat of dot-printed ceramic was tested to determine its effectiveness when used as an additional barrier to the existing fiberglass insulation.

The ceramic barrier and fiberglass insulation batts were encapsulated with the standard metallized PVF moisture barrier film. The ceramic barrier was installed on the outboard face of the insulation batts (within the film) to form a flame penetration barrier between the external flames and the interior of the test apparatus. The insulation batts and the ceramic barrier were clamped in place around the perimeter. This arrangement was very effective, preventing burnthrough for nearly 5 minutes. During a posttest inspection, it was observed that the majority

of the ceramic barrier had remained in place. However, in one area, it was also clear that the barrier had opened and allowed flames to penetrate.

Figure 24 illustrates the gas concentration histories obtained from the fiberglass/ceramic barrier insulation system test. Five minutes into the test, concentrations of 2,525 ppm CO, 15,308 ppm CO_2, 116 ppm HCN, 291 ppm NH_3, 153 ppm CH_2CHCHO, 59 ppm C_6H_6, 101 ppm $C_6H_5NH_2$, and 48 ppm C_6H_5OH were measured. The $\Delta CO_2/\Delta CO$ ratio was 6.0. At 5 minutes, the H_2O concentration reached 2.4%. The concentrations of hydrocarbons measured in the test box were far below the level to cause a flashover event. The LEL of CH_4, C_2H_6, and C_3H_8 were 5.0%, 3.0%, and 2.1%, respectively (1% = 10,000 ppm). The 5-minute concentration of CH_4 was 494 ppm. The 5-minute concentrations of C_2H_2, C_2H_4, and C_2H_6 were 130, 215, and 35 ppm, and C_3H_8 was 94 ppm. C_6H_6, C_6H_5OH, and $C_6H_5NH_2$ were 59, 48, and 101 ppm, respectively. A rough estimate of the percentage of LEL of the hydrocarbons as propane can be made by assuming that it is proportional to the number of carbon atoms. Table 1 provides the contribution of C1, C2, C3, and C6 hydrocarbons to the percentage of LEL as propane (as determined by FTIR analysis). Collectively, the combined effect of these gases was only about 5% of the propane LEL. The fibers used in the ceramic barrier are composed of aluminum oxide, silicone dioxide, and boron oxide. The moderate HCN and NH_3 levels may be due to binders in the ceramic paper and/or fiberglass insulation.

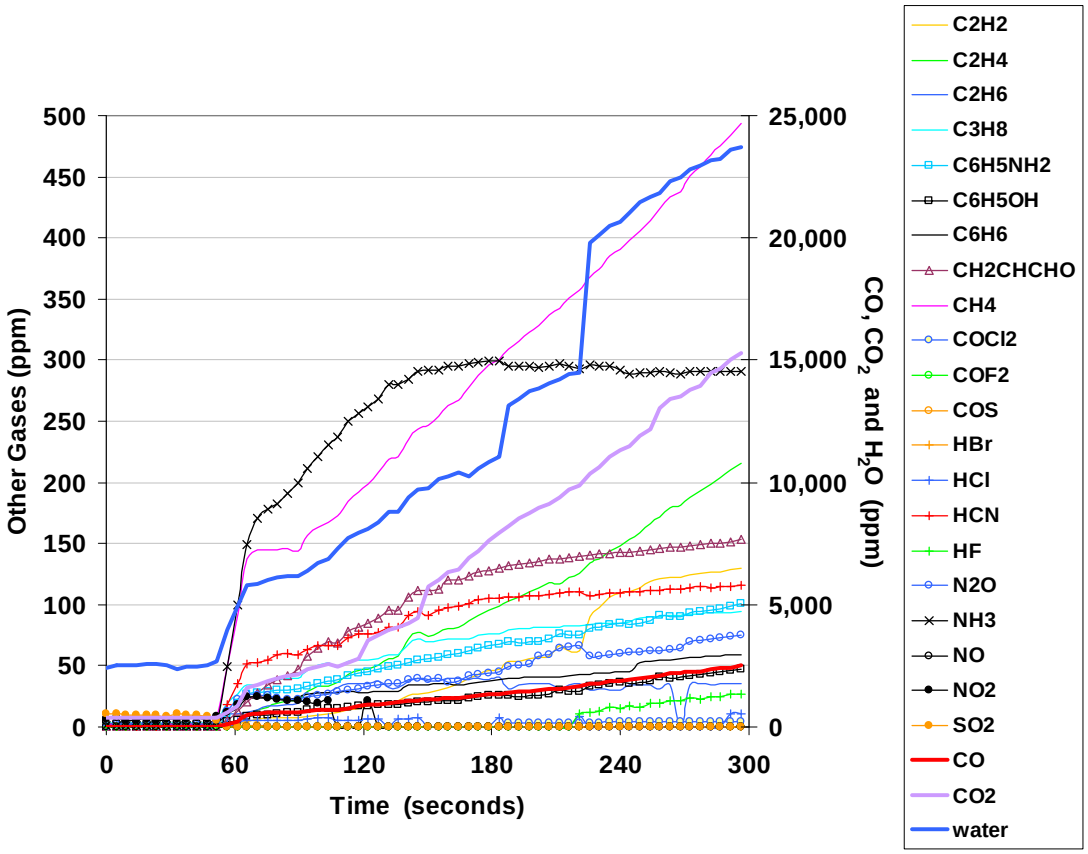

Figure 24. Concentration Histories of Ceramic Barrier Insulation System Box Test Obtained by FTIR Analysis

Table 1. Computation of the Percentage of the LEL as Propane at 5 Minutes for a Fiberglass/Ceramic Barrier Insulation System Test

Number of Carbons	Gases	Concentration as Propane (ppm)	Percentage of LEL as Propane
1	CH_4	494/3 = 165	(165/21,000)*100 = 0.78
2	C_2H_2, C_2H_4, C_2H_6	(130 + 215 + 35) *2/3 = 254	(254/21,000)*100 = 1.21
3	C_3H_8, CH_2CHCHO	94 + 153 = 247	(247/21,000)*100 = 1.18
6	C_6H_6, C_6H_5OH, $C_6H_5NH_2$	(59.3 + 47.5 + 101)* 6/3 = 207	(207/21,000)*100 = 1.98
1, 2, 3, and 6		165 + 254 + 247 + 415 = 1080	(1080/21,000)*100 = 5.14

3.3.2 The PAN Insulation System.

Another series of tests were conducted using an oxidized PAN fiber blanket material supplied by TexTech Industries of North Monmouth, Maine. The material was similar to the heat-stabilized PAN material supplied by the Orcon Corporation (Curlon®) that was initially burnthrough tested in the full-scale test apparatus. The TexTech blanket material contained 25% Nomex, 25% Preceramic (silica), 20% poly(phenylene oxide) sulfide, 20% PAN, and 10% Kevlar® (the PAN used in this blanket contained about 70% carbon, 20% nitrogen, and 10% oxygen). These PAN-like materials are unique because they could potentially be used as drop-in replacements for the current fiberglass insulation (i.e., they possess some qualities similar to fiberglass for the intended use in aircraft applications, such as noise attenuation). The PAN-like blanket material supplied by TexTech was extremely effective at resisting flame penetration for at least 5 minutes.

Early, large spikes in the concentrations of NH_3, HCN, CH_4, and H_2O can be observed at 106 seconds in figure 25. This is consistent with the high position of the sample probe and the auto-accelerated exothermic stabilization reaction of the remaining unstabilized PAN. The PAN was probably not fully stabilized. Above 220°C, these stabilization reactions are spontaneous, with a rapid uncontrolled release of heat [9]. During stabilization, the dehydrogenation reactions evolved as H_2O, the decarbonization reaction evolved as CO_2, and the nitriles evolved as HCN. The carbonization reactions of stabilized PAN can be accelerated by this initial large exotherm, resulting in the early spikes. It is clear that the spikes are not primarily due to a pressure event, since the spike was very minor for many of the gases.

In the 300°-350°C range, the main reactions of the carbonization process occurred on the chain ends, generating NH_3, H_2O, CO_2, HCN, and low molecular weight nitriles. In the 700°-1000°C range, substantial amounts of HCN, NH_3, N_2, and water with lesser amounts of low molecular weight nitriles, CO_2, CO, H_2, and methane were expected to be generated [10].

Figure 25 illustrates the gas concentration histories obtained by FTIR for the PAN insulation system test. Five minutes into the test, concentrations of 0.46% CO, 1.18% CO_2 (1.6% with the CO_2 analyzer), 467 ppm HCN, 377 ppm NH_3, 266 ppm SO_2, 79 ppm C_6H_6, 70 ppm $C_6H_5NH_2$, 56 ppm CH_2CHCHO, 39 ppm COS, 0 ppm NO, and 22 ppm HF were measured. The $\Delta CO_2/\Delta CO$ ratio was 2.5, and a concentration of 18.2% oxygen and 1.2% H_2O was measured.

The hydrocarbon composition at 5 minutes, based on FTIR analysis, is shown in table 2. Observed THCs were 0.06% as propane, based on the FTIR measurements, and 0.08% as propane (table 2), based on the THC analyzer, or 3% to 4% of the propane LEL, respectively. The concentration histories obtained by gas analyzers are illustrated in figure 26.

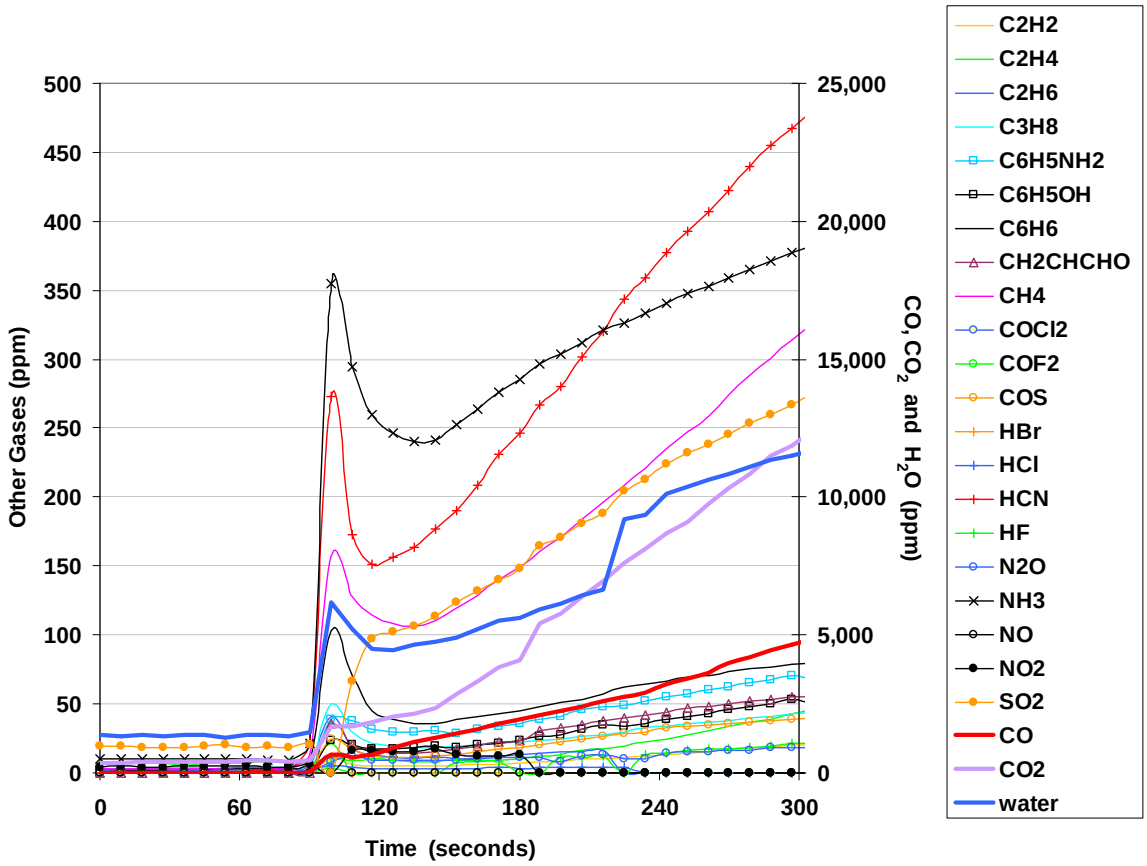

Figure 25. Concentration Histories of PAN Insulation System Box Test Obtained by FTIR Analysis

Table 2. Computation of the Percentage of the LEL as Propane at 5 Minutes for PAN Insulation System Test

Number of Carbons	Gases	Concentration as Propane (ppm)	Percentage of LEL as Propane
1	CH_4	313.9/3 = 104.6	(104.6/21,000)*100 = 0.050
2	C_2H_2, C_2H_4, C_2H_6	(20.2 + 342.7 + 0) * 2/3 = 41.9	(41.9/21,000)*100 = 0.20
3	C_3H_8, CH_2CHCHO	42.9 + 55.5 = 97.4	(97.4/21,000)*100 = 0.46
6	C_6H_6, C_6H_5OH, $C_6H_5NH_2$	(78.7 + 52.7 + 70.7) * 6/3 = 403.2	(403.2/21,000)*100 = 1.92
1, 2, 3, and 6	All the above	104.6 + 41.9 + 97.4 + 403.2 = 647.2	(647.2 / 21,000)*100 = 3.08

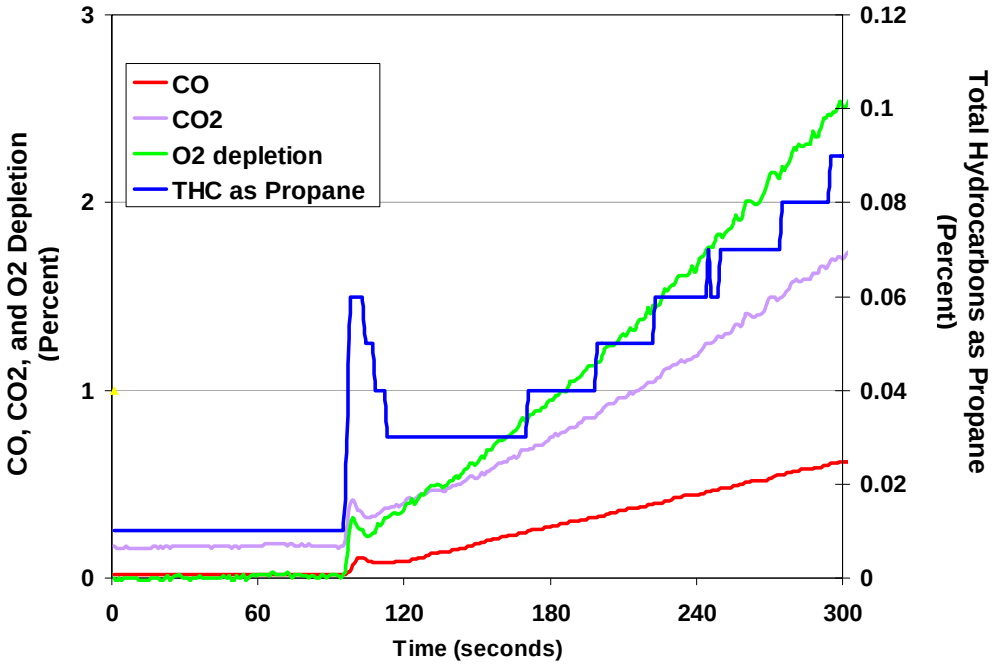

Figure 26. Concentration Histories of PAN Insulation System Box Test Obtained by Gas Analyzers

3.4 INITIAL LABORATORY-SCALE EVALUATION OF CARBON/EPOXY MATERIAL (NO ENCLOSURE).

A multi-ply, epoxy-impregnated carbon fiber composite material was evaluated. The 40- by 40-inch test panels were fabricated by Integrated Technologies, Inc. (Everett, WA 98203) from material supplied by Toray Composites (America) that is qualified for the Boeing 787 aircraft as Boeing Materials Specification BMS 8-276. The composite panels for the test program were fabricated by stacking the BMS 8-276 pre-preg tape in a repeating orientation sequence of -45°, 0°, 45°, and 90° with respect to the reference direction and symmetrically with respect to the mid-plane of the panel to provide a final composite having uniform strength and stiffness in the fiber plane after curing. In the present panels, the (-45°, 0°, 45°, 90°) sequence was repeated 4 times for a total of 16 layers. This "quasi-isotropic" lay-up was cured at 177°C (350°F) under 1.4 MPa (200 psi) of hydrostatic pressure for 2 hours to consolidate the 16 plies and chemically react (cure) the liquid resin system into a highly cross-linked, rigid binder for the carbon fiber reinforcement. After processing, the carbon fiber-reinforced epoxy composite was a flat panel, having a final thickness of 3.2 mm (1/8 inch) and a final density of 1530 ±30 kg/m^3.

The thermal, combustion, and flammability properties of this composite material have been reported [11]. Decomposition from products has been characterized by Jones and Pedrick [12]. The predegradation products HCl and HF probably arise from reagent impurities. The postdegradation products are H_2S, CH_4, and HCN. The major identified products in the primary degradation are $C_6H_5NH_2$, H_2O, C_3H_8, and SO_2. C_6H_6, methylaniline ($C_6H_5NHCH_3$), and ethylaniline ($C_6H_5NHCH_2CH_3$) have also been identified.

Because the carbon/epoxy material incorporated an epoxy resin system, it was initially speculated that a combustible mix of gases could be produced and emitted from the backface side of the test sample. Since the steel box enclosure did not incorporate any type of pressure relief blowout panels to alleviate a spike in pressure in the event of rapid combustion of these gases, the initial burnthrough test was run using the standard open-frame sample holder. The heated gas-sampling line was initially located centrally on the unexposed side of the test apparatus, near the top of the test sample holder, to capture any gases generated from the back surface of the test sample. Relatively constant concentrations of H_2O, CO_2, SO_2, $C_6H_5NH_2$, NH_3, HCl, CH_4, and C_3H_8 were observed for the open-frame test (figures 27 and 28). These gases may be, in part, decomposition products of the oil-fired burner. Except for H_2O and CO_2, the measured gas concentrations were all below 10 ppm.

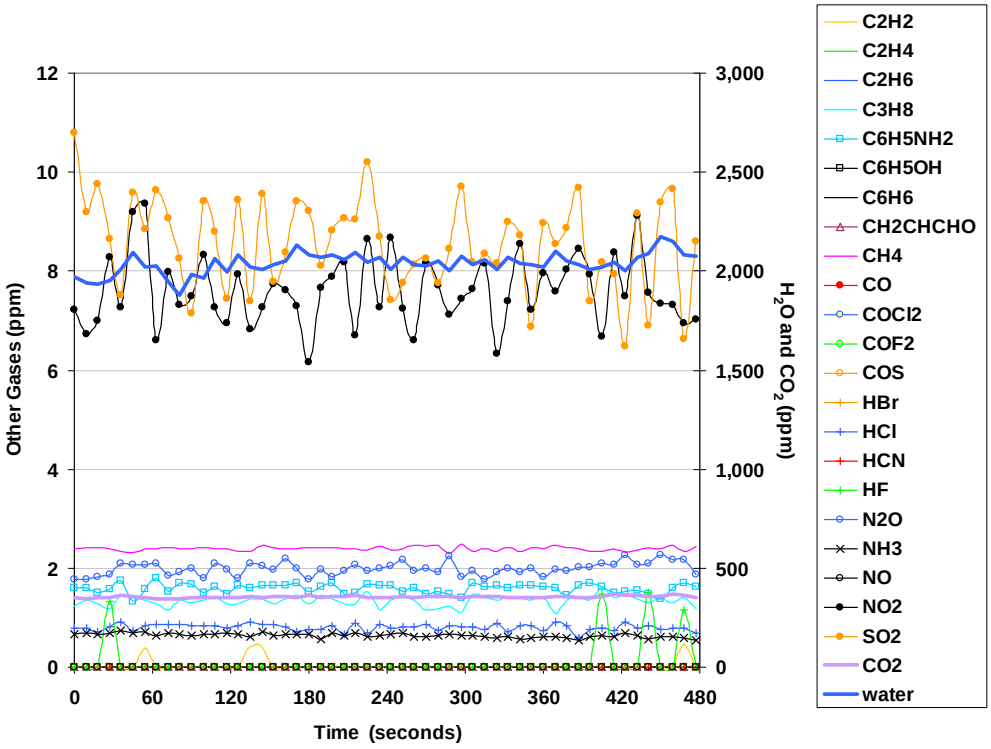

Figure 27. Concentration Histories of the Backface of the Carbon/Epoxy Material With no Enclosure Obtained by FTIR Analysis

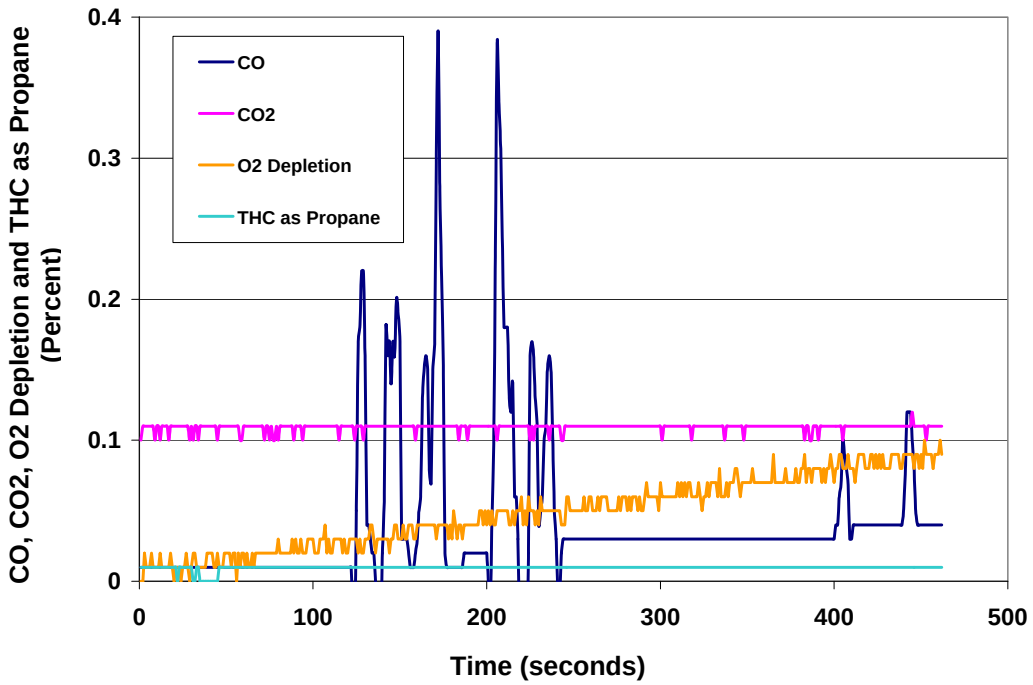

Figure 28. Concentration Histories of the Backface of the Carbon/Epoxy Material With no Enclosure Obtained by Gas Analyzers

Once the burnthrough test was underway, it was apparent that low levels of decomposition gases were being emitted from the backface of the test sample. The carbon/epoxy structural composite material test sample was exposed to the burnthrough test burner for over 7 minutes, at which point the burner flame was turned off. A concentrated area on the backface of the test sample began to smoke at approximately 4 minutes into the test. To gauge the composition of the gases within the smoke plume, the test probe was repositioned into the plume at 7 minutes. The gas analysis equipment was run for an additional 90 seconds before termination (figure 29). There was no significant change in gas concentrations.

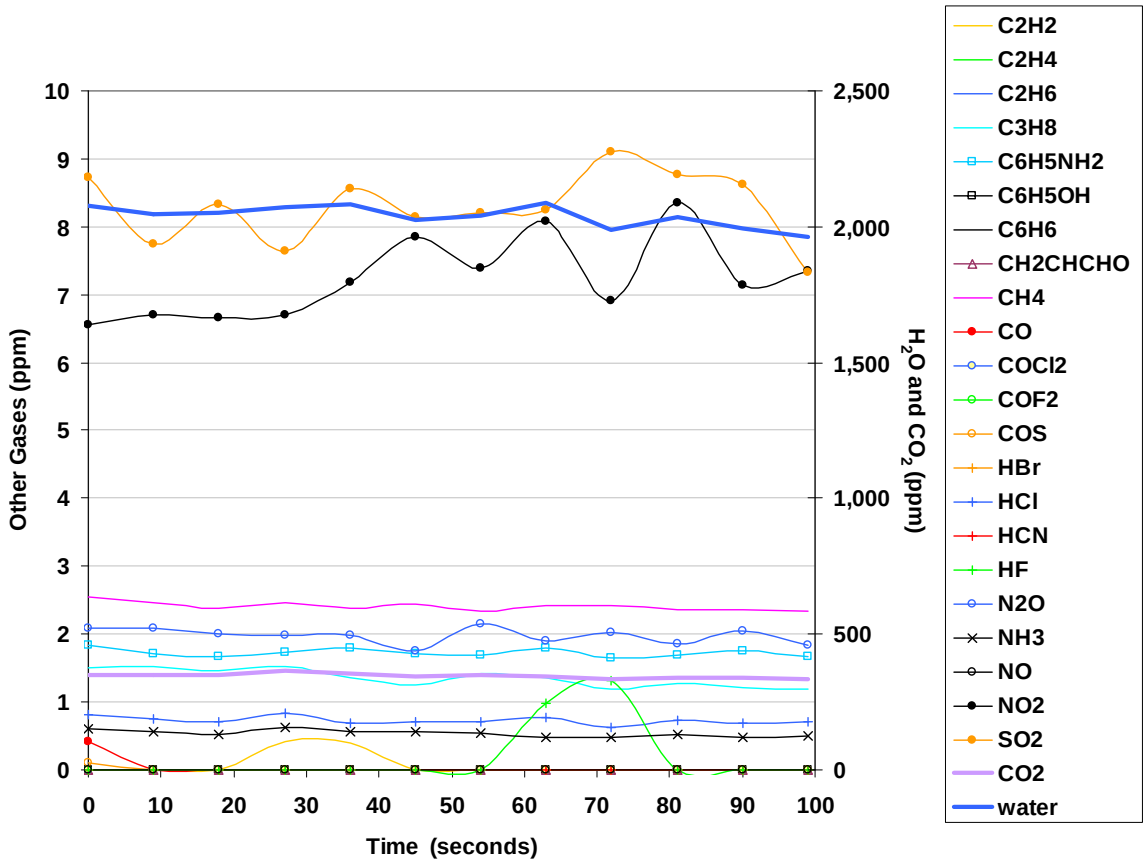

Figure 29. Posttest FTIR Analysis of the Carbon/Epoxy Material Backface in Open Frame With Probe Positioned Closer to the Sample Within the Smoke Plume From the Panel Backface

3.5 EVALUATION OF CARBON/EPOXY STRUCTURAL COMPOSITE.

Following the open-frame test of the carbon/epoxy material, in which a very small amount of constituents were released from the nonexposed side of the test sample, it was agreed that a safe test could be run using the steel box enclosure. To ensure safety, a 6- by 6-inch blowout panel was installed in the box to prevent a catastrophic overpressure in the event of gas ignition. The composite panel was mounted into the recessed area of the box opening, and the securing flange and bolts were installed and tightened.

Five minutes into the test, concentrations of 56 ppm CO, 464 ppm CO_2, 0 ppm HCN, 4 ppm NH_3, 34 ppm SO_2, 9 ppm C_6H_6, 0.8 ppm COS, 0 ppm CH_2CHCHO, and 6 ppm $C_6H_5NH_2$ were measured (figures 30 and 31). The observed $\Delta CO_2/\Delta CO$ ratio, corrected for the initial concentrations of CO and CO2, was 1.8. A concentration of 21% O_2 and 3714 ppm H_2O was measured at 5 minutes. The hydrocarbon composition at 5 minutes, based on FTIR analysis, is shown in table 3. Observed THCs were as high as 0.008% as propane, or 0.4% of the propane LEL.

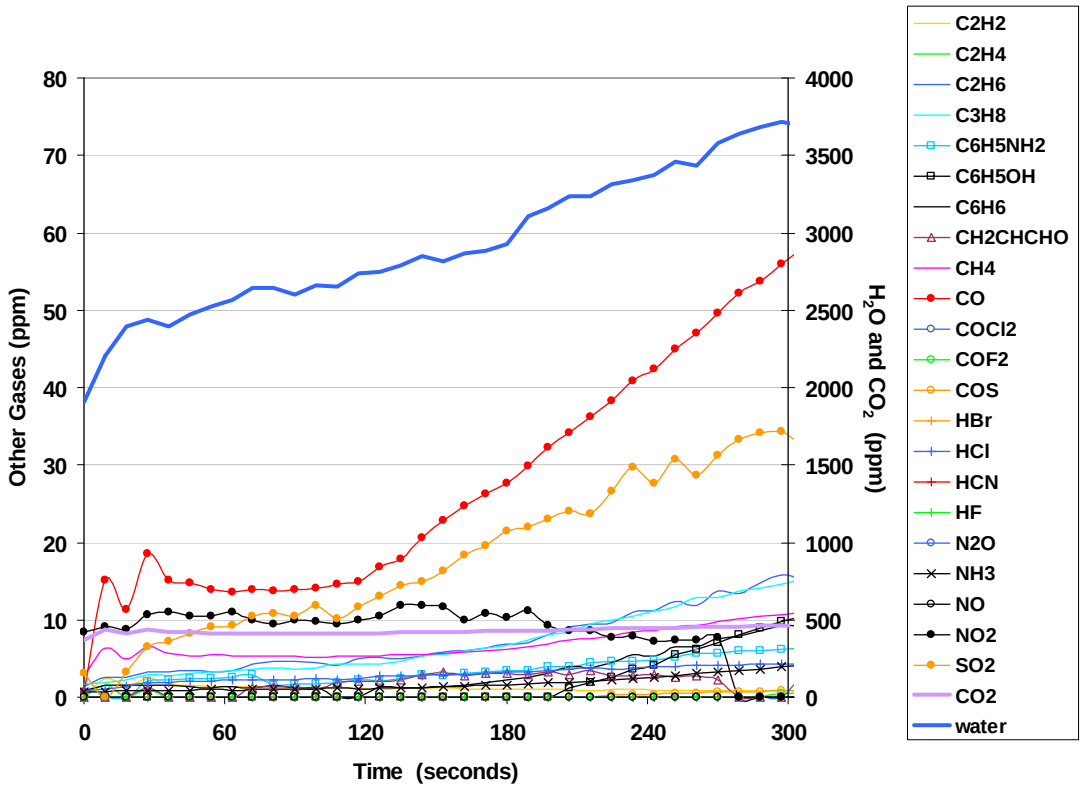

Figure 30. Concentration Histories of the Carbon/Epoxy Material Box Test 1 Obtained by FTIR Analysis

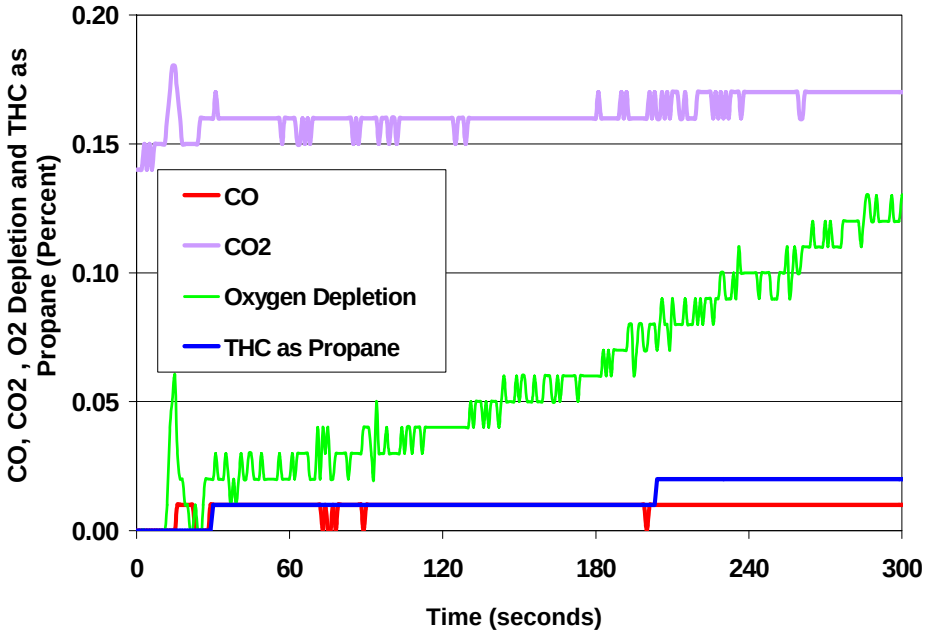

Figure 31. Concentration Histories of the Carbon/Epoxy Material Box Test 1 Obtained by Gas Analyzers

Table 3. Computation of the Percentage of LEL as Propane at 5 Minutes for Carbon/Epoxy Structural Composite Material Test

Number of Carbons	Gases	Concentration as Propane (ppm)	Percentage of LEL as Propane
1	CH_4	10.7/3 = 3.6	(3.6/21,000)*100 = 0.017
2	C_2H_2, C_2H_4, C_2H_6	(0.9 + 0 + 16.0) *2/3 = 11.2	(11.2/21,000)*100 = 0.053
3	C_3H_8, CH_2CHCHO	14.5 + 0 = 14.5	(14.5/21,000)*100 = 0.069
6	C_6H_6, $C_6H_5NH_2$, C_6H_5OH	(9.3 + 9.8 + 6.1)* 6/3 = 50.3	(50.3/21,000)*100 = 0.24
1, 2, 3, and 6		3.6 + 11.2 + 14.5 + 50.3 = 79.6	79.6 (21,000)*100 = 0.379

Additional tests were conducted using the carbon/epoxy material to assess test reproducibility, and the results were reasonably consistent. The test results for the second test were discarded due to test data acquisition problems. The results of the third test are shown in figure 32.

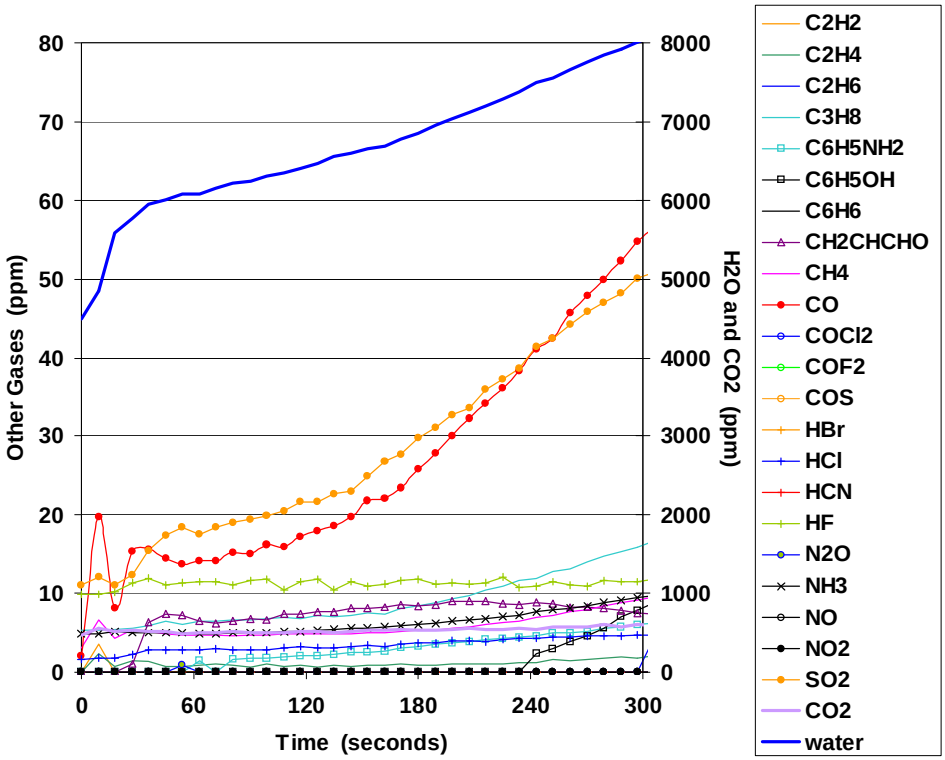

Figure 32. Concentration Histories of the Carbon/Epoxy Material Box Test 3 Obtained by FTIR Analysis

3.6 COMPARISON OF TEST RESULTS.

Figures 33 and 34 compare the FTIR-derived gas concentrations at 5 minutes for the three material systems tested in this study. As shown in figure 33, both the ceramic barrier and the

PAN insulation systems generated greater quantities of CO, CO_2, H_2O, and THC than the carbon/epoxy material.

Similarly, as shown in figure 34, all other gases measured also resulted in higher quantities during tests of the ceramic barrier and PAN insulation systems compared to the carbon/epoxy material.

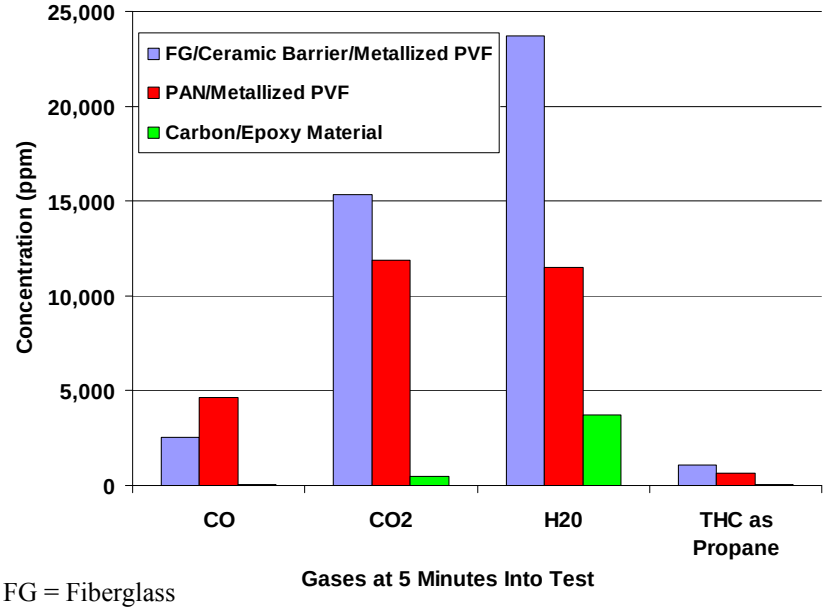

FG = Fiberglass

Figure 33. Comparison of Box Test Concentrations Obtained at 5 Minutes by FTIR for the Three Material Systems: CO, CO_2, H_2O, and THC

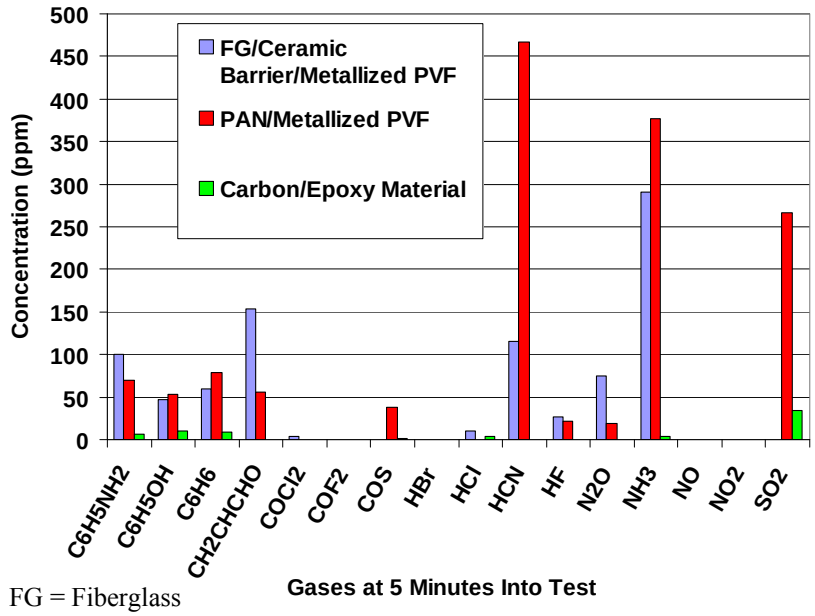

FG = Fiberglass

Figure 34. Comparison of Box Test Concentrations Obtained at 5 Minutes by FTIR for all Other Gases

4. FULL-SCALE EVALUATION OF INSULATION MATERIALS PREVIOUSLY TESTED IN THE LABORATORY-SCALE APPARATUS.

Subsequent full-scale tests were conducted using a B-707 fuselage to establish realistic levels of combustion products generated inside an intact fuselage during exposure to an external fuel fire, when using burnthrough-compliant materials identical to those previously tested in the laboratory-scale apparatus. The full-scale tests used a fire-hardened fuselage section, in which skin/insulation materials could be installed and evaluated against a standard 8- by 10-foot fuel pan fire, as discussed in section 1.2. By determining actual levels of decomposition gases inside the fuselage, comparisons could be made between full-scale results and those previously obtained using the laboratory-scale apparatus. This comparison should allow the determination of a ratio, or scaling factor, between the two test methods. By determining this ratio, an appropriate gas concentration acceptance level could be established for the laboratory-scale apparatus.

Since the ratio of the exposed area of the insulation material divided by the volume of the enclosure used to capture emitted gases was much greater in the laboratory-scale apparatus than in the more realistic full-scale apparatus, it was anticipated that the gas concentrations obtained in the laboratory-scale apparatus would be significantly greater.

4.1 FULL-SCALE TEST APPARATUS DESCRIPTION.

The next phase of the program involved the use of a full-scale test apparatus in which burnthrough-compliant insulation systems could be evaluated under realistic conditions. The full-scale test apparatus was developed previously to evaluate various types of thermal acoustic insulation (the results of these early tests were used to develop the laboratory-test standard for evaluating insulation burnthrough resistance). The full-scale test apparatus consisted of a 20-foot-long steel cylinder constructed from curved C-channel. The steel test section was integrated into an existing B-707 fuselage, which was cut in half to allow the insertion of the test apparatus between the two fuselage halves (figure 35). The test apparatus had an 8- by 8-foot section of the outer skin removed, which could be outfitted with thermal acoustic insulation samples. Measurements of temperature and smoke levels were taken inside the test apparatus along with video coverage at several locations to determine the occurrence of insulation blanket burnthrough. In addition, extensive measurement of gas decomposition products was performed using four sets of continuous gas analyzers, an FTIR analyzer, and an FID THC analyzer (figure 36).

Figure 35. Full-Scale Test Apparatus Configuration for Evaluating Decomposition Products From Various Insulation Samples

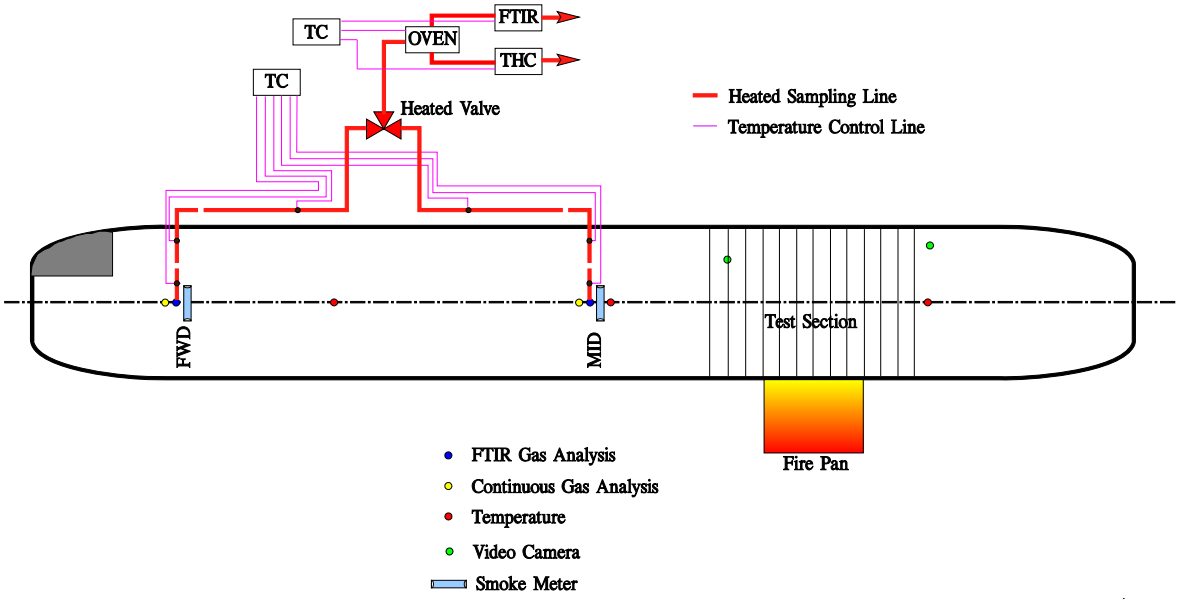

Figure 36. Full-Scale Test Apparatus Instrumentation

For the full-scale tests, the test apparatus was configured with two large openings approximately 4 by 8 feet, situated adjacent to the fuel pan. Insulation blankets were installed over the openings and clipped at the blanket perimeter to prevent the fuel fire flames from penetrating areas other than through the blanket (figure 37).

Figure 37. Full-Scale Test Apparatus Showing Typical Clipping Arrangement of Insulation Blankets

The external face of the test apparatus was outfitted with two 4- by 8-ft pieces of aluminum skin to produce a realistic, fuselage structure. A 0.0625-in.-thick 2024T3 aluminum skin was used for all tests (figure 38).

Figure 38. External Face of the Full-Scale Test Apparatus Showing Aluminum Skin

4.2 GAS-SAMPLING METHODOLOGY FOR THE FTIR AND THC ANALYZERS DURING FULL-SCALE TESTS.

Figure 39 shows a schematic of the FTIR and THC sampling system used during the full-scale tests. The two identical sampling paths leading to the analyzers were heated to minimize condensation of analytes in the sampling system. The flexible, heated, Teflon®-lined, 1/4-inch-diameter (0.64-cm) sample lines ran from the test fuselage to a three-way valve located outside the oven. Each heated sample line was composed of one 3-foot section, one 6-foot section, and one 40-ft section, each separately thermostated to 160°C. The oven was also thermostated to 160°C. The path from the oven to the FID THC analyzer was thermostated to the working temperature of that analyzer, 160°C. The line leading from the oven to the FTIR sample cell and the FTIR were thermostated to 170°C, the temperature at which most of the FTIR calibration standard library was developed.

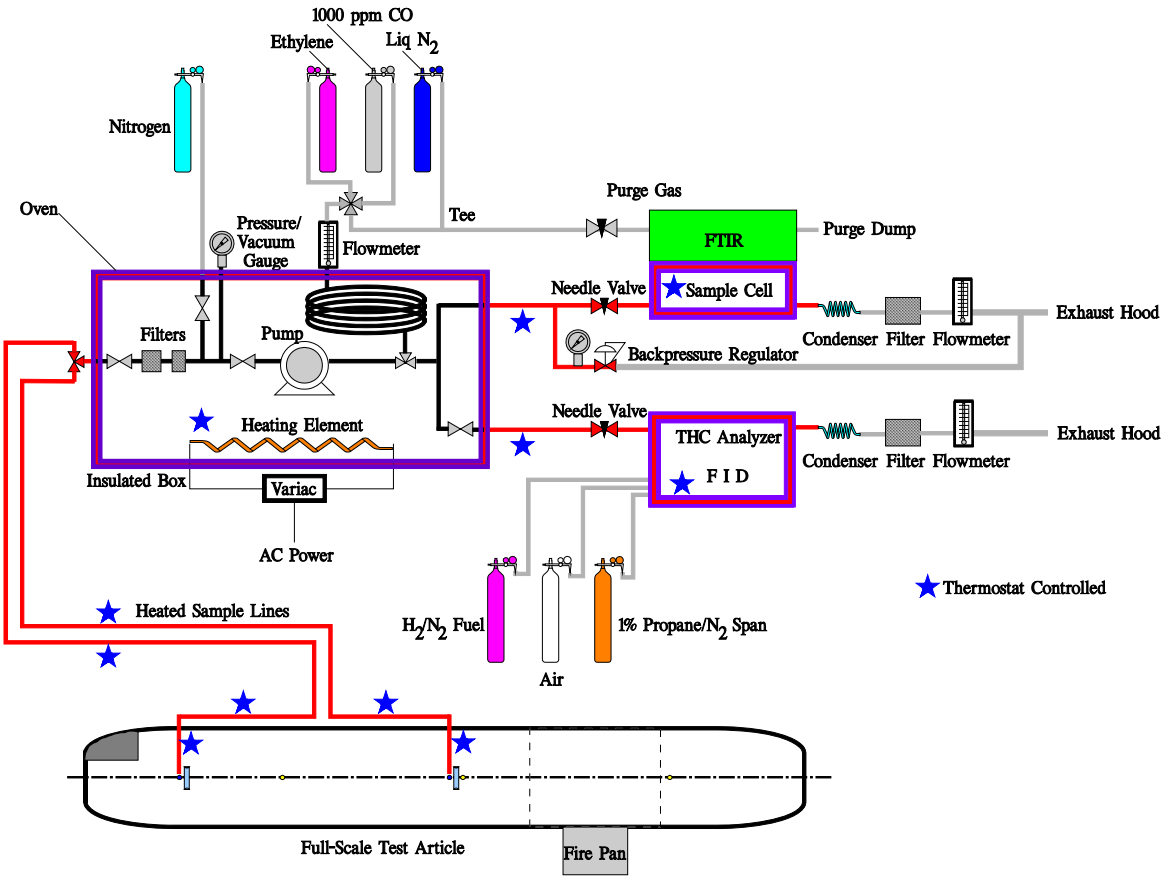

Figure 39. Schematic of FTIR and THC Gas-Sampling System

The sample line intakes were located at two stations inside the test fuselage, one approximately in the middle of the fuselage length, closer to the fire pan, and the other at a forward location, closer to the forward exit door. The middle and forward sampling locations are 18 and 53 feet, respectively, from the centerline of the fire pan when measured axially (the stations are 35 feet apart). Both stations were located at a height of 5′6″ from the floor. The three-way valve was manually switched during the test, so that measurements could be obtained at both locations

(although this sampling method resulted in more complete coverage of the test fuselage, it created gaps in the data when the valve was switched to the opposite station).

The oven, downstream plumbing, instrumentation, and flow rates matched those of the laboratory-scale gas-sampling system, with the exception of the THC analyzer: an FID-based analyzer was used in the full-scale system, whereas an NDIR-based analyzer was used in the laboratory-scale tests.

4.3 FULL-SCALE EVALUATION OF INSULATION MATERIALS MEETING THE NEW BURNTHROUGH STANDARD.

4.3.1 The PAN Insulation System.

The first full-scale test was conducted using the same PAN insulation system that was tested in the laboratory-scale apparatus. Blanket material containing PAN fibers supplied by TexTech Industries was encapsulated in the standard PVF moisture barrier film (per figure 22). The PAN-containing blanket material was extremely effective at resisting flame penetration for at least 5 minutes during the laboratory-scale evaluations.

During the full-scale test, the PAN material remained intact for the length of the test, approximately 5 minutes. After fuel pan ignition, there was a noticeable amount of smoke produced by the pyrolysis of the PAN material on the inboard (protected) side of the test apparatus. After approximately 2 minutes however, the level of smoke being produced by the material decreased dramatically. This reduction in smoke production indicated the combustion of the binders within the PAN material (used to hold the fibers together) had ceased, or the binder material was consumed. A posttest inspection revealed the PAN material to be completely free of any penetrations or failure points (figures 40 and 41).

Figure 40. Posttest Inspection of PAN Material, Shown From Inboard Side

Figure 41. Posttest Inspection of PAN Material, Shown From External Side

Early large spikes in the concentrations of NH_3, HCN, CH_4, and H_2O were observed at 105 seconds at the midstation, 5′6″ height (figure 42). This is consistent with the relatively high position of the sample probe and the auto-accelerated exothermic stabilization reaction of the remaining unstabilized PAN. The PAN was probably not fully stabilized prior to testing. Above 220°C, these stabilization reactions are spontaneous, with a rapid uncontrolled release of heat [10]. During stabilization, the dehydrogenation reactions evolved as H_2O, the decarbonization reaction evolved as CO_2, and the nitriles evolved as HCN. The carbonization reactions of stabilized PAN can be accelerated by this initial large exotherm, resulting in the early spikes. It can be observed that the spikes are not primarily due to a pressure event, since the spike was very minor for many of the gases. In the 300°-350°C range, the main reactions of the carbonization process occur on the chain ends, generating NH_3, H_2O, CO_2, HCN, and low molecular weight nitriles. In the 700°-1000°C range, substantial amounts of HCN, NH_3, N_2, and water with lesser amounts of low molecular weight nitriles, CO_2, CO, H_2, and methane are expected to be generated [12]. Five minutes into the test, concentrations of 0.019% CO, 0.175% CO_2 (0.19% with the CO_2 analyzer), 16.4 ppm HCN, 5.6 ppm NH_3, 19.8 ppm SO_2, 15 ppm C_6H_6, 4.6 ppm $C_6H_5NH_2$, 0 ppm COS, 0 ppm NO, and 0 ppm HF were measured at the mid station using FTIR. A concentration of 20.4% oxygen was measured. The $\Delta CO_2/\Delta CO$ ratio, corrected for the initial concentration of CO and CO_2, was 10.3. The $\Delta CO_2/\Delta CO$ ratio for the laboratory-scale test was 2.5; thus, the full-scale ratio was 4.1 times that of the laboratory-scale test, indicating infiltration of external combustion gases into the fuselage.

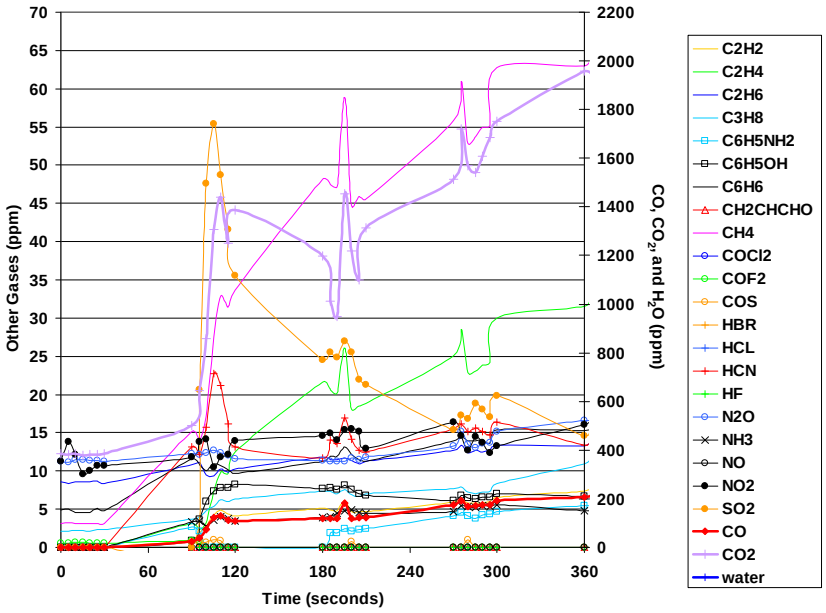

Figure 42. Concentration Histories of PAN Insulation System Full-Scale Test at Midstation, 5′6″ Height, Obtained by FTIR Analysis

Similar results were obtained at the forward station, also at a height of 5′6″ (figure 43). The $\Delta CO_2/\Delta CO$ ratio for the forward station was 7.0. The ratio for the laboratory-scale test was 2.5; thus, the ratio for the full-scale test is 2.8 times greater than the ratio observed in the laboratory-scale test, also indicating significant infiltration of external combustion gases into the fuselage.

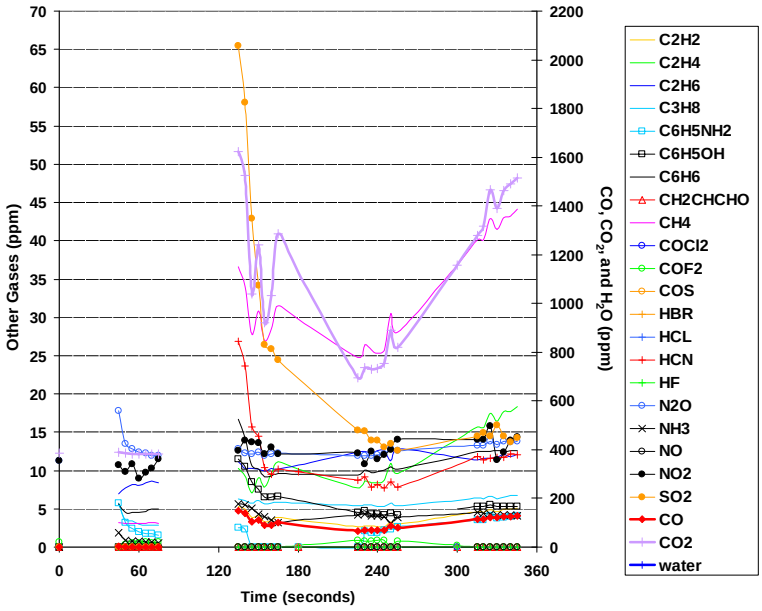

Figure 43. Concentration Histories of PAN Insulation System Full-Scale Test at Forward Station, 5′6″ Height, Obtained by FTIR Analysis

The gas yield histories obtained by continuous gas analyzers are illustrated in figures 44 and 45. As shown, the concentrations for carbon monoxide were very low, reaching a maximum of about 0.025% at 5 minutes. Similarly, for carbon dioxide, the concentrations only reached about 0.020% at 5 minutes.

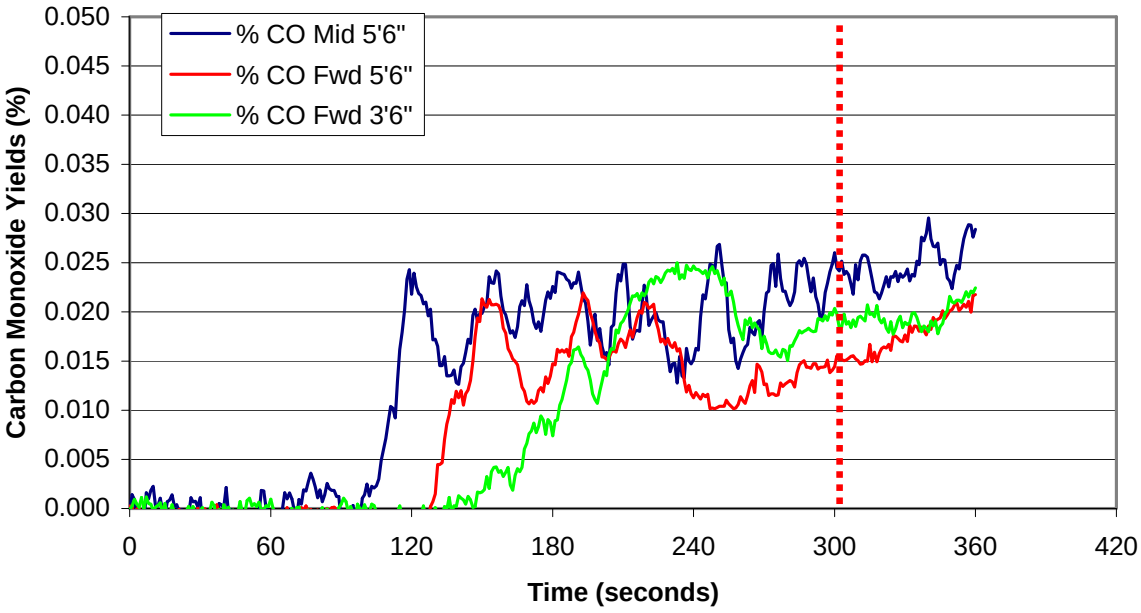

Figure 44. Carbon Monoxide Yield Histories of PAN Insulation System Full-Scale Test Obtained by Gas Analyzers

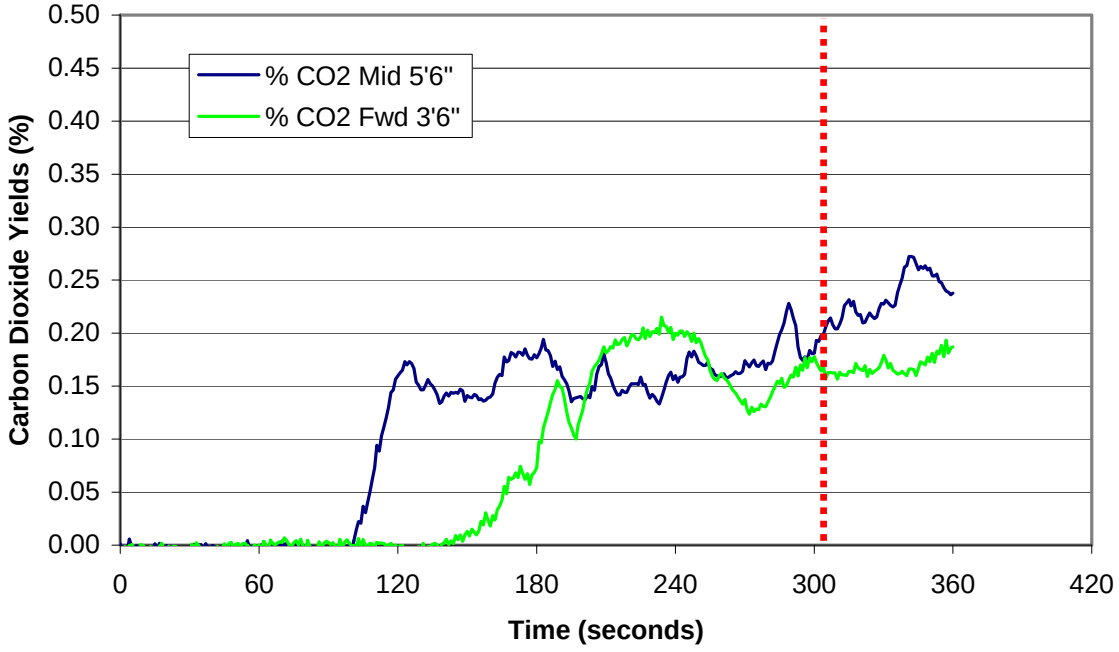

Figure 45. Carbon Dioxide Yield Histories of PAN Insulation System Full-Scale Test Obtained by Gas Analyzers

A comparison of the gas yields is shown in figure 46. With the exception of water, all gas concentrations were higher at the midstation, which was expected due to the closer proximity to the fire.

A chart of the yields obtained by FTIR is compared to those obtained by the gas analyzers for CO, CO_2, and THC as propane in figure 47. The results indicate slightly higher values obtained when using the gas analyzers for CO and CO_2, but slightly higher values are obtained for THC when using the FTIR. In general, the results indicate a high level of correlation between the two, which are distinctly different methods of measurement.

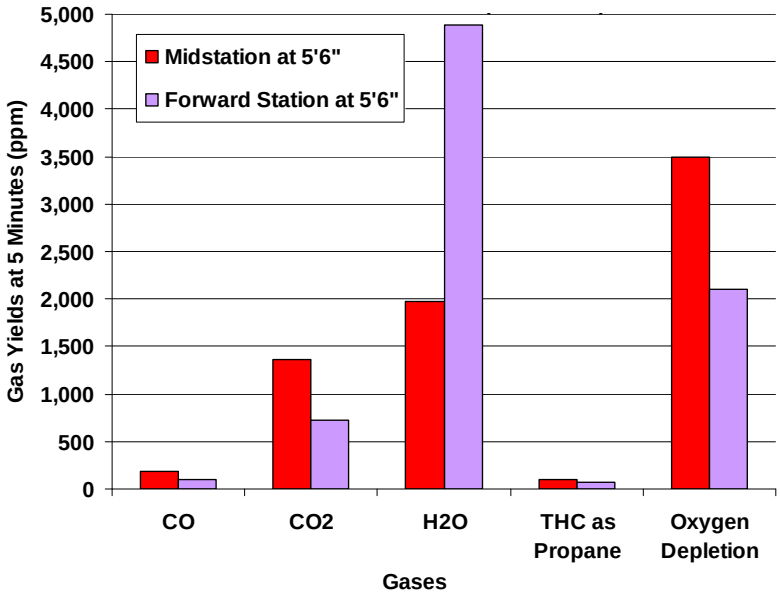

Figure 46. Comparison of PAN Insulation System Gas Yield at the Mid- and Forward Stations

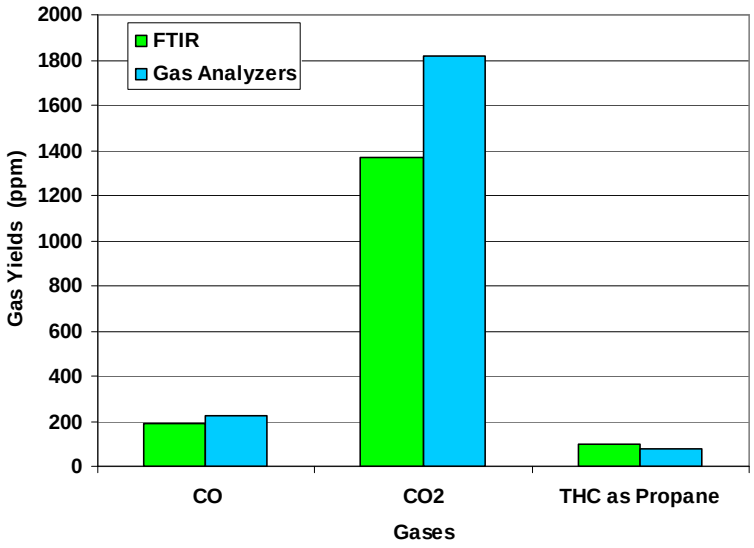

Figure 47. Comparison of Gas Yields Obtained by FTIR and Gas Analyzers for the PAN Insulation System at Midstation, 5′6″ Height, at 5 Minutes

4.3.2 Fiberglass/Ceramic Barrier Insulation System.

The next full-scale test was conducted using fiberglass batting with a thin, paper-like ceramic barrier encapsulated in the metallized PVF film covering. This arrangement was identical to the laboratory-scale apparatus.

The ceramic barrier was installed on the outboard face of the insulation batting (within the film) to form a flame penetration barrier between the external flames and the interior of the fuselage. The insulation batting, along with the ceramic barrier, was clamped in place around the perimeter of the 4- by 8-ft openings, similar to the previous test using PAN material. The clamping process also held the ceramic barrier in place (figure 48).

Figure 48. Installation of Blankets Containing the Thin, Ceramic Barrier and Fiberglass Insulation

Although this installation methodology had proven effective during the laboratory-scale tests, as well as the previous test using a blanket material containing PAN fibers, the extremely large spacing of the frame members supporting the blankets was too great, leading to an early failure of the ceramic barrier that allowed flame penetration. By allowing flame penetration, the data was unusable, since the purpose of the tests was to determine the contribution of gases from the decomposition of the material itself, not from the fuel fire combustion products. During a posttest inspection, it was observed that the majority of the ceramic barrier had opened and allowed flames to penetrate (figure 49).

Figure 49. Posttest Inspection Shows Failure of the Ceramic Barrier During Initial Configuration

A subsequent test was arranged with more realistic spacing between frame members (figure 50). During the configuration of the apparatus, two additional curved C-channels were installed to cut down on the span between frame members.

Figure 50. Modified Blanket Installation Configuration Using a Fiberglass/Ceramic Barrier

The modified installation method proved successful during a repeat test in which the ceramic barrier was able to prevent fuel fire flame penetration for the duration of the test, approximately 5 minutes. A posttest inspection revealed the ceramic barrier material to be completely free of any penetrations or failure points (figure 51).

Figure 51. Posttest Inspection of the Fiberglass/Ceramic Barrier Insulation System

Additional inspection of the inboard side of the insulation revealed the fiberglass batting to be largely consumed, leaving only the ceramic barrier (figure 52).

Figure 52. Posttest Inspection of Inboard Side of the Fiberglass/Ceramic Barrier Insulation System

Figure 53 shows the gas concentration histories obtained by FTIR at the midstation, 5′6″ height, for the second fiberglass/ceramic barrier insulation system test. At 4 minutes 20 seconds into the test, concentrations of 100 ppm CO, 3100 ppm CO_2, 0 ppm HCN, 4.5 ppm NH_3, 0 ppm CH_2CHCHO, 9.5 ppm C_6H_6, and 5.5 ppm $C_6H_5NH_2$, and 10 ppm C_6H_5OH were measured. The $\Delta CO_2/\Delta CO$ ratio was 27. The $\Delta CO_2/\Delta CO$ ratio for the laboratory-scale test was 6.0; thus, the full-scale ratio was 4.5 times that of the laboratory-scale test, indicating infiltration of external combustion gases into the fuselage. Also at 4 minutes 20 seconds, the H_2O concentration reached 0.6%. The concentrations of hydrocarbons measured in the fuselage were far below the level to cause a flashover event. The LEL of CH_4, C_2H_6, and C_3H_8 were 5.0%, 3.0%, and 2.1%, respectively. The 4-minute 20-second concentration of CH_4 was 35 ppm. The 5-minute concentrations of C_2H_2, C_2H_4, and C_2H_6 were 13, 22, and 0 ppm, respectively, and C_3H_8 and C_6H_6 were 29 and 10 ppm, respectively.

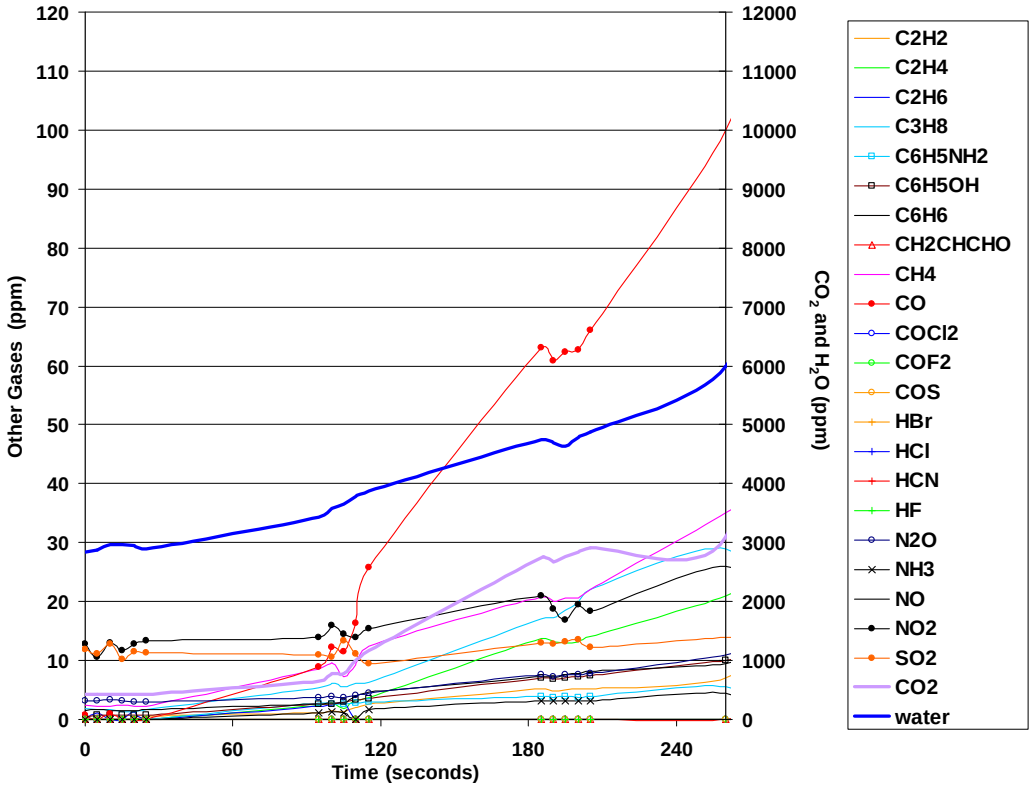

Figure 53. Concentration Histories of the Fiberglass/Ceramic Barrier Insulation System Full-Scale Test at Midstation, 5′6″ Height, Obtained by FTIR Analysis

At the forward station, the concentrations were slightly less than at the midstation (figure 54). At 4 minutes into the test, the following concentrations were observed: 48 ppm CO, 2215 ppm CO_2, 0 ppm HCN, 2 ppm NH_3, 0 ppm CH_2CHCHO, 6 ppm C_6H_6, 3 ppm $C_6H_5NH_2$, and 6 ppm C_6H_5OH. The $\Delta CO_2/\Delta CO$ ratio was 36. In comparison, the $\Delta CO_2/\Delta CO$ ratio for the laboratory-scale test was 6.0; thus, the full-scale ratio was 6 times greater than the laboratory-scale ratio. This indicates infiltration of the external combustion gases into the fuselage. Also at 4 minutes, the H_2O concentration reached 0.45%. The concentrations of hydrocarbons measured in the fuselage were far below the level to cause a flashover event. The LEL of CH_4, C_2H_6, and C_3H_8

were 5.0%, 3.0%, and 2.1%, respectively. The 4-minute concentration of CH_4 was 16 ppm. The 4-minute concentrations of C_2H_2, C_2H_4, and C_2H_6 were 4, 9, and 0 ppm, respectively, and C_3H_8 and C_6H_6 were 17 and 6 ppm, respectively.

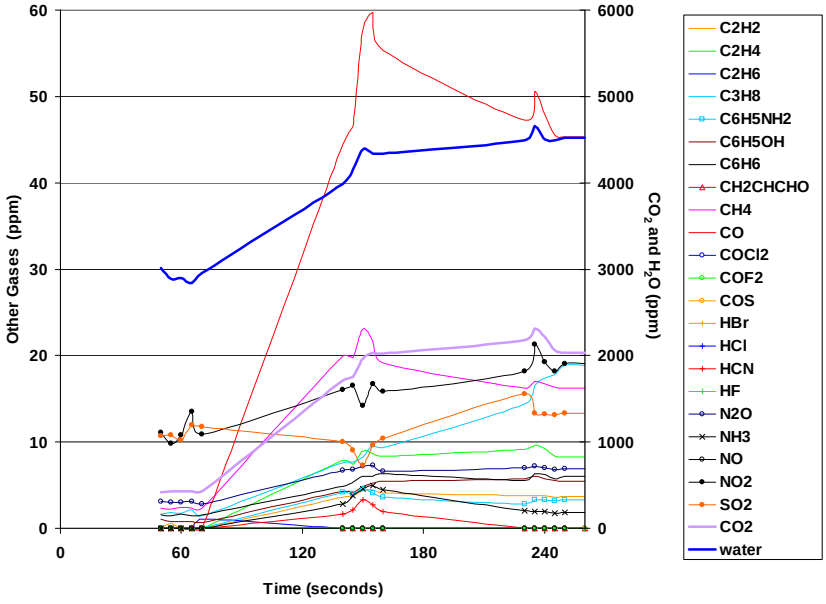

Figure 54. Concentration Histories of the Fiberglass/Ceramic Barrier Insulation System Full-Scale Test at Forward Station, 5′6″ Height, Obtained by FTIR Analysis

The gas yield histories obtained by continuous gas analyzers are illustrated in figures 55 and 56. As shown, the yields for CO were very low, reaching a maximum of about 0.015% at 4 minutes 30 seconds. Similarly, for CO_2, the yields only reached about 0.30% at the 4-minute 30-second point. These low readings indicate the ceramic barrier was effective at keeping fire gases out of the fuselage and did not indicate any significant contribution from the insulation material itself.

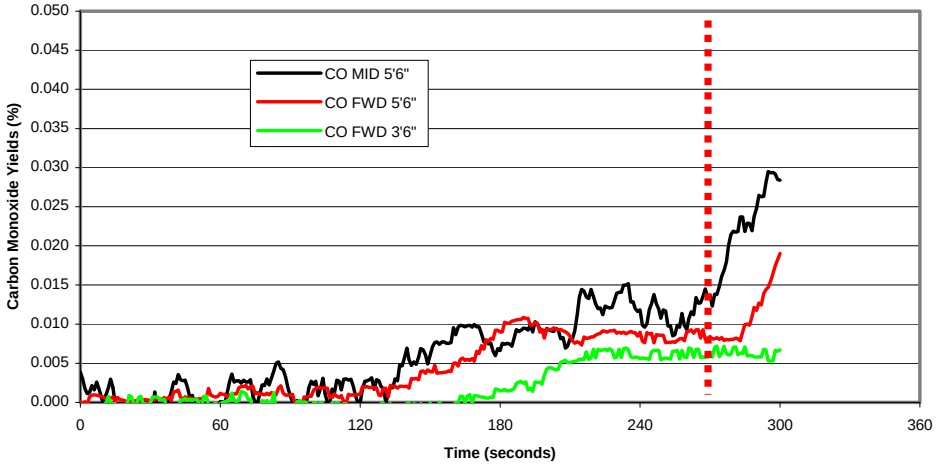

Figure 55. Carbon Monoxide Yield Histories of the Fiberglass/Ceramic Barrier Insulation System Full-Scale Test Obtained by Gas Analyzers

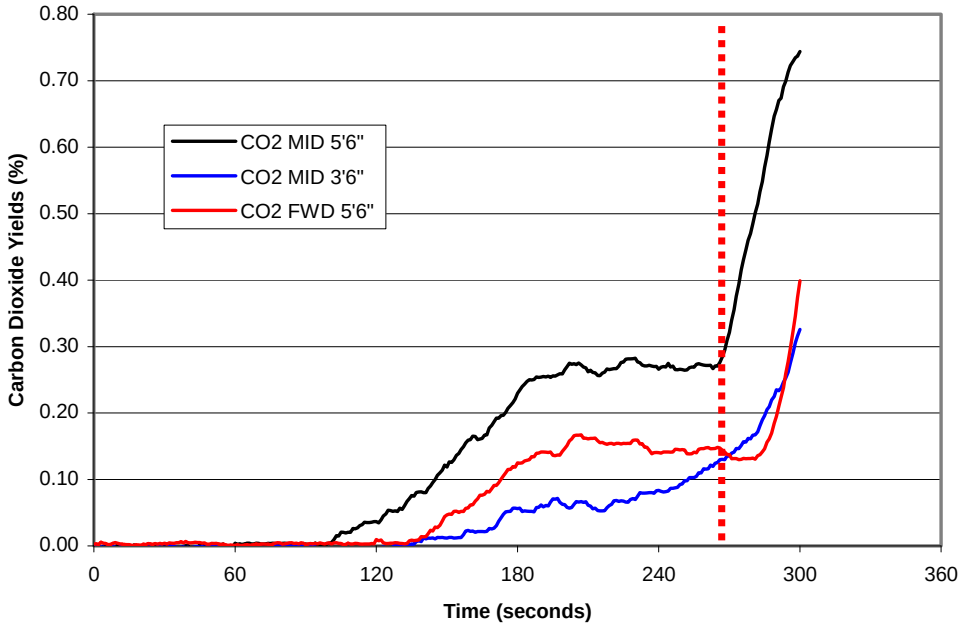

Figure 56. Carbon Dioxide Yield Histories of the Fiberglass/Ceramic Barrier Insulation System Full-Scale Test Obtained by Gas Analyzers

A comparison of the gas yields is shown in figure 57. All gas yields were higher at midstation, which was expected due to the closer proximity to the fire.

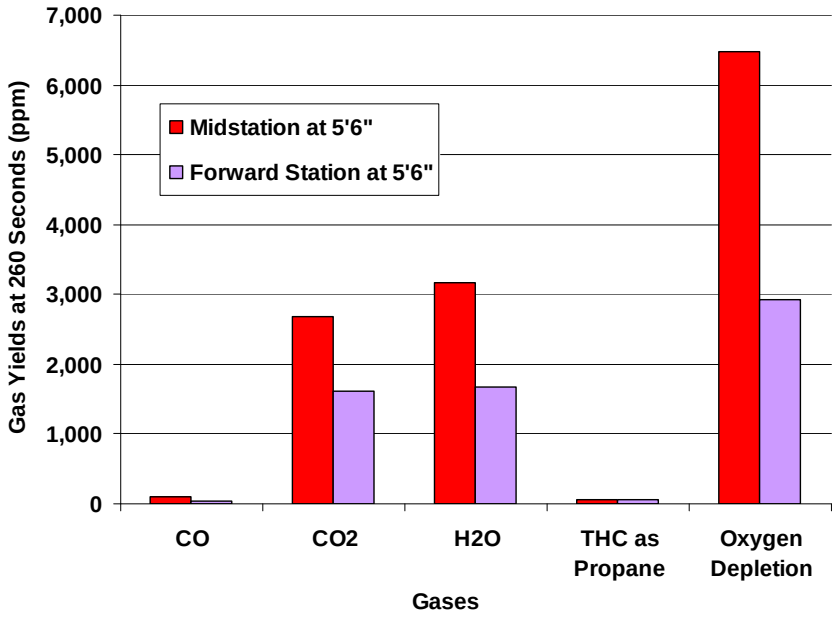

Figure 57. Comparison of the Fiberglass/Ceramic Barrier Insulation System Gas Yields at 260 Seconds at the Mid- and Forward Stations

A chart of the yields obtained by FTIR is compared to those obtained by the gas analyzers for CO, CO_2, and THC as propane (figure 58). Replacing the CO and CO_2 gas analyzers' left detectors prior to this test resulted in excellent agreement with the FTIR and gas analyzer data.

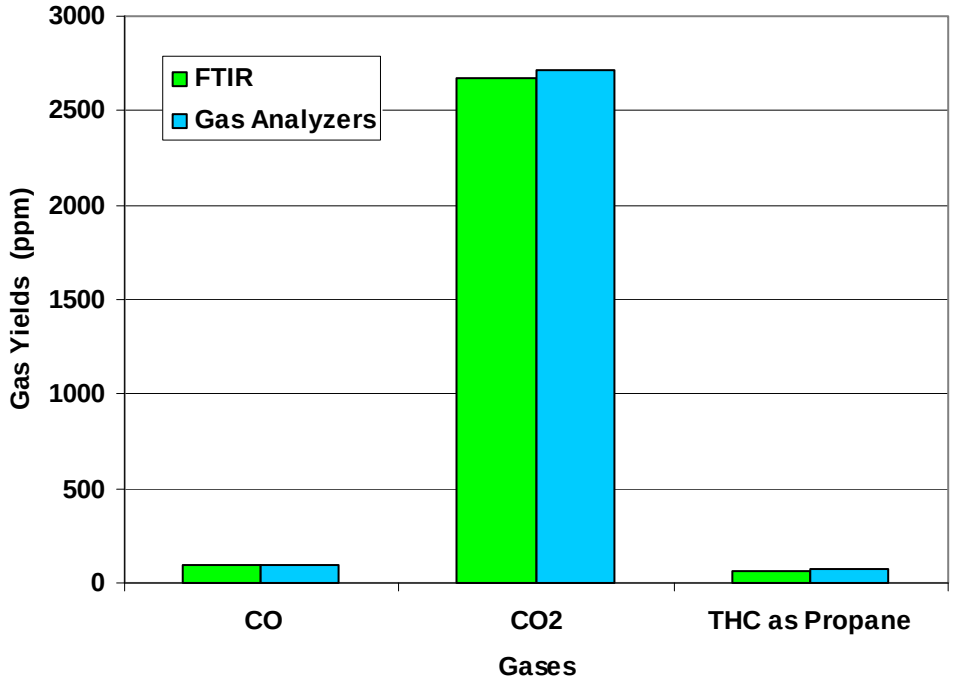

Figure 58. Comparison of Gas Yields Obtained by FTIR and Gas Analyzers at Midstation, 5′6″ Height, for the Fiberglass/Ceramic Barrier Insulation System (260 seconds)

4.4 FULL-SCALE EVALUATION OF CARBON/EPOXY STRUCTURAL COMPOSITE MATERIAL.

A multi-ply, epoxy-impregnated carbon fiber composite material was evaluated. The two 4- by 8-ft test panels were fabricated by Integrated Technologies, Inc. (Everett, WA 98203) from material supplied by Toray Composites (America), which is qualified for the B-787 aircraft as BMS 8-276 (for a detailed description of this material, refer to section 3.4). After processing, the carbon fiber-reinforced epoxy composite was a flat panel, having a final thickness of 3.2 mm (1/8 inch) and a final density of 1530 ±30 kg/m^3. Thermal, combustion, and flammability properties of this composite material have been reported [11].

For the full-scale tests, the two epoxy/carbon structural composite panels were mounted onto the steel test apparatus structure with 5/16-inch-diameter bolts and large flange washers. Each panel was restrained at the top with three bolts and at the midpoint with two additional bolts and washers. The bottom edges of the panels were placed just below the edge of the fuel pan, in order to hold them tight to the test apparatus structure. A high-temperature-resistant ceramic mat material was used to cover the fuselage structure at the perimeter of the two openings. The ceramic mat protected the steel frames from becoming warped during fire conditions and served as a gasket for the composite panels to mate to, forming a protective seal against the fuel fire. Additional flanges constructed of thin-gauge sheet steel were added to the test apparatus exterior

surface to prevent the seepage of fuel fire gases into the fuselage through the long edges of the panels. The flanges were placed in the center section, between the two panels and on the outer sides (figure 59). All efforts were made to minimize the amount of holes drilled through the panels to prevent the passage of fire gases into the fuselage, which would cause erroneously high readings in the gas collection systems.

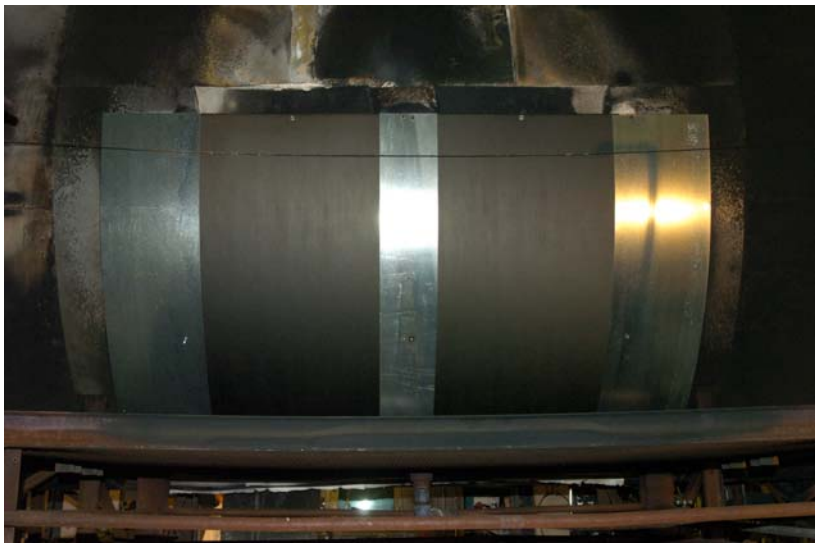

Figure 59. Carbon/Epoxy Structural Composite Material Mounted to the Steel Test Apparatus

It should be noted that the panels were constructed in a flat configuration, but were flexible enough to fit the contour of the test fuselage without difficulty, albeit with noticeable preload.

Following the fuel pan ignition, there was no apparent effect for the first 30 seconds. From approximately 30 seconds to 1 minute, there was noticeable bubbling of the inboard face of the structural composite, although it did not lead to any type of flame penetration. It was later discovered that the small amount of bending of the flat panels to fit the contour of the fuselage magnified the preloading condition during the fire exposure, causing a slight delamination of the interior face. The delamination appeared to be confined to the inner face ply only and did not significantly contribute to the outcome of the test.

Starting at approximately 2 minutes 15 seconds, a small fissure formed at the edge of one panel, causing the release of smoke into the fuselage. Three additional small fissures formed between 2 minutes 30 seconds and 3 minutes at other locations near the edges of the panels. The smoke production steadily increased from these areas, with the exception of one area near the center former, which appeared to be producing a majority of the smoke at 4 minutes. At 5 minutes, moderate to heavy smoke was coming from several areas along an imaginary horizontal line about midway along one of the panels. Although the smoke production was worsening, a decision was made to allow the test to continue beyond 5 minutes, since no visible burnthrough had occurred. At 6 minutes 30 seconds, a visible breach began at the edges of both panels (along the center former), allowing flames to enter. The external fire was extinguished at approximately 7 minutes, although localized flaming was still visible until 7 minutes 45 seconds.

A posttest inspection revealed the inner surface to be largely intact, with only a localized area near the center former fire damaged to the point of allowing direct flame penetration. The entire inner surface showed evidence of delamination, but there were no other visible penetrations (figure 60).

Figure 60. Posttest Inspection of the Inboard Surface of the Carbon/Epoxy Structural Composite Material

A posttest inspection of the outer face of the panels revealed significant delamination of the outermost layers. In some instances, the carbon fibers had fallen away from the face of the panel (figure 61). Although the delamination was significant to the outer layers, there was enough integrity in the remaining layers to keep the panels complete for removal. After removing the central flange that overlapped the panels, additional segments of the carbon fibers collapsed, as the flange had been holding them in place.

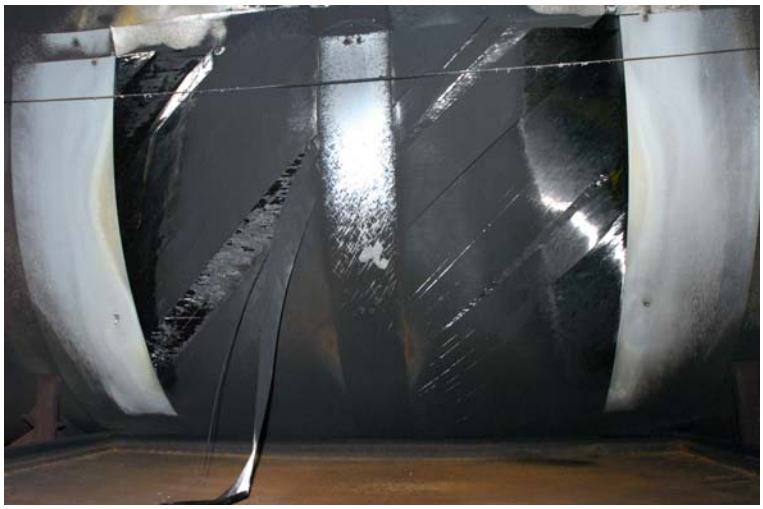

Figure 61. Posttest Inspection of the Outboard Surface of the Carbon/Epoxy Structural Composite Material

Figure 62 illustrates the gas concentration histories obtained by FTIR analysis at the midstation, 5′6″ height, for the epoxy/carbon structural composite panel test. Five minutes into the test, concentrations of 7 ppm CO, 399 ppm CO_2, 0 ppm HCN, 1.4 ppm NH_3, 0 ppm CH_2CHCHO, 9.2 ppm C_6H_6, 3.3 ppm $C_6H_5NH_2$, and 9.4 ppm C_6H_5OH were measured. Also at 5 minutes, the H_2O concentration reached 0.35%. The concentrations of hydrocarbons measured in the fuselage were far below the level to cause a flashover event. The LEL of CH_4, C_2H_6, and C_3H_8 were 5.0%, 3.0%, and 2.1%, respectively. The 5-minute concentration of CH_4 was 13 ppm. The 5-minute concentrations of C_2H_2, C_2H_4, and C_2H_6 were 0, 0, and 11 ppm, respectively, and C_3H_8 and C_6H_6 were 5.4 and 9.2 ppm, respectively. The $\Delta CO_2/\Delta CO$ ratio was 5.5. The $\Delta CO_2/\Delta CO$ ratio for the laboratory-scale test was 1.8; thus, the full-scale ratio was 3.1 times greater than the laboratory-scale ratio, indicating infiltration of external combustion gases into the fuselage.

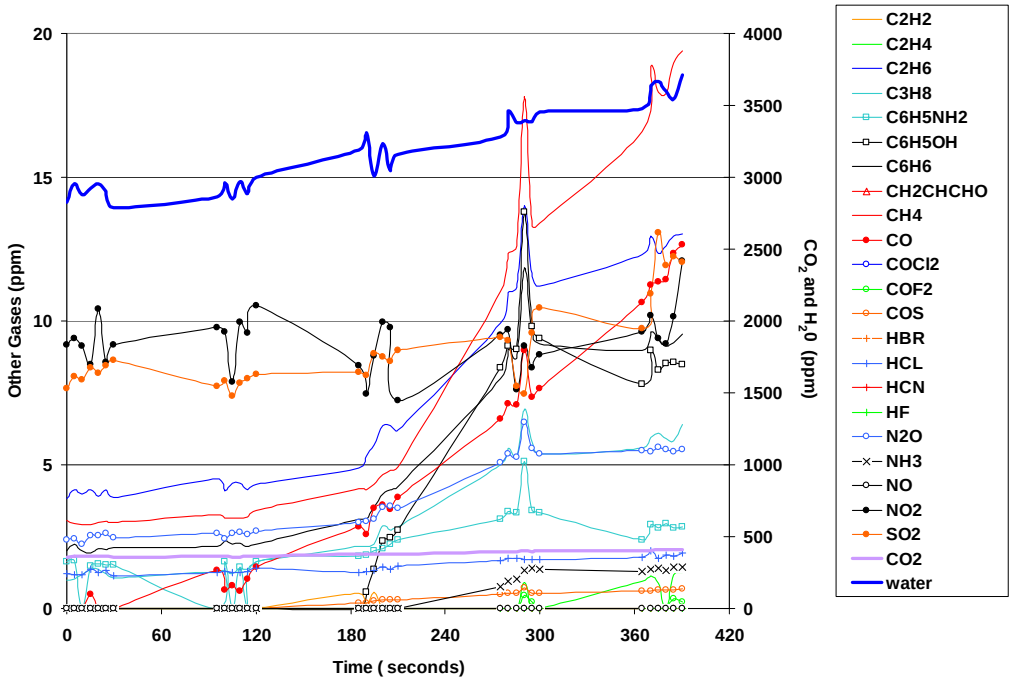

Figure 62. Concentration Histories of the Carbon/Epoxy Structural Composite Full-Scale Test at Midstation, 5′6″ Height, Obtained by FTIR Analysis

At the forward station, the concentrations were slightly less than at midstation (figure 63). At 5 minutes 20 seconds into the test, the following concentrations were observed: 5.6 ppm CO, 391 ppm CO_2, 0 ppm HCN, 1 ppm NH_3, 0 ppm CH_2CHCHO, 6.4 ppm C_6H_6, 2 ppm $C_6H_5NH_2$, and 5.7 ppm C_6H_5OH. The $\Delta CO_2/\Delta CO$ ratio was 7.1. The $\Delta CO_2/\Delta CO$ ratio for the laboratory-scale test was 1.8; thus, the full-scale ratio is 3.9 times greater than the laboratory-scale ratio, indicating infiltration of external combustion gases into the fuselage. Also at 5 minutes 20 seconds, the H_2O concentration reached 0.33%. The concentrations of hydrocarbons measured in the fuselage were far below the level to cause a flashover event. The LEL of CH_4, C_2H_6, and C_3H_8 were 5.0%, 3.0%, and 2.1%, respectively. The 5-minute 20-second concentration of CH_4 was 8.9 ppm. The 5-minute 20-second concentrations of C_2H_2, C_2H_4, and C_2H_6 were 0, 0, and 8.6 ppm, respectively; and C_3H_8 and C_6H_6 were 3.8 and 6.4 ppm, respectively.

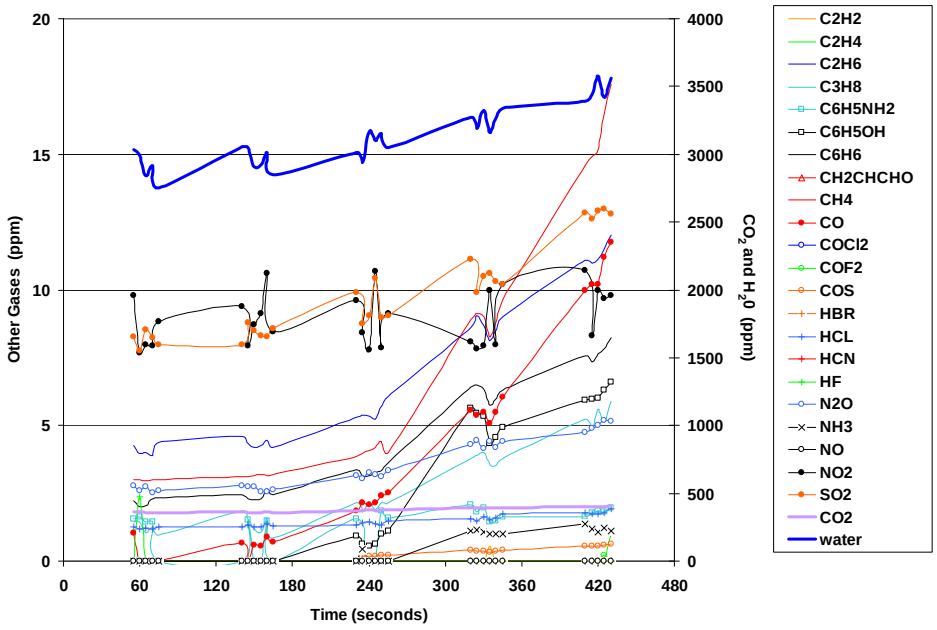

Figure 63. Concentration Histories of the Carbon/Epoxy Structural Composite Full-Scale Test at Forward Station, 5′6″ Height, Obtained by FTIR Analysis

The concentration histories obtained by continuous gas analyzers are illustrated in figures 64 and 65. As shown, the concentrations for CO were extremely low, reaching a maximum of about 0.004% at 5 minutes. Similarly, for CO_2, the concentrations only reached about 0.02% at the 5-minute point. The instability of the data is the result of the extremely low readings, which are at the limit of detection for these types of gas analyzers.

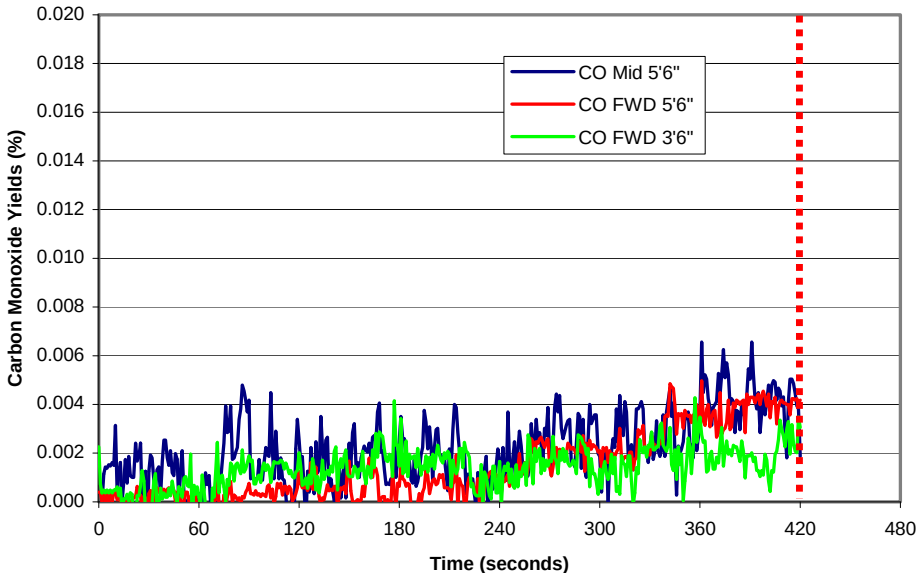

Figure 64. Carbon Monoxide Yield Histories for the Carbon/Epoxy Structural Composite Full-Scale Test Obtained by Gas Analyzers

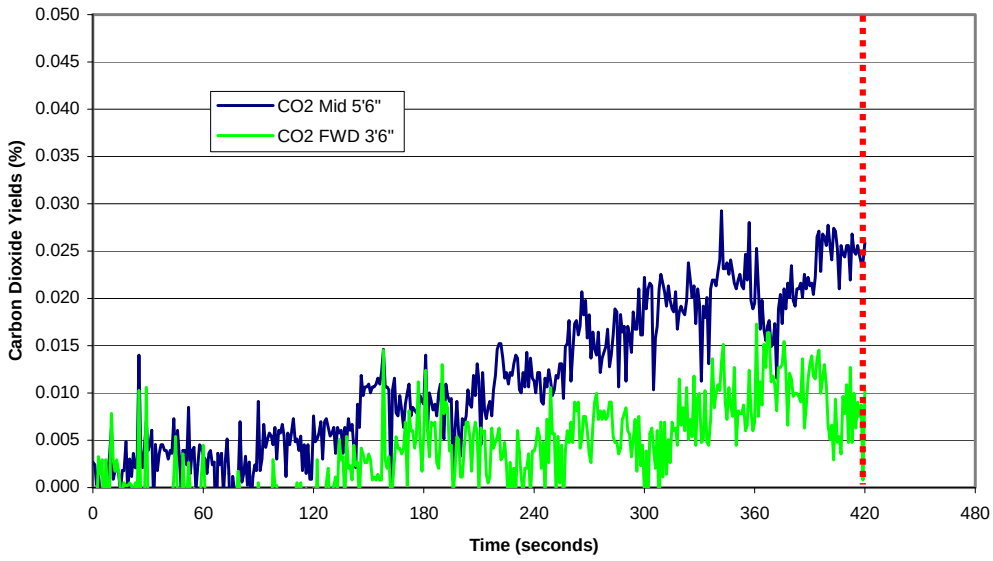

Figure 65. Carbon Dioxide Yield Histories for the Carbon/Epoxy Structural Composite Full-Scale Test Obtained by Gas Analyzers

A comparison of the gas yields based on FTIR data is shown in figure 66. The reported yields are the difference between the 5-minute concentrations and the initial concentrations. All gas concentrations were higher at the midstation, which was expected due to the close proximity to the fire.

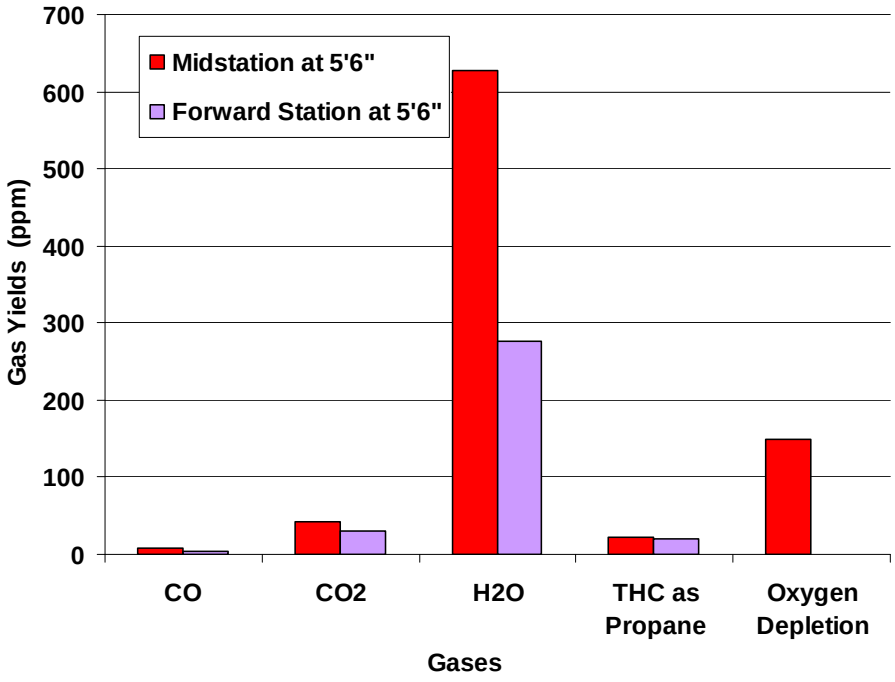

Figure 66. Gas Yield Comparison for the Carbon/Epoxy Structural Composite Material at Two Cabin Locations at 5 Minutes

The values obtained by FTIR are compared to the values obtained by the gas analyzers in figure 67. The agreement between the FTIR and the gas analyzer was good for the THC as propane. However, the CO and CO_2 gas analyzers recorded significantly higher levels than the FTIR. A posttest three-point calibration check of the gas analyzers revealed a change since the full six-point calibration check, indicating a Luft detection gas leak, requiring replacement of all the Luft detectors. In addition, instrument drift (namely, zero drift) and span drift may have accounted for some of the discrepancy. The span gases used for the gas analyzers were 2% CO and 10% CO_2. Lower span gas concentrations should have been used for these analyzers when monitoring gas concentrations at such low levels. Subsequent tests revealed much better agreement to the FTIR results.

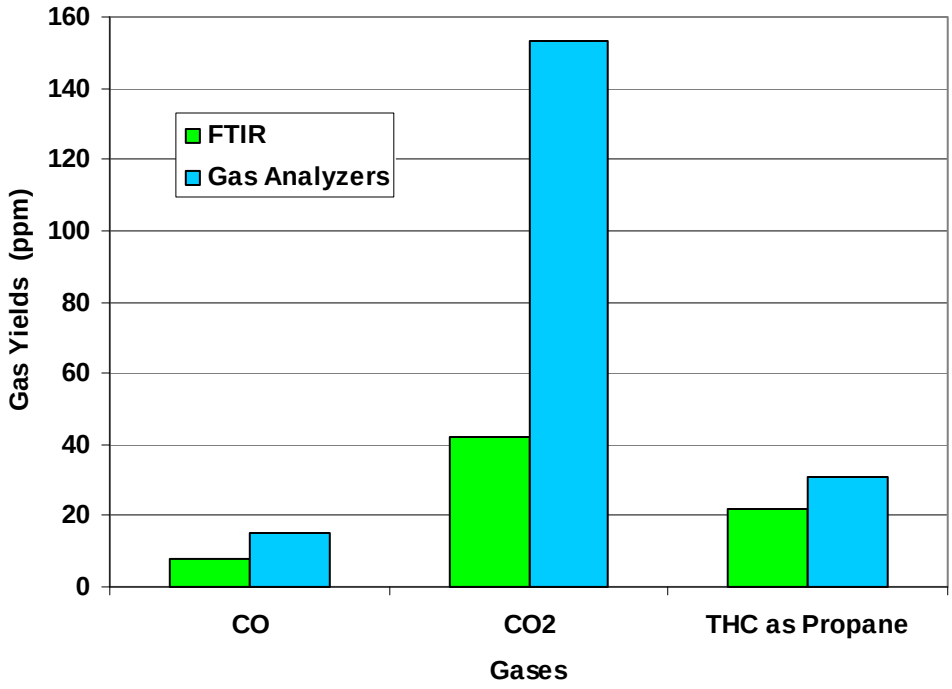

Figure 67. Comparison of Gas Yields Obtained by FTIR and Gas Analyzers for the Carbon/Epoxy Structural Composite Material at Midstation, 5′6″ Height, at 5 Minutes

5. DETERMINATION OF SCALING FACTORS.

The goal of the full-scale tests was to relate the concentration of thermal decomposition products that could accumulate inside an intact fuselage (when using a burnthrough-resistant insulation) to the amount accumulated in the laboratory-scale box test, when using identical materials. By comparing the results of the full- and laboratory-scale tests, empirical scaling factors can be obtained for a multitude of gases. The study focused on the gas concentrations generated from the insulation materials only, and not from additional cabin materials such as carpet, seats, or interior panels. In the case of the structural composite, this material was evaluated in a similar manner, as it was used as the burnthrough-resistant barrier in lieu of insulation blankets. All three full-scale tests were performed using the identical insulation and structural composite materials that were previously tested in the laboratory-scale box test.

The objective of comparing the full- and laboratory-scale test results was to determine the correlation between the measured gas levels. This relationship could then be used to establish appropriate acceptance levels in the laboratory equipment (for some or all of the gases measured during the tests). The use of scaled laboratory equipment to predict full-scale outcomes has been the accepted methodology for most other FAA fire test methods, since conducting full-scale tests is expensive and cumbersome, and only intended for developing the basic data to be used in the laboratory test design.

It should be noted that other factors may effect the results obtained in the full-scale apparatus compared to those obtained in the laboratory-scale apparatus. Measured gas levels may be a function of gas stratification, mixing, sampling location, surface absorption and absorption of water-soluble gases onto moist surfaces, and reaction with other gases.

In this report, scaling factors are defined in general terms as the ratio of laboratory-scale gas yields divided by the full-scale test gas yields. There are three scaling factors of interest:

1. The theoretical scaling factor as described in section 5.1.

2. The experimental scaling factor is described in section 5.2, which includes the contribution of combustion gases and fuel vapors from the external fire that infuse into the fuselage through the insulation system. The experimental scaling factor also includes losses due to condensation and absorption onto internal fuselage surfaces, as well as stratification, buoyancy, and circulation effects. The experimental scaling factor increases if surface losses, condensation, or an additional chemical reaction occurs, depleting the measured gases inside the test fuselage.

3. The corrected scaling factor is described in section 5.3, which does not include the contribution of infiltrating gases, surface losses, and the loss of gases due to chemical reactions. For each gas sampling location in the test fuselage, the corrected scaling factor should be the same for each reaction product at a given sampling location.

If 2. is less than 3. for gases such as CO and CO_2, which are not absorbed appreciably on surfaces, then the infiltrating fuel combustion products contribute to the experimental scaling factor.

If 2. is more than 3. for gases such as NH_3, which is absorbed readily on moist surfaces, then surface losses contribute to the experimental scaling factor for that gas.

5.1 THEORETICAL SCALING FACTORS.

5.1.1 Calculation of Volume in the Full- and Laboratory-Scale Apparatuses.

To accurately calculate the total volume of the full-scale test apparatus, it was divided into three sections: forward, mid, and aft (figure 68). The forward and aft sections encompassed the volume above the cabin floor only, whereas the midsection volume included the spaces both above and below the floor. This occurred since the floor was partly removed from the midsection, enabling gases to flow freely in the entire volume above and below the floor. The

volume below the floor was confined however, as the midsection lower lobe contained walls that prevented gas permeation forward and aft. When combined, the total volume of the test apparatus exceeded 9250 cubic feet.

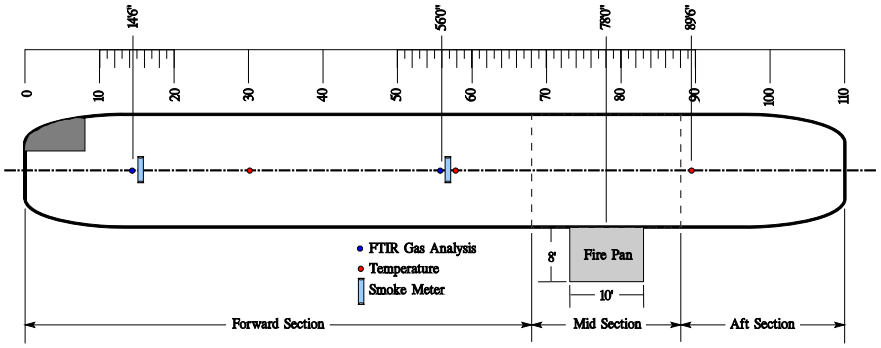

Forward Volume = Cabin Area x Fwd Length = (109899/144) x 68 = 5189.7 cu ft

Mid Volume = Total Cabin Area x Mid Length = (172031/144) x 20 = 2389.4 cu ft

Aft Volume = Cabin Area x Aft Length = (109899/144) x 22 = 1679 cu ft

Total Volume = Forward Volume + Mid Volume + Aft Volume

Total Volume = 5189.7 + 2389.4 + 1679 = 9258.1 cu ft

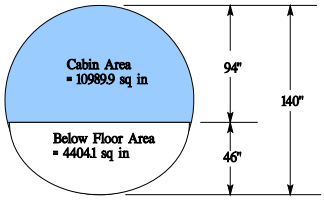

Figure 68. Volume Calculation of Full-Scale Test Apparatus

A similar calculation of the laboratory-scale apparatus volume was done, as shown in figure 69. This calculation was not as complex as the fuselage calculation, but simply, the volume of the cube minus the volume of the corner that was missing (to facilitate moving the apparatus under the overhead exhaust hood).

Box Volume = Cube Volume - Corner Volume

= (48 x 48 x 48) - 1/2 x (21 x 11.6 x 48)

= 110592 cu in - 5846 cu in

= 104746 cu in x (1 cu ft / 1728 cu in)

= 60.62 cu ft

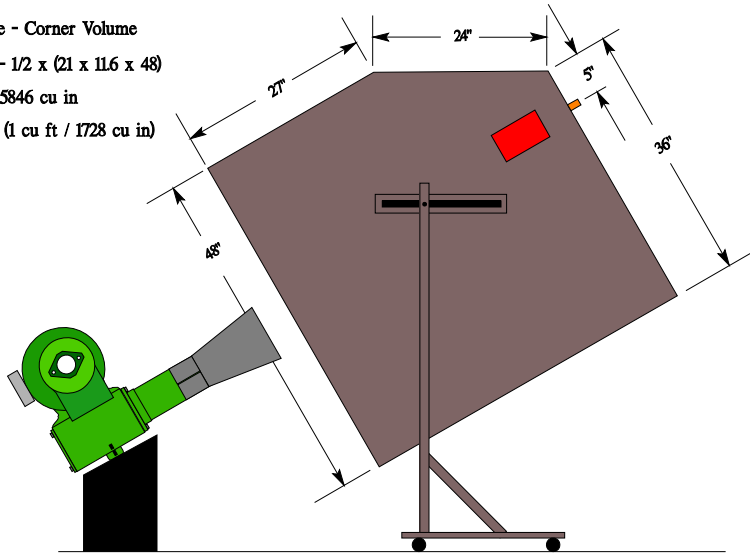

Figure 69. Volume Calculation of Laboratory-Scale Test Apparatus

In addition to the volume calculations, the amount of exposed material area to the fire threat was considered in both the laboratory- and full-scale tests. In both cases, the amount of material exposed was calculated, which was the entire area of each sample. The calculations were as follows:

- Exposed area of material in the full-scale test: (2 sheets) x 4 x 8 feet = 64 ft^2
- Exposed area of material in the laboratory-scale test: 36.5 x 36.5 inches = 1332.25 in^2 = 9.25 ft^2

5.1.2 Calculation of Theoretical Volumetric Scaling Ratio.

The full- and laboratory-scale apparatuses were not perfectly scaled to each other in terms of exposed sample area and the volume of the gas collection mechanism. The concentrations obtained in the laboratory-scale test were expected to be much higher than those obtained during the full-scale tests, simply because of the large difference in volume between the two. To better understand the relationship between the two apparatuses, a ratio of exposed test specimen area to the collection volume was calculated for each case:

- The ratio of the laboratory-scale volume to the exposed area is 60.62 ft^3/9.25 ft^2, or simply, 6.55 cubic feet of collection volume per square foot of exposed material area for this arrangement.
- The ratio of the full-scale volume to the exposed area is 9258.1 ft^3/64 ft^2, or simply, 144.7 cubic feet of collection volume per square foot of exposed material area for this arrangement.

By comparing the two test situations, a theoretical volumetric scaling ratio can be obtained. The volumetric scaling ratio between full- and laboratory-scale tests is 144.7/6.55 = 22.1. This indicates that the full-scale apparatus has approximately 22.1 times more collection volume per exposed sample area than the laboratory-scale apparatus. This would suggest that the resulting gas concentrations obtained in the laboratory apparatus would be 22.1 times more concentrated, or 22.1 times greater, assuming perfect mixing.

5.2 EXPERIMENTAL SCALING FACTORS.

5.2.1 Comparison of Gas Yields.

The actual tabulated 5-minute gas yield data obtained in the full- and laboratory-scale tests are shown in table 4. The reported 5-minute gas yields are the differences between the 5-minute concentrations and the initial concentrations. From the table, the first column lists the 21 gases measured, followed by the next three groups of columns that list the full-scale, 5-minute gas yields (in ppm) for the three material systems at both the mid- and forward-cabin sampling locations, all at a sampling height of 5′6″ (green, yellow, and blue columns). The last three columns list the gas yields obtained during the laboratory-scale tests. In this table, the FTIR data are shown for gases where multiple analysis methods were used.

Table 4. Comparison of Full-Scale (5′6″ Height) and Laboratory-Scale Gas Yields

Gas	Full-Scale Gas Yields at 5 Minutes (ppm)						Laboratory-Scale Gas Yields at 5 Minutes (ppm)		
	PAN/Metallized PVF		Fiberglass/Ceramic Barrier/ Metallized PVF (260 Sec)		Structural Composite				
	Midstation at 5′ 6″	Forward Station at 5′ 6″	Midstation at 5′ 6″	Forward Station at 5′ 6″	Midstation at 5′ 6″	Forward Station at 5′ 6″	PAN/ Metallized PVF	Fiberglass/ Ceramic Barrier/ Metallized PVF	Structural Composite
$C_6H_5NH_2$	4.6	3.3	5.5	3.3	1.7	0.3	68.7	91.1	6.1
C_6H_5OH	7.0	4.6	9.6	5.0	9.4	4.0	52.2	39.0	9.8
C_6H_6	10.5	10.4	8.1	4.6	7.2	3.2	76.6	52.5	8.3
CH_2CHCHO	0.0	0.0	0.0	0.0	0.0	0.0	55.5	146.0	0.0
$COCl_2$	0.0	0.0	0.0	0.0	0.0	0.0	0.0	3.9	0.0
COF_2	0.0	0.2	0.0	0.0	0.0	0.0	0.0	0.0	0.4
COS	0.0	0.6	0.0	0.0	0.5	0.3	38.7	0.0	0.8
HBr	0.0	0.0	0.0	0.0	0.0	0.0	0.0	0.0	0.0
HCl	0.0	0.0	0.0	0.0	0.5	0.3	0.0	0.0	3.4
HCN	16.4	10.8	0.0	0.0	0.0	0.0	467.0	111.7	0.0
HF	0.0	0.0	0.0	0.0	0.0	0.0	14.5	19.3	0.0
N_2O	4.0	9.9	7.8	3.7	3.0	1.0	18.8	62.6	0.0
NH_3	5.6	4.3	4.5	1.8	1.4	1.0	367.2	289.2	3.3
NO	0.0	0.0	0.0	0.0	0.0	0.0	0.0	0.0	0.0
NO_2	2.0	1.2	13.1	6.2	0.0	0.0	0.0	0.0	0.0
SO_2	19.8	2.1	2.0	1.3	2.8	2.6	246.6	0.0	31.2
CO	190.9	104.8	99.2	44.5	7.7	4.2	4645.8	2116.2	55.3
CO_2	1367.6	730.3	2674.7	1608.0	42.0	30.0	11506.6	12657.0	96.7
H_2O	1973.9	4885.0	3160.6	1684.0	627.0	276.0	10164.8	19430.0	1808.3
THC as Propane	97.9	72.2	68.2	55.2	22.0	20.8	629.7	903.5	22.0
Oxygen Depletion	3500.0	2100.0	6470.0	2920.0	150.0	No Data	3000.0	No Data	1200.0

5.2.2 Comparison of Experimental Scaling Factors.

The corresponding scaling factors are shown in table 5. The first three sets of columns in table 5 (green, yellow, and blue) display the scaling factors relating the 5-minute laboratory- and full-scale yields for each material system. These columns are the laboratory-scale yield divided by the full-scale yield for both sampling locations. The far right column displays the theoretical scaling factor for comparison.

Table 5. Comparison of Scaling Factors for the Three Material Systems Tested

Gas	PAN/Metalized PVF (5 Minutes)		Fiberglass/Ceramic Barrier/Metalized PVF (260 Seconds)		Structural Composite (5 Minutes)		Theoretical Scaling Factor
	Midstation	Forward Station	Midstation	Forward Station	Midstation	Forward Station	
$C_6H_5NH_2$	14.8	21.0	16.6	27.9	3.5	21.2	22.1
C_6H_5OH	7.4	11.4	4.1	7.8	1.0	2.4	22.1
C_6H_6	7.3	7.4	6.5	11.5	1.2	2.6	22.1
CH_2CHCHO	*	*	*	*	*	*	22.1
$COCl_2$	*	*	*	*	*	*	22.1
COF_2	*	*	*	*	*	*	22.1
COS	*	63.4	*	*	1.6	2.5	22.1
HBr	*	*	*	*	*	*	22.1
HCl	*	*	*	*	7.0	11.8	22.1
HCN	28.5	43.4	*	*	*	*	22.1
HF	*	*	*	*	*	*	22.1
N_2O	4.7	1.9	8.0	16.8	0.0	0.0	22.1
NH_3	66.2	85.0	64.3	159	2.4	3.3	22.1
NO	*	*	*	*	*	*	22.1
NO_2	*	*	*	*	*	*	22.1
SO_2	12.4	120	*	*	11.1	12.2	22.1
CO	24.3	44.3	21.3	47.6	7.2	13.2	22.1
CO_2	8.4	15.8	4.7	7.9	2.3	3.2	22.1
H_2O	5.1	2.1	6.1	11.5	2.9	6.6	22.1
THC as propane	6.4	8.7	13.3	16.4	1.0	1.1	22.1
Oxygen depletion	0.9	1.4	No data	No data	8.0	No data	22.1

*Not scalable since gas was not detected in laboratory- and/or full-scale tests.

The scaling factors are also shown graphically in figures 70, 71, and 72 (the theoretical scaling factor of 22.1 is indicated as dashed lines in these figures). From these data and charts, the 5-minute scaling factors (laboratory-scale yield divided by full-scale yield at 5 minutes) are generally lower at the midstation compared to the forward station. This is due to the higher yields obtained at midstation, which was closer to the fire. Because the scaling factors are calculated by dividing the laboratory-scale yield by the full-scale yield, the higher full-scale yields result in lower scaling factors at midstation.

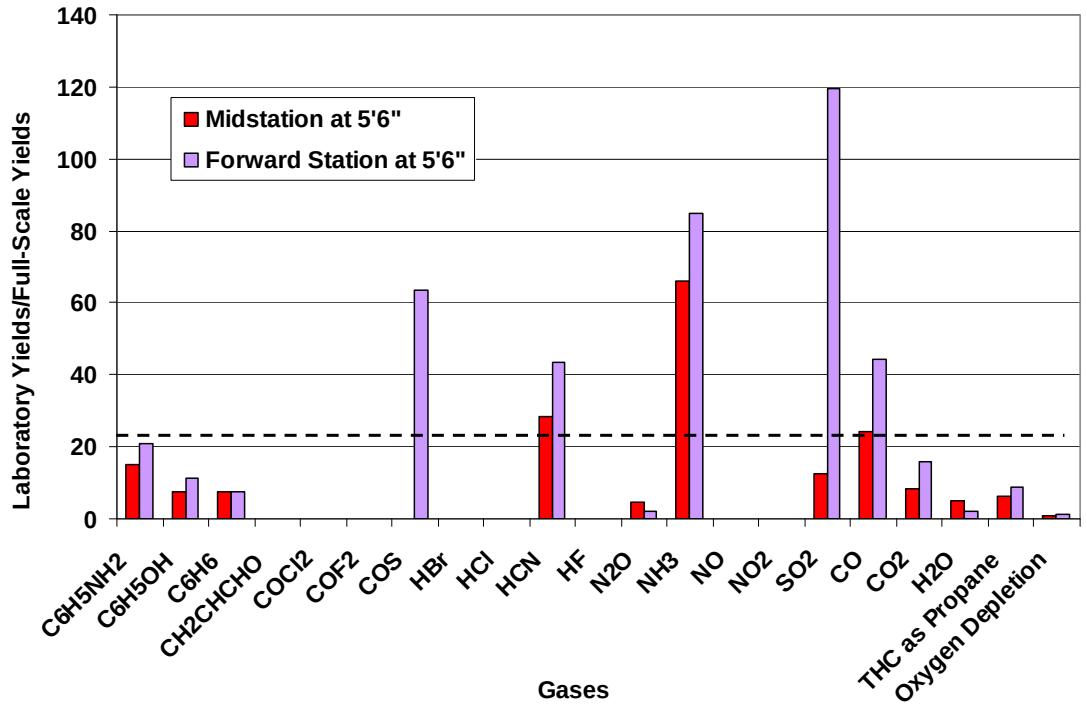

Figure 70. Scaling Comparison of Test Results Using PAN Insulation

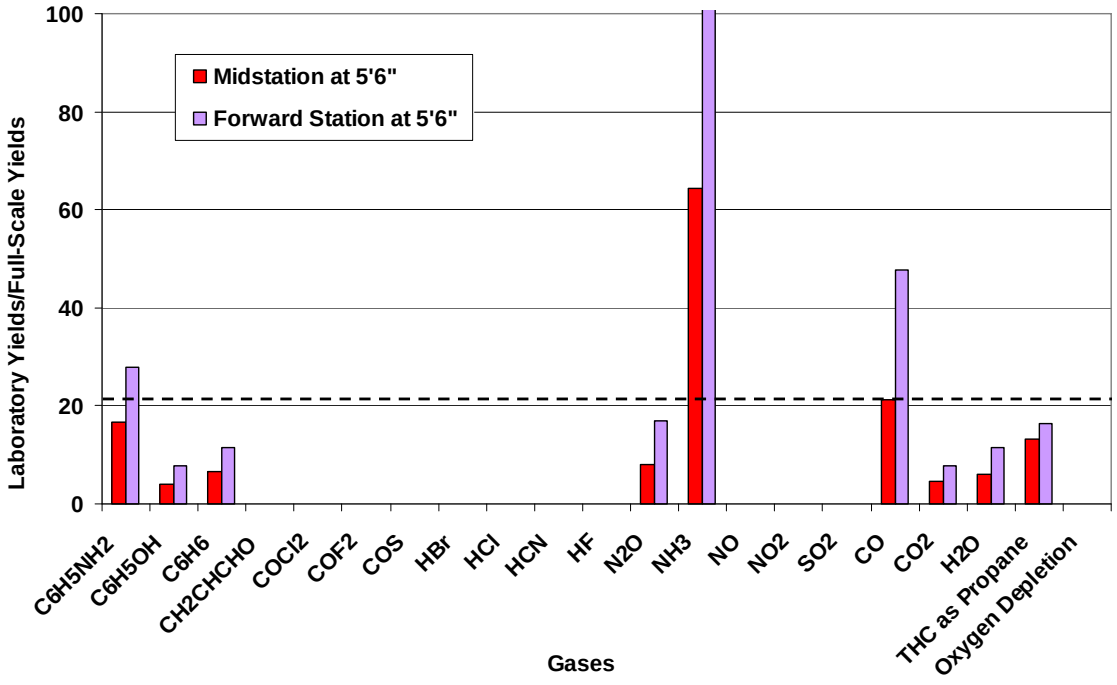

Figure 71. Scaling Comparison of Test Results Using the Fiberglass/Ceramic Barrier Insulation

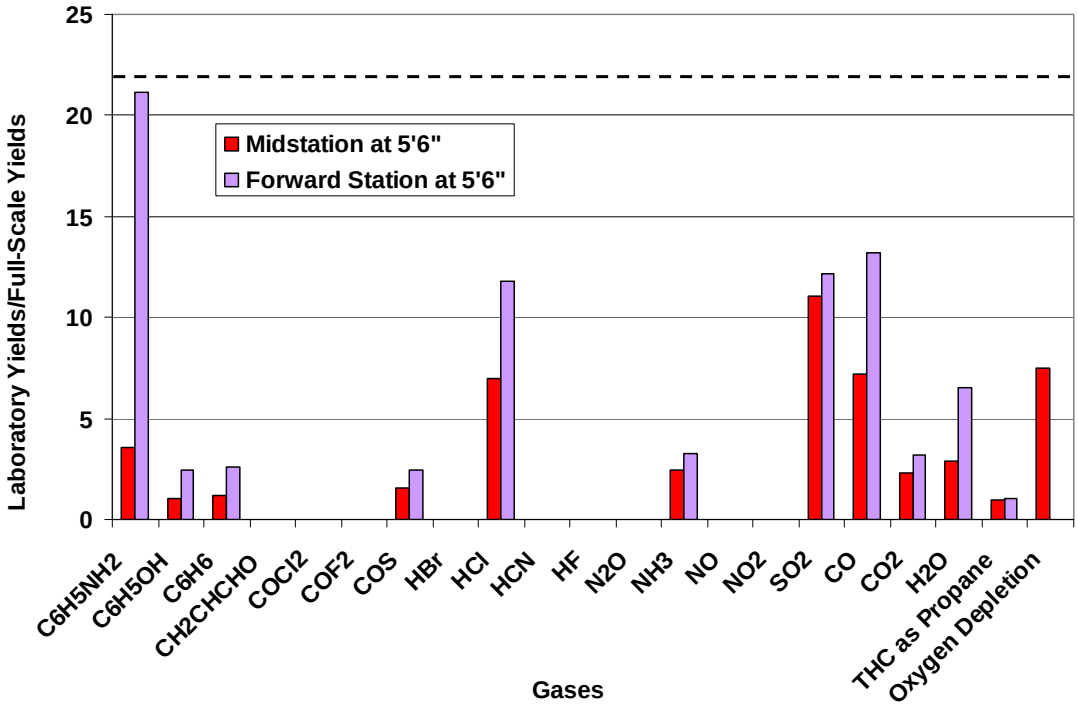

Figure 72. Scaling Comparison of Test Results Using Carbon/Epoxy Structural Composite

5.2.3 Assessment of Experimental Scaling Factors.

Figure 73 shows a comparison of the experimental scaling factors for all three material systems tested. The experimental gas scaling factors range from 1 to 159, deviating significantly from the theoretical scaling factor of 22.1. It appears that the scaling matches reasonably well on a per-gas basis at each sampling position for the PAN insulation system and the fiberglass/ceramic barrier insulation system. However, the scaling results from the carbon/epoxy structural composite appear to be much lower for most of the gases. For example, when measuring NH_3 at midstation at a height of 5′6″, the scaling factors are very high but match fairly closely to each other for both tests using insulation systems (66.2 for the PAN system and 64.3 for the fiberglass/ceramic barrier system), which is well above the theoretical value of 22.1. However, when the structural composite was tested, a scaling factor of 2.4 was obtained for NH_3, which was well below the theoretical value of 22.1. Infiltration of external fuel combustion products into the fuselage and internal surface losses may account for the scaling factor differences.

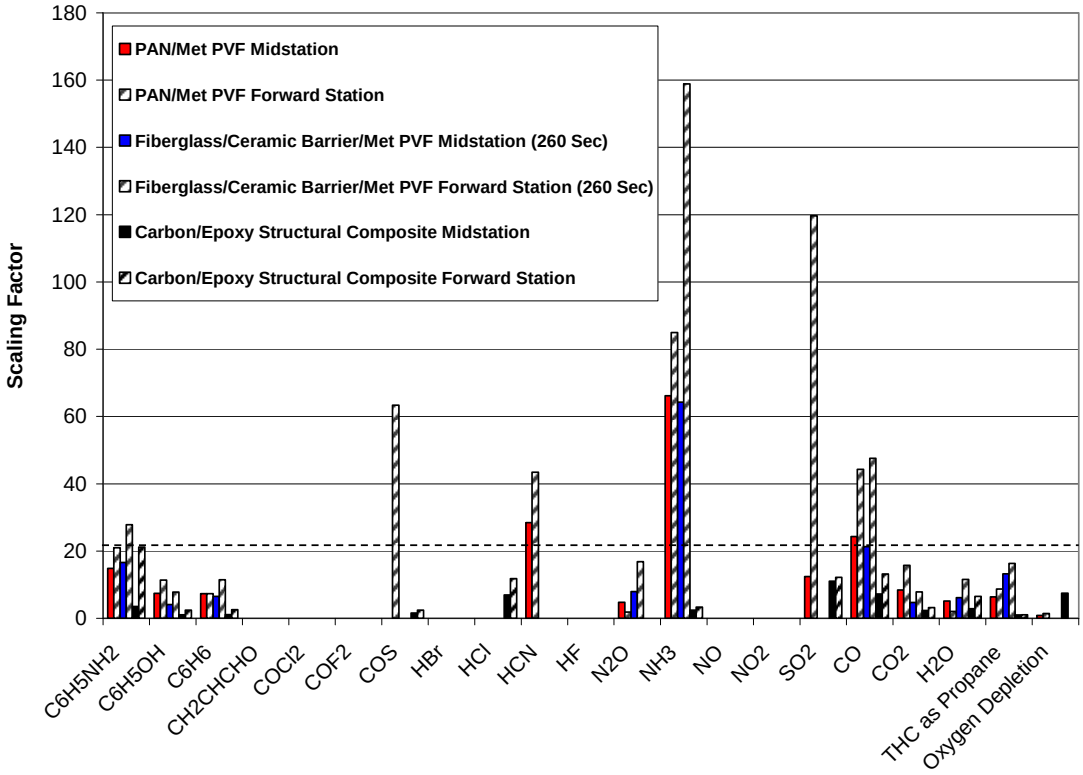

Figure 73. Scaling Comparison of Gas Yields for the Three Material Systems Tested for Mid- and Forward Stations, at a Height of 5′6″

Similarly, when measuring CO at midstation at 5′6″, the scaling factors matched fairly closely to the theoretical value of 22.1 for both tests using insulation systems (24.3 for the PAN system and 21.3 for the fiberglass/ceramic barrier system). However, when the structural composite was tested, a scaling factor of 7.2 for CO was obtained, which was well below the theoretical value. As indicated from the bar chart, the scaling factors for the structural composite material were lower than the other material systems tested for most of the measured gases, indicating higher-than-predicted, full-scale test concentrations. Low scaling factors for THC as propane and for gases, such as CO_2, H_2O, and O_2 depletion, may be due to infiltration of the fuel combustion products into the fuselage.

One possible explanation for this was the development of a small breach in the center seam between the two structural composite panels during the full-scale tests. Although the structural composite material performed extremely well at blocking the fuel fire flames, it was difficult to prevent the fire from eventually penetrating along the center seam between the two panels. This occurred approximately 3 minutes into the test when the curved steel channel member began to warp from the fire. This warpage eliminated the initial tight seal that existed between the composite material and the face of the curved steel channel at the beginning of the test. Although the breach was fairly small, it may have allowed the combustion gases from the external fire to infiltrate into the fuselage. The increased concentration in the full-scale test would result in a lower ratio of laboratory-scale to full-scale gas yields than would be expected with no gas infiltration into the fuselage.

Another possible contributing factor was that very low gas concentrations were observed for the structural composite full-scale tests compared to the other insulation systems tested, so the scaling was likely more sensitive to combustion gas infiltration, even in small quantities, from the burning external fuel fire during the full-scale test.

The assumption of perfect mixing is not likely to be valid during full-scale tests due, in part, to the sheer volume of the test apparatus itself. This large volume may prevent or limit the level of homogeneous gas mixing throughout the test apparatus, as the mixing level is highly time-dependent and may not reach a perfect mix until well after the data collection process has stopped. Under these circumstances, the levels obtained closer to the fire would be more highly concentrated (per volume), and the levels obtained further from the fire would be more diluted. This would cause the scaling ratios to be lower at the midstation than at the forward station. In reviewing the scaling data generated for all the tests, this was found to be true for all gases measured in all cases except two: N_2O and H_2O, during the PAN insulation test.

The theoretical scaling factor of 22.1 also assumes no condensation of gases to the surrounding interior structure or water solubility on these surfaces. The coarse, porous interior surface of the full-scale test apparatus provided a higher surface area compared to the relatively smooth interior surface of the laboratory-scale box test. Higher surface effects per unit volume are also expected for the fuselage due to the relative shapes of the two test apparatuses. The full-scale test apparatus has a larger surface-to-volume ratio than the laboratory-scale box test. A perfect sphere has a minimum surface to volume ratio. These surface effects would cause the full-scale gas yields to be somewhat lower, hence raising the scaling ratios. This could explain why NH_3 and SO_2, both highly water-soluble gases, have high scaling factors.

Stratification of the hot decomposition products in the upper levels was also expected, and these stratification profiles may differ for the large- and laboratory-scale tests, contributing to the deviation from the theoretical scaling factor of 22.1.

It is difficult to explain the relationship for each gas measured in the laboratory- and full-scale test configurations, as there may be a number of other factors involved that cannot be determined, which could influence the amount of each gas recorded. Although the theoretical volumetric scaling ratio of 22.1 between the two test apparatuses was clear, it was based on perfect mixing and the assumption of no gains or losses of combustion products in either apparatus. However, the data suggest that these assumptions may not be valid, and therefore, a simple volumetric scaling ratio may not be the best method for establishing the acceptable levels in the laboratory apparatus for each of the gases measured.

5.3 CORRECTED SCALING FACTORS.

The scaling factors shown in table 5 and figure 73 range from 1 to 66 for the midstation and 1 to 159 for the forward station. The analysis below determines the corrected scaling factors obtained when the contribution of infiltrating external gases and wall and reaction losses are removed, leaving only the contribution from the thermal decomposition of the insulation systems within the fuselage.

5.3.1 Infiltration of External Fuel Decomposition Products Into the Full-Scale Test Fuselage.

Fuel pan combustion gases could infiltrate into seams and openings in the fuselage or through the insulation system itself. The measured structural composite CO_2 concentration yields in table 4 were 42.0 and 30.0 ppm at 5 minutes for the mid and forward stations, respectively. The measured structural composite CO yields were 7.7 ppm and 4.2 ppm. It has been determined in section 3.1 that the $\Delta CO_2/\Delta CO$ ratio for the burner fire (no test sample) used in the laboratory-scale tests is in the order of 300 and is expected to be similar for the full-scale tests, since the incident heat flux of the two fires matches. Therefore, the expected infiltration of CO relative to CO_2 into the fuselage should be very low. If the 5-minute structural composite yields of CO_2 were due to infiltration only, then the expected infiltration of CO based on the 300/1 $\Delta CO_2/\Delta CO$ ratio would be approximately 0.1. The very low, yet higher-than-expected levels of CO measured during the full-scale structural composite test may be due to the decomposition of the other residual materials or soot within the aircraft.

Video documentation of the interior of the full-scale test fuselage indicated little to no infiltration of external fire gases was seen during the structural composite material test. Since the external fuel fire was identical for all three material system tests, and little to no infiltration was observed for the structural composite, the higher-than-expected levels of decomposition products observed for the burnthrough-resistant conventional batt-style insulation systems were likely due to the permeation of fire gases through the insulation itself, and not the result of entry through small openings and seams in the intact test fuselage. The more porous nature of the conventional batt-style insulation systems resulted in more significant infiltration of fuel combustion gases and fuel vapors into the fuselage. This generally occurred after 1 minute of fuel fire exposure, when the metallized PVF film melted and no longer formed an impermeable barrier to the external fire gases.

5.3.2 Scaling Factors With Contribution of Infiltrating Gases and Surface and Reaction Losses Removed.

5.3.2.1 Theory.

The stoichiometry of the thermal decomposition of each chemical in a given insulation material should be identical for both the small- and full-scale tests since the samples are exposed to the same heat flux. For a given chemical reaction, the ratio of the yields of two thermal decomposition products expressed as the change in concentration (Δppm (v/v)) are identical to the ratio of the number of moles of the reaction products. For any balanced chemical reaction with two or more reaction products

$$aA \rightarrow bB + cC + \ldots nN$$

The following equality holds for

$$\frac{b}{c} = \frac{n_B}{n_C} = \frac{\nu_B}{\nu_C} = \frac{\dfrac{\nu_B}{\nu_{compartment}} \times 10^{+6}}{\dfrac{\nu_C}{\nu_{compartment}} \times 10^{+6}} = \frac{ppm_B}{ppm_C}$$

Since the reactions are the same for the laboratory- and full-scale tests

$$\frac{\left(\dfrac{b}{c}\right)_{Full-Scale}}{\left(\dfrac{b}{c}\right)_{Lab-Scale}} = \frac{\left(\dfrac{ppm_B}{ppm_C}\right)_{Full-Scale}}{\left(\dfrac{ppm_B}{ppm_C}\right)_{Lab-Scale}} = 1$$

where

n_B = the number of moles of a chemical compound B in an enclosure
ν_B = the volume of chemical B in an enclosure
$\nu_{compartment}$ = the volume of the compartment

For this pyrolysis reaction, assuming C is carbon monoxide (CO) and the change in the concentration of gas B is ΔB and the change in the concentration of CO is ΔCO, then

$$\left(\frac{\Delta B}{\Delta CO}\right)_{Full-Scale,5\ minutes} = \left(\frac{\Delta B}{\Delta CO}\right)_{Lab-Scale,5\ minutes}$$

The above relation holds true when there are no gains and losses of combustion products in the fuselage.

The experimental scaling factors need to be corrected to remove the contribution of infiltrating gases, and wall and reaction losses. To accomplish this, the first-order approximation for the corrected experimental scaling factor can be obtained for each gas and each material by applying a correction multiplier to the experimental scaling factor: The ΔB/ΔCO ratio for the full-scale test at 5 minutes divided by the ΔB/ΔCO ratio for the laboratory-scale test at 5 minutes. The multiplier is unity if there is no infiltration of outside gases, and no reaction or wall losses. The first-order approximation of the scaling factor for each gas G, assuming no infiltration of CO from the external fire with a correction for infiltration (or loss of gas B), is shown in equation 1.

$$SF_{B,5\ minutes_{1stOrderApproximation}} = \frac{\left(\dfrac{\Delta B}{\Delta CO}\right)_{Full-Scale,5\ minutes}}{\left(\dfrac{\Delta B}{\Delta CO}\right)_{Lab-Scale,5\ minutes}} \times SF_{B,5\ minutes_{Experimental}} \qquad (1)$$

This scaling factor is independent of the stoichiometry of the reactions.

5.3.2.2 Application.

The first-order correction multiplier for the 5-minute experimental scaling factors, assuming no infiltration of CO are shown in table 6.

Table 6. First-Order Correction Multiplier for 5-Minute Experimental Scaling Factors, Assuming no Infiltration of CO

Gas	PAN/Metallized PVF		Fiberglass/Ceramic Barrier/Metallized PVF (260 Seconds)		Structural Composite	
	Mid	Forward	Mid	Forward	Mid	Forward
CO_2	2.89	2.81	4.52	6.04	3.10	3.90
THC as propane	3.77	5.07	1.57	2.90	7.19	12.4
H_2O	4.72	21.3	3.47	4.12	2.50	2.01
HCN	0.855	1.03	*	*	*	*
$C_6H_5NH_2$	1.63	2.13	1.29	1.72	2.00	0.65
C_6H_5OH	3.27	3.91	5.25	6.10	6.88	5.38
C_6H_6	3.34	6.02	3.29	4.17	6.23	5.08
COS	*	0.687	*	*	4.49	4.92
N_2O	5.18	23.4	2.66	2.42	*	*
NH_3	0.371	0.519	0.332	0.296	3.05	3.99
SO_2	1.95	0.378	*	*	0.645	1.10
O_2 depletion	28.4	31.0	**	**	0.898	**

*$\Delta B = 0$ for laboratory- and/or full-scale tests
**Not measured

Table 7 shows that applying a first-order correction multiplier from table 6 to the experimental scaling factors in table 5 resulted in uniform scaling for all gases for each material and location for the conventional batt-style insulation materials. The structural composite, which had much lower gas yields had its scaling factors increase substantially, but are a third of the value of the scaling factors for the conventional style insulation systems. Table 7 also shows that the scaling factors are dependant on the gas sampling position, with much higher scaling factors resulting at the forward sampling position, further from the fire. Higher scaling factors were expected at the more distant sampling location, as they are a ratio of laboratory-scale yields divided by the full-scale yields (a lower full-scale yield will result in a higher scaling factor).

Table 7. Laboratory- and/or Full-Scale Gas Yields Scaling Factors at 5 Minutes With First-Order Correction for Gas Infiltration, Wall Losses and Reactions, Assuming no Infiltration of CO

Gas	PAN/Metalized PVF		Fiberglass/Ceramic Barrier/Metalized PVF (260 Seconds)		Structural Composite	
	Mid at 5′6″	Forward at 5′6″	Mid at 5′6″	Forward at 5′6″	Mid at 5′6″	Forward at 5′6″
CO_2	24.3	44.4	21.2	47.7	7.1	12.5
THC as propane	24.2	44.1	20.8	47.6	7.6	13.6
H_2O	24.1	44.7	21.2	47.4	7.3	13.3
HCN	24.3	44.5	*	*	*	*
$C_6H_5NH_2$	24.3	44.3	21.4	47.6	7.2	13.1
C_6H_5OH	24.4	44.5	21.3	47.6	7.1	13.2
C_6H_6	24.4	44.4	21.3	47.9	7.2	13.1
COS	*	43.6	*	*	7.2	12.3
N_2O	24.3	44.4	21.3	40.7	*	*
NH_3	24.6	44.1	21.3	47.0	7.3	13.2
SO_2	24.2	45.2	*	*	7.2	13.4
O_2 depletion	24.3	44.2	**	**	7.2	**
Average	24.3	44.4	21.2	46.7	7.2	13.1

*Can not scale since analyte gas was not detected in laboratory- and/or full-scale tests.
**Not measured.

The corrected scaling factors in table 7 for the PAN/Metallized PVF at the mid and forward station were based on full 5-minute laboratory- and full-scale tests. The fiberglass/ceramic barrier scaling factors were based on a 260-second, full-scale test and were slightly lower.

The amount of CO that infiltrated the test fuselage from the external fuel fire or that originated from the decomposition of other materials inside the fuselage can be recursively estimated by applying equation 2 in place of equation 1. The solution is obtained when the scaling factors for the structural composite match the average of the scaling factors of the PAN/Metallized PVF insulation system. A small infiltration of 5.4- and 3.1-ppm CO for the mid and forward sampling stations, respectfully, would account for the low structural composite scaling factors. Replacing equation 1 with the following equation brings the structural composite scaling factors up to match the scaling factors of the conventional insulation systems (table 8).

$$SF_{B,5\ minutes_{1stOrderApproximation}} = \frac{\left(\frac{\Delta B}{\Delta CO - \Delta CO_{infiltrating}}\right)_{Full-Scale,5\ minutes}}{\left(\frac{\Delta B}{\Delta CO}\right)_{Lab-Scale,5\ minutes}} \times SF_{B,5\ minutes_{Experimental}} \quad (2)$$

Table 8. Laboratory- and/or Full-Scale Gas Yields Scaling Factors at 5 Minutes With Second-Order Correction for CO Infiltration

Gas	PAN/Metallized PVF		Fiberglass/Ceramic Barrier/Metallized PVF (260 Seconds)		Structural Composite	
	Mid at 5′6″	Forward at 5′6″	Mid at 5′6″	Forward at 5′6″	Mid at 5′6″	Forward at 5′6″
CO	25.0	45.7	22.5	51.1	23.7	48.9
CO_2	25.0	45.7	22.4	51.3	23.0	47.2
THC as propane	24.9	45.4	22.5	51.2	25.1	50.9
H_2O	24.7	46.1	22.4	50.9	23.9	49.3
HCN	25.2	46.3	*	*	*	*
$C_6H_5NH_2$	25.0	45.6	22.6	51.1	25.8	48.9
C_6H_5OH	25.1	45.9	22.5	51.1	23.7	74.0
C_6H_6	25.1	45.7	22.6	52.0	23.7	48.9
COS	*	44.9	*	*	23.7	45.9
N_2O	25.0	45.7	22.5	43.8	*	*
NH_3	25.3	45.5	22.6	50.5	24.2	48.9
SO_2	24.9	46.6	*	*	23.6	49.8
O_2 depletion	25.0	45.7	**	**	23.7	**
Average	25.0	45.8	22.5	50.3	24.0	48.7***

*Cannot scale since analyte gas was not detected in laboratory- and/or full-scale tests.
**Not scalable since oxygen not measured
***The highest value was dropped for the average.

Equation 1 is sufficient for a particular insulation system only if the 5-minute ΔCO yield is much greater than the $\Delta CO_{infiltration}$ through that insulation system. This is the case for the conventional batt-style insulation materials tested. The table 7 scaling factors (assuming no CO infiltration) are similar for both conventional style insulation systems, despite vastly different experimental 5-minute CO yields observed for both tests as shown in table 4.

Table 9 shows the optimized scaling divisor that could be applied to future laboratory-scale test yields to predict full-scale gas yields. These scaling factors predict the concentrations of the decomposition products of the insulation system. They were corrected to remove the

contribution of infiltrating external fire gases through the insulation system and chemical reaction and wall losses.

Table 9. Laboratory- and/or Full-Scale Corrected Gas Yields Scaling Factors for Predicting Gas Concentrations in Full-Scale Fuselage at 5 Minutes

Station	Corrected Scaling Factor (corrected to remove the contribution of external gas infiltration, assuming no CO infiltration)	Corrected Scaling Factor (corrected to remove the contribution of external gas infiltration, including CO infiltration)
Mid at 5′6″	24	25
Forward at 5′6″	44	50

The theoretical scaling factor of 22.1, assuming perfect mixing is very close to the corrected scaling factors of 24 and 25 obtained at the midstation, 5′6″ high sampling position.

6. TOXICITY.

Toxicity limits for future, burnthrough-compliant aircraft insulation systems could be set based on an equivalent level of safety with the two batting-style insulations systems tested under full-scale conditions (i.e., the PAN insulation system and the fiberglass system with the ceramic barrier). The limits could be based on a 5-minute exposure period. The 5-minute period is based on an analysis of past accidents, which suggests that a large majority of passengers completed the evacuation phase at this point. Limits could be based on a fraction of a 5-minute incapacitating and/or lethal concentration or they could be based on 5-minute exposure limits extrapolated from existing standards. Existing standards, intended for other purposes, include "Documentation for Immediately Dangerous to Life and Health Concentrations (IDLH)," published by the U.S. National Institute for Occupational Safety and Health (NIOSH) and "Emergency Response Planning Guidelines" (ERPG). ERPGs are developed by the Emergency Response Planning committee of the American Industrial Hygiene Association.

The definition for the cited exposure limits are listed below:

- Lethal Concentratrion, 50% (LC_{50})—5 minutes is the predicted concentration that would cause lethality to 50% of an exposed population based on the Fractional Effective Dose (FED) model developed by Speitel [13].

- Incapacitation Concentration—5 minutes is the predicted concentration that would cause incapacitation to 50% of an exposed population based on the FED model developed by Speitel [13].

- ERPG-2 is the maximum airborne concentration below which it is believed nearly all individuals could be exposed for up to 1 hour without experiencing or developing irreversible or other serious health effects or symptoms which could impair an individuals ability to take protective action.

- ERPG-3 is the maximum airborne concentration below which it is believed that nearly all individuals could be exposed for up to 1 hour without experiencing life-threatening health effects.

- IDLH is defined by NIOSH as exposure to airborne contaminants that is "likely to cause death or immediate or delayed permanent adverse health effects or prevent escape from such an environment." The IDLH is based on a 30-minute exposure.

Table 10 shows the exposure limits from various references for the gases selected from the 24 gases that were measured for the laboratory- and full-scale tests. For each selected gas, several columns of exposure limits are displayed for various exposure times. ERPGs and IDLHs extrapolated to 5-minute exposures are also listed in table 10. The minimum of the 5-minute exposure limits is shown in the seventh column of table 10. IDLH values were not extrapolated for CO_2, since the concentration-time products change with concentration. Care should be taken in calculating the extrapolated 5-minute toxicological limits in the absence of other toxicological data, since the 5-minute values were derived assuming that Haber's Rule holds. Haber's Rule assumes that the concentration-time product required to produce an effect is constant.

For example, the second and third columns labeled "Incapacitation Concentration" and "LC_{50}" lists the predicted concentration that would cause incapacitation and lethality, respectively to 50% of exposed people for a 5-minute exposure to a constant gas concentration, based on a FED model developed by Speitel [13]. This model predicts the amount of time a human has to escape an aircraft fire, using regression equations based on numerous sources for many animal species over a wide exposure concentration range. The effect of CO_2 increasing the uptake of other gases is included in this model. This survival model uses incapacitation data to obtain a fractional effective dose for incapacitation (FED_I) and lethality data to obtain a fractional effective dose for lethality (FED_L). The time when either FED reaches 1 determines the exposure time available to escape from an aircraft cabin fire and to survive postexposure. Speitel has shown that the primary toxic contribution of CO_2 in aircraft cabin fires is the increased uptake of other gases induced by the inhalation of CO_2 [13]. In Speitel's models, the multiplication factor for the enhanced uptake of other gases, V_{CO_2}, is factored into the concentration term in the regression equations for all hazards with the exception of CO_2, O_2, and temperature, where

$$V_{CO_2} = \frac{e^{0.2496 \times C_{CO_2} + 1.9086}}{6.8} \quad \text{and} \quad C_{CO_2} = \%CO_2$$

Table 10. Exposure Limits of Gases From Various References

Gas	Exposure Limits From Various References (ppm)								
	5-Minute Exposure						60-Minute Exposure		30-Minute Exposure
	Incapacitation Concentration	LC_{50}	Derived From 60-Minute ERPG-2	Derived From 60-Minute ERPG-3	Derived From 30-Minute IDLH	Minimum 5-Minute Exposure Limit	ERPG-2 (2008)	ERPG-3 (2008)	IDLH (1995)
$C_6H_5NH_2$	*	*	*	*	600	600	*	*	100
C_6H_5OH	*	*	600	2,400	1500	600	50	200	250
C_6H_6	*	*	1800	12,000	3000	1,800	150	1000	500
CH_2CHCHO	10,928	7,783	2.4	24	12	2.4	0.2	2	2
$COCl_2$	*	100	2.4	12	12	2.4	0.2	1	2
COF_2	3832** (HF)	3,614** (HF)	120	300	90	90	10 (HF)	25 (HF)	15 (HF)
COS	500* (500 for 15 minutes, brain damage)	333* (1000 for 15 minutes)	360	1,200	*	333	30 (H_2S)	100 (H_2S)	*
HBr	16,830 (HCl)	15,900 (HCl)	240	1,800	180	180	20 (HCl)	150 (HCl)	30
HCl	16830	15,900	240	1,800	300	240	20	150	50
HCN	176	560	120	300	300	120	10	25	50
HF	7663	7,227	240	600	180	240	20	50	30
N_2O	*	*	*	*	*		*	*	*
NH_3	*	*	1800	9,000	1800	1,800	150	750	300
NO	12,850 (NO_2)	4,260 (NO_2)	900	1,800	600	600	75 (NO_2)	150 (NO_2)	100
NO_2	2570	852	180	360	120	120	15	30	20
SO_2	*	2,115	36	180	600	36	3	15	100
CO	6,850	16,600	4200	6,000	7200	4,200	350	500	1,200
CO_2	88,000	*	*	*	*	88,000	*	*	40,000
Oxygen depletion	136,000	*	*	*	*	136,000	*	*	*

* = Data not available
** = Extrapolated from the LC50
(X) = Estimated value based on gas X (e.g., LC_{50} for COF_2 is estimated based on LC_{50} of HF)

Note there is a 2 to 3 order of magnitude variation for the different 5-minute toxicity limits in table 10 for CH_2CHCHO, HF, HBr, and HCl. Incapacitation and lethality are suitable limits to use for survival modeling. However, the limits drop considerably when health effects are also considered, as is the case for ERPG and IDLH limits, which are set to protect sensitive populations. There are significant gaps in health effect toxicity data and some ERPGs and IDLHs may be set lower than they would be if sufficient health effect data was available to ensure safety.

6.1 SELECTION OF GASES TO BE EVALUATED.

Table 11 shows the laboratory-scale and full-scale gas yields at 5 minutes and the calculated FEDs for survival and health effects. Simple FEDs were calculated as the ratio of the maximum full-scale 5-minute yield to the 5-minute exposure limits for each gas. More accurate FEDs can be calculated using the FED modeling developed by Speitel [13]. The calculated FED ratios in table 11 are based on survival and ERPG3-based health effects. The survival FED ratios are based on the lower of the 5-minute incapacitation concentration and LC_{50} for each gas.

The FEDs shown in the last 4 columns of table 11 are based on the experimental yields and the yields corrected for gas infiltration. The corrected yields were obtained by dividing the 5-minute laboratory-scale yields by the scaling divisor, 25.

The simple ratio method used in table 11 significantly overestimates the survival FEDs for gases that deviate greatly from Haber's Rule such as HCN, CO_2 and O_2 depletion, as observed in the second-to-last column in table 11. However, it errs on the side of safety and may be useful to assess toxicity for the other gases.

It is clear from the 5-minute exposure FEDs in the last four columns in table 11 that there is a negligible survival hazard for the three insulation systems tested. It is also clear, based on ERPG-3-based health limits, that there is a small health hazard for these materials.

Table 11. Fractional Effective Dose at 5 Minutes

Gas	Laboratory-Scale Gas Yields at 5 Minutes (ppm)			Maximum Full-Scale Gas Yields at 5 Minutes Into Test (Experimental) (ppm)			Maximum Full-Scale Gas Yields at 5-Minutes (Predicted From Laboratory-Scale Using Scaling Factor = 25) (ppm)			Maximum FED (Experimental) Maximum 5-Minute Yield/Minute Limit		Maximum FED (No Gas Infiltration) Maximum 5-Minute Yield/Minute Limit	
	PAN/ Metalized PVF	Fiberglass/ Ceramic Barrier/ Met PVF	Structural Composite	PAN/ Metalized PVF	Fiberglass/ Ceramic Barrier/ Metalized PVF	Structural Composite	PAN/ Metalized PVF	Fiberglass/ Ceramic Barrier/ Metalized PVF	Structural Composite	Based on Survival	Based on Health Effects (ERPG-3)	Based on Survival	Based on Health Effects (ERPG-3)
$C_6H_5NH_2$	68.7	91.1	6.1	4.63	5.5	1.73	2.7	3.6	0.2	*	*	*	*
C_6H_5OH	52.2	39.0	9.8	7.02	9.57	9.4	2.1	1.6	0.4	*	0.004	*	0.001
C_6H_6	76.6	52.5	8.3	10.5	8.05	7.21	3.1	2.1	0.3	*	0.001	*	0.000
CH_2CHCHO	55.5	146	0.0	0	0	0	2.2	5.8	0.0	0	0	0.001	0.242
$COCl_2$	0.0	3.9	0.0	0	0	0	0.0	0.2	0.0	0	0	0.002	0.017
COF_2	0.0	0.0	0.4	0.21	0	0	0.0	0.0	0.0	0	0.001	0.000	0
COS	38.7	0.0	0.8	0.61	0	0.53	1.5	0.0	0.0	0.002	0.001	0.005	0.001
HBr	0.0	0.0	0.0	0	0	0	0.0	0.0	0.0	0	0	0.000	0.000
HCl	0.0	0.0	3.4	0	0	0.49	0.0	0.0	0.1	0	0	0.000	0.000
HCN	467	111.7	0.0	16.4	0	0	18.7	4.5	0.0	0.093 (0)**	0.055	0.106 (0)**	0.062
HF	14.5	19.3	0.0	0	0	0	0.6	0.8	0.0	0	0	0.000	0.001
NH_3	367	62.6	0.0	5.55	4.5	1.36	14.7	2.5	0.0	*	0.001	*	0.002
NO	0.0	289	3.3	0	0	0	0.0	11.6	0.1	0 (0)**	0	0.003	0.006
NO_2	0.0	0.0	0.0	2.02	13.13	0	0.0	0.0	0.0	0.015 (0)**	0.036	0	0.000
SO_2	247	0.0	0.0	19.8	2.04	2.82	9.9	0.0	0.0	0.009 (0.002)**	0.110	0.005 (0.001)**	0.055
CO	4,646	0.0	31.2	191	99.2	7.7	186	0.0	1.2	0.028 (0.028)**	0.032	0.027 (0.027)**	0.031
CO_2	11,507	2,116	55.3	1368	2675	42	460	84.6	2.2	0.030 (0)**	*	0.005 (0) **	*
Oxygen depletion	10,165	12,657	96.7	3500	6470	150	407	506	3.9	0.048 (0)**	*	0.004 (0)**	*

*Data not available
**Calculated from reference 13

7. SUMMARY.

A laboratory-scale test method was developed for evaluating the products of combustion emitted from fuselage/insulation samples designed to remain intact during exposure to a simulated external jet fuel fire. The equipment used in the test (an oil-fired burner and a 4- by 4- by 4-foot steel cube box used to mount representative test samples) effectively simulated the desired postcrash fire condition. The cube box also served as an enclosure to collect and analyze emitted gases during fire exposure.

Test samples representing three fuselage constructions were tested using laboratory- and full-scale apparatuses to measure the emission of combustion gases from the nonexposed side when subjected to a simulated external jet fuel fire. Two fuselage configurations were initially evaluated, consisting of aluminum skin and accompanying insulation materials that met the new FAA thermal-acoustic insulation burnthrough standard: a PAN fiber-containing material and a ceramic-based, lightweight barrier in conjunction with standard fiberglass batting. These two configurations were primarily run to establish a baseline of the amount and type of gases emitted during exposure for comparing other fuselage and insulation samples to. In addition, a third fuselage construction was tested consisting of a prototype carbon/epoxy structural composite material (without thermal acoustic insulation). It was determined that the multi-ply, structural composite material produced minimal quantities of smoke, toxic gases, and hydrocarbons during a 5-minute exposure. Approximately 7 plies of the 16-ply test panel were penetrated by the fire. Overall, the aluminum skin/insulation configurations generated much higher gas concentrations than the composite material during the 5-minute exposure.

Theoretical, experimental, and corrected scaling factors relating the full- and laboratory-scale 5-minute gas concentrations were determined for gases of toxicological significance for the three insulation systems (the experimental scaling factors were corrected for infiltration of external combustion gases). These corrected scaling factors can be applied to future laboratory-scale tests to predict full-scale toxic gas concentrations. Toxicity criteria can be applied to these simulated full-scale concentrations to assess the hazard of toxic thermal decomposition products.

The explosive hazard of the buildup of combustible gases for full-scale fire tests of insulation systems was found to be insignificant.

The theoretical scaling factor of 22.1, assuming perfect mixing, is very close to the corrected scaling factor of 24 and 25 (assuming no CO infiltration and including CO infiltration, respectively) obtained at midstation at a height of 5′6″. It is more conservative than the 24 and 25 scaling factor values, in that it slightly overestimates the concentration in the full-scale test fuselage midstation sampling station at a height of 5′6″.

Applying the aircraft-appropriate theoretical, perfect mixing scaling divisor to the box test data would provide a practical method for estimating gas concentrations to be used in a hazard assessment of the pyrolysis products for burnthrough-resistant aircraft insulation systems exposed to an external fuel fire. This scaling factor does not consider infiltration of external gases or losses due to chemical reactions or absorption onto surfaces.

When exposed to the thermal conditions of the external fuel fire, the melting of the metallized PVF insulation batting film used with the conventional batt-style insulation systems allowed the fire gases to permeate the insulation and enter the fuselage. In contrast, the structural composite material prevented the penetration of external fire gases into the aircraft. Consideration should be given to upgrade the PVF batting film used in the conventional style insulation systems with a more thermally robust film that could help reduce permeation of external combustion gas through the insulation for 5 minutes.

8. CONCLUSIONS.

Laboratory- and full-scale tests demonstrated that the oil-fired burner and accompanying 4- by 4- by 4-foot steel cube box used to mount representative test samples provided a suitable test method to evaluate potentially hazardous gases emitted from a variety of fuselage and insulation samples. The method of clamping the test samples in place onto the box enclosure proved to be effective at minimizing the collection of combustion by-products produced by the oil-fired burner flame itself. This was important, as the intent was to sample only gases that would emanate from the unexposed side of the test samples during exposure, simulating a continuous fuselage under realistic conditions. The intrusion of oil-fired burner by-products into the box enclosure would adversely impact the gas analysis.

In addition, a higher confidence level in the Fourier Transform Infrared data for carbon monoxide, carbon dioxide, and total hydrocarbons as propane was gained by using a second analyzer for each of these gases. The second analyzers were nondispersive infrared analyzers and a flame ionization detector-based total hydrocarbon analyzer.

The test method could be used to evaluate the potential toxicity of insulation constructions and innovations that meet the new burnthrough test requirements, to ensure that harmful gases will not result inside an intact fuselage subjected to an external fuel fire, despite the high burnthrough performance associated with a particular system. It also could be used to evaluate the toxic contribution of the basic fuselage structure whenever a nonmetallic material is used as the primary component.

Applying the aircraft-appropriate theoretical, perfect mixing scaling divisor to the laboratory-scale test data provides a practical method for estimating gas concentrations to be used in a hazard assessment for a particular aircraft when exposed to an external fuel fire.

9. REFERENCES.

1. Sarkos, C.P., "Development of Improved Fire Safety Standards Adopted by the Federal Aviation Administration," AGARD-CPP-467-5, *Propulsion and Energetics Panel 73rd Symposium on Aircraft Fire Safety*, Sintra, Portugal, May 22-26, 1989.

2. Sarkos, C.P., Webster, H., Geyer, G., Do, D., Wright, J., Collins, J., and Hampton, L., "Full-Scale Fuselage Burnthrough Tests," *The European Cabin Safety Conference*, Gatwick International Airport, Sussex, United Kingdom, September 18-21, 1990.

3. Webster, H., et al., "Full-Scale Air Transport Category Fuselage Burnthrough Tests," FAA report DOT/FAA/CT-TN89/65, February 1990.

4. Webster, H., "Fuselage Burnthrough From Large Exterior Fuel Fires," FAA report DOT/FAA/CT-90/10, July 1994.

5. Marker, T.R., "Full-Scale Test Evaluation of Aircraft Fuel Fire Burnthrough Resistance Improvements," FAA report DOT/FAA/AR-98/52, January 1999.

6. Marker, T.R., "Development of Improved Flammability Criteria for Aircraft Thermal Acoustic Insulation," FAA report DOT/FAA/AR-99/44, September 2000.

7. Cherry, R. and Warren, K., "Fuselage Burnthrough Protection for Increased Postcrash Occupant Survivability: Safety Benefit Analysis Based on Past Accidents," FAA report DOT/FAA/AR-99/57, September 1999.

8. Cherry, R., "A Benefit Analysis for Cabin Water Spray Systems and Enhanced Fuselage Burnthrough Protection," FAA report DOT/FAA/AR-02/49, April 2003.

9. Speitel, L.C., "Fourier Transform Infrared Analysis of Combustion Gases," FAA report DOT/FAA/AR-01/88, October 2001.

10. Kroschwitz, J.I., ed., *High Performance Polymers and Composites*, Encyclopedia Reprint Series, John Wiley & Sons, New York, 1991, pp. 20-65.

11. Quintiere, J.G., Walters, R.N., and Crowley, S., "Flammability Properties of Aircraft Carbon-Fiber Structural Composites," FAA Report DOT/FAA/AR-07/57, October 2007.

12. Jones, E.G. and Pedrick, D.L., "Polymer Degradation," WL-TR-93-4020, final report for 12/08/88-11/08/92, Systems Research Laboratories, Inc., A Division of ARVIN/ CALSPAN, 2800 Indian Ripple Road, Dayton, Ohio, February 1993.

13. Speitel, L.C., "Toxicity Assessment of Combustion Gases and Development of a Survival Model," FAA report DOT/FAA/AR-95/5, July 1995.

14. "Documentation for the Threshold Limit Values and Biological Exposure Indices, 6th Edition, 1991 American Conference of Governmental Industrial Hygenists, Inc., Cincinnati, Ohio, ISBN: 0-936712-96-1.